Higher Structures 9(1):88–178, 2025.

HIGHER STRUCTURES

Higher algebra of A_∞ and ΩBAs-algebras in Morse theory I

Thibaut Mazuir[a]

[a]*Institut für Mathematik, Humboldt Universität zu Berlin, Germany*

Abstract

Elaborating on works by Abouzaid and Mescher, we prove that for a Morse function on a smooth compact manifold, its Morse cochain complex can be endowed with an ΩBAs-algebra structure through counts of perturbed Morse gradient trees. This rich structure descends to its already known A_∞-algebra structure. We then introduce the notion of ΩBAs-morphism between two ΩBAs-algebras and prove that given two Morse functions, one can construct an ΩBAs-morphism between their associated ΩBAs-algebras through counts of 2-colored perturbed Morse gradient trees. This continuation morphism is a quasi-isomorphism and induces a standard A_∞-morphism between the induced A_∞-algebras. We work with integer coefficients, and provide to this extent a detailed account on the sign conventions for A_∞-algebras, ΩBAs-algebras, A_∞-morphisms and ΩBAs-morphisms, using polytopes and moduli spaces of metric trees which explicitly realize the dg operadic objects encoding them. Our proofs also involve showing at the level of polytopes that an ΩBAs-morphism between ΩBAs-algebras naturally induces an A_∞-morphism between A_∞-algebras. This paper is adressed to people acquainted with either differential topology or algebraic operads, and written in a way to be hopefully understood by both communities. It comes in particular with a short survey on operads, A_∞-algebras and A_∞-morphisms, the associahedra and the multiplihedra. All the details on transversality, gluing maps, signs and orientations for the moduli spaces defining the algebraic structures on the Morse cochains are thorougly carried out. It moreover lays the basis for a second article in which we solve the problem of finding a satisfactory notion of higher morphisms between A_∞-algebras and between ΩBAs-algebras, and show how this higher algebra of A_∞ and ΩBAs-algebras provides a natural framework to give a higher categorical meaning to the fact that continuation morphisms in Morse theory are well-defined up to homotopy at the chain level.

Communicated by: Alexander A Voronov.
Received: 19th September, 2021. Accepted: 30th December, 2024.
MSC: 18M70; 18N70; 53D30; 52B05; 52B11; 37D15.
Keywords: Morse theory, operads, homotopy theory, polytopes, symplectic topology, combinatorics.

Email address: thibaut.mazuir@hotmail.fr (Thibaut Mazuir)

DOI: 10.21136/HS.2025.03

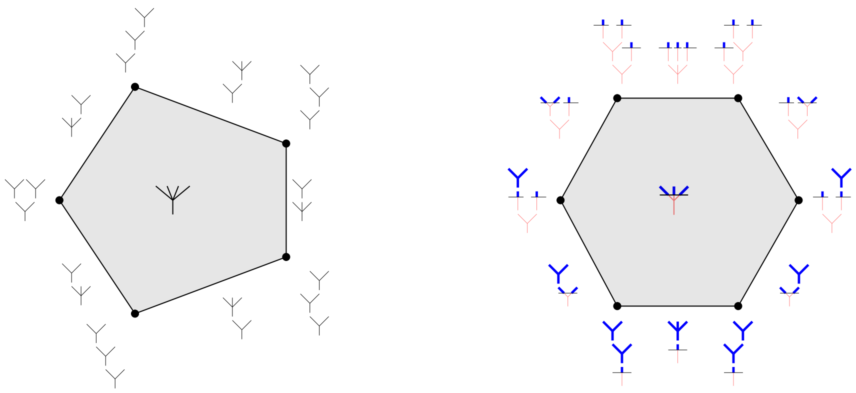

The associahedron K_4 and the multiplihedron J_3 …

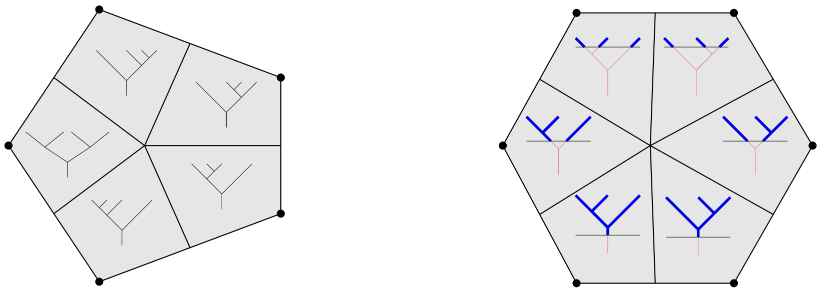

… and their ΩBAs-cell decompositions

Introduction

Context and main goal — The notion of *A_∞-algebra* was first introduced in the seminal work of Stasheff on iterated loop spaces [39] to describe *strongly homotopy associative algebras*: it corresponds to the datum of a cochain complex A endowed with operations $m_n : A^{\otimes n} \to A$ for $n \geqslant 2$, such that m_2 represents the multiplication on A and the operations m_n are the higher homotopies encoding the lack of associativity of m_2. This structure is in fact encoded by an operad: the operad A_∞, which is the minimal model of the operad As encoding associative algebras, as explained in [25] for instance.

Morse theory corresponds to the study of manifolds endowed with a *Morse function*, i.e. a function whose critical points are non-degenerate (see [36]). Given a smooth compact manifold M, Fukaya constructed in [13] an A_∞-category whose objects are functions f_i on the manifold M, whose spaces of morphisms between two functions f_i and f_j (such that $f_i - f_j$ is Morse) are the Morse cochain complexes $C^*(f_i - f_j)$, and whose higher multiplications are defined by counts of Morse ribbon trees. Adapting this construction to the case of a single Morse function f on the manifold M, Abouzaid defines in [3] an A_∞-algebra structure on the Morse cochains $C^*(f)$ through counts of *perturbed Morse gradient ribbon trees*. His work was subsequently continued by Mescher in [35]. See also [11] and [1].

The goal of this work in three articles is to study the unicity up to homotopy of the strongly homotopy associative algebra structure on the Morse cochains $C^*(f)$. The main objectives of this first paper are as follows:

1. We provide a quick and self-contained survey on operads and strongly homotopy associative structures for the use of geometers. We give special attention to the definition of the polytopes and moduli spaces of metric trees encoding these structures, and also prove some folklore theorems in the process.
2. We prove that the Morse cochains can in fact be endowed with an ΩBAs-*algebra* structure (an alternative and refined notion of strongly homotopy associative algebra) and construct *continuation morphisms* between the Morse cochains of two different Morse functions: these continuation morphisms are ΩBAs-*morphisms* (a newly defined notion of morphisms between ΩBAs-algebras which preserve the product up to homotopy) and induce isomorphisms in homology. This is a first step towards the formulation of the unicity up to homotopy of the ΩBAs-algebra structure on the Morse cochains at the chain-level.
3. We carry out a detailed study of the analysis, and the signs and orientations involved in the definition of these structures, and construct explicit gluing maps for the moduli spaces of perturbed Morse trees used therein. This completes in particular some of the proofs of Abouzaid in [3] which were only sketched in his paper. Our proofs are moreover written in a way to be hopefully accessible to people from the algebraic operads community.

Outline of the paper — Our first part begins with concise and self-contained recollections on the theory of algebraic (nonsymmetric) operads, that we subsequently specialize to the case of A_∞-algebras, A_∞-morphisms between them and their homotopy theory. We resort in particular to the convenient setting of operadic bimodules to define the operadic bimodule M_∞ encoding A_∞-morphisms between A_∞-algebras. We then recall how the operad A_∞ and the operadic bimodule M_∞ can be realized using families of polytopes, respectively known as the associahedra and the multiplihedra. The associahedra can themselves be realized as geometric moduli spaces: the compactified moduli spaces of stable metric ribbon trees $\overline{\mathcal{T}}_n$. These moduli spaces come with a refined cell decomposition encoding the operad ΩBAs. Likewise, the multiplihedra can be realized as the compactified moduli spaces of 2-colored metric stable ribbon trees $\overline{\mathcal{CT}}_n$. Endowing these moduli spaces with a refined cell decomposition, we introduce a new operadic bimodule: the *operadic bimodule* $M_{\Omega BAs}$, encoding ΩBAs-*morphisms* between ΩBAs-algebras.

> *The* operadic bimodule $M_{\Omega BAs}$ *is the quasi-free* $(\Omega BAs, \Omega BAs)$*-operadic bimodule generated by the set of 2-colored stable ribbon trees*
>
> $M_{\Omega BAs} := \mathcal{F}^{\Omega BAs,\Omega BAs}($ 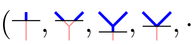 $, \cdots)$,
>
> *where a 2-colored stable ribbon tree* t_c *with* $e(t)$ *internal edges and whose gauge crosses* j *vertices has degree* $|t_c| := j - e(t) - 1$*. The differential of a 2-colored stable ribbon tree* t_c *is given by the signed sum of all 2-colored stable ribbon trees obtained from* t_c *under four families of tree transformations prescribed by the top dimensional strata in the boundary of the compactified moduli space* $\overline{\mathcal{CT}}_n(t_c)$*. (Definition 3.2.13 p.109 and Definition 3.2.19 p.111)*

The ΩBAs framework provides another template to study algebras which are associative up to homotopy, together with morphisms between them which preserve the product up to homotopy. These sections are followed by a comprehensive study on the A_∞ and ΩBAs sign conventions. In the A_∞ case, we show how the two usual sign conventions for A_∞-algebras and A_∞-morphisms are naturally induced by the shifted bar construction viewpoint. Using the Loday realizations of the associahedra [29] and the Forcey–Loday realizations of the multiplihedra [20], we give a complete proof of the following two folklore theorems:

The codimension 1 boundaries of the Loday realizations of the associahedra and of the Forcey–Loday realizations of the multiplihedra determine the usual sign conventions for A_∞-algebras and A_∞-morphisms between them. (Theorem 2.2.1 p.101 and Theorem 2.3.1 p.102)

In the ΩBAs case, we start by recalling the formulation of the operad ΩBAs by Markl and Shnider in [28]. We then proceed to study the moduli spaces of stable 2-colored metric ribbon trees $\mathcal{CT}_n(t_c)$ and compute the signs arising in the top dimensional strata of their boundary in Propositions 5.2.14 to 5.2.18 (p.130 to 134). This allows us to complete our definition of the operadic bimodule $M_{\Omega BAs}$ by making explicit the signs for the action-composition maps and the differential. We subsequently prove the following two propositions:

We give an alternative and more geometric construction of the morphism of operads $A_\infty \to \Omega BAs$ defined in [28], using the realizations of the associahedra as geometric moduli spaces. (Proposition 3.1.15 p.106) We build an explicit morphism of operadic bimodules $M_\infty \to M_{\Omega BAs}$ applying the same ideas to the moduli spaces realizing the multiplihedra. (Proposition 3.2.25 p.112)

In the second part of this paper, we adapt the constructions of Abouzaid [3], using the terminology of Mescher [35], to perform two constructions on the Morse cochains $C^*(f)$. Firstly, we introduce the notion of smooth choices of perturbation data $\mathbb{X}_n$ on the moduli spaces $\mathcal{T}_n$ that we use to define the moduli spaces of perturbed Morse gradient trees $\mathcal{T}_t^{\mathbb{X}_t}(y; x_1, \dots, x_n)$ modeled on a stable ribbon tree type t.

Under some generic assumptions on the choice of perturbation data $\{\mathbb{X}_n\}_{n\geqslant 2}$, the moduli spaces $\mathcal{T}_t^{\mathbb{X}_t}(y; x_1, \dots, x_n)$ are orientable manifolds. If they have dimension 0, they are compact. If they have dimension 1, they can be compactified to compact manifolds with boundary, whose boundary is modeled on the boundary of the moduli spaces $\mathcal{T}_n(t)$. (Theorem 6.4.5 p.145 and Theorem 6.4.6 p.145)

In this context, *generic* means that the set of perturbation data for which the moduli spaces $\mathcal{T}_t^{\mathbb{X}_t}(y; x_1, \dots, x_n)$ are orientable manifolds is residual in the sense of Baire in the space of all perturbation data. We then show that under a generic choice of perturbation data $\{\mathbb{X}_n\}_{n\geqslant 2}$ the Morse cochains $C^*(f)$ can be endowed with an ΩBAs-algebra structure, through counts of perturbed Morse ribbon trees:

Defining for every n and every stable ribbon tree type t of arity n the operation m_t as

$$\begin{aligned} m_t : C^*(f) \otimes \cdots \otimes C^*(f) &\longrightarrow C^*(f) \\ x_1 \otimes \cdots \otimes x_n &\longmapsto \sum_{|y| = \sum_{i=1}^n |x_i| - e(t)} \# \mathcal{T}_t^{\mathbb{X}}(y; x_1, \cdots, x_n) \cdot y \ , \end{aligned}$$

these operations endow the Morse cochains $C^*(f)$ with an ΩBAs-algebra structure. (Theorem 6.5.1 p.146)

The ΩBAs formalism is the natural and intrisic combinatorial viewpoint arising when realizing the moduli spaces of stable metric ribbon trees in Morse theory. We recover the A_∞-algebra structure of [3] using the morphism of operads $A_\infty \to \Omega BAs$ of Proposition 3.1.15: it corresponds to forgetting about all operations of the ΩBAs-algebra structure but the ones labeled by binary ribbon trees, and defining each operations m_n of the A_∞-algebra structure as a signed sum of all operations associated to binary ribbon trees of arity n. We point out that this viewpoint is also more ad hoc to resort to when defining *smooth* choices of perturbation data, as we work in

that case with the natural smooth structures on the moduli spaces $\mathcal{T}_n(t)$, rather than proving that the moduli spaces $\mathcal{T}_n$ can be endowed with a smooth structure compatible with the operadic composition and inducing the natural smooth structure on each cell $\mathcal{T}_n(t)$.
Given now two Morse functions f and g, we can perform the same constructions in Morse theory using this time the moduli spaces $\mathcal{CT}_n$ as blueprints. The counterparts of Theorems 6.4.5 and 6.4.6 (Theorem 7.3.3 p.152 and Theorem 7.3.4 p.153) still hold. Moreover, given two generic choices of perturbation data $\mathbb{X}^f$ and $\mathbb{X}^g$, we construct an ΩBAs-morphism between the ΩBAs-algebras $C^*(f)$ and $C^*(g)$ through counts of 2-colored perturbed Morse gradient trees. This construction provides a first geometric and explicit instance of the newly defined notion of ΩBAs-morphism:

Let $(\mathbb{Y}_n)_{n\geqslant 1}$ be a generic choice of perturbation data on the moduli spaces $\mathcal{CT}_n$. Defining for every n and every 2-colored stable ribbon tree type t_c of arity n the operations μ_{t_c} as

$$\begin{aligned} \mu_{t_c}^{\mathbb{Y}} : C^*(f) \otimes \cdots \otimes C^*(f) &\longrightarrow C^*(g) \\ x_1 \otimes \cdots \otimes x_n &\longmapsto \sum_{|y| = \sum_{i=1}^n |x_i| + |t_c|} \# \mathcal{CT}_{t_c}^{\mathbb{Y}}(y; x_1, \cdots, x_n) \cdot y \ . \end{aligned}$$

these operations fit into an ΩBAs-morphism $\mu^{\mathbb{Y}} : (C^*(f), m_t^{\mathbb{X}^f}) \to (C^*(g), m_t^{\mathbb{X}^g})$. (Theorem 7.4.1 p.154)

We moreover show that:

The ΩBAs-morphism $\mu^{\mathbb{Y}}$ is a quasi-isomorphism. (Theorem 7.4.5 p.154)

This ΩBAs-morphism yields in particular an A_∞-morphism between two A_∞-algebras, using the morphism of operadic bimodules of Proposition 3.2.25. These constructions are followed by a section dedicated to a comprehensive proof of Theorem 6.4.5, which clarifies and completes the arguments in [3, Section 7]. We resort in particular to an argument commonly attributed to Taubes to prove the existence of generic choices of *smooth* perturbation data. Our last section on signs and orientations is dedicated to a thorough sign check for Theorems 6.5.1 and 7.4.1. We introduce for this purpose the notion of *twisted A_∞-algebra*:

A twisted A_∞-algebra *is a dg module A endowed with two different differentials ∂_1 and ∂_2, and a sequence of degree $2-n$ operations $m_n : A^{\otimes n} \to A$ such that*

$$[\partial, m_n] = - \sum_{\substack{i_1+i_2+i_3=n \\ 2 \leqslant i_2 \leqslant n-1}} (-1)^{i_1+i_2 i_3} m_{i_1+1+i_3}(\mathrm{id}^{\otimes i_1} \otimes m_{i_2} \otimes \mathrm{id}^{\otimes i_3}) \ ,$$

where $[\partial, \cdot]$ denotes the bracket for the maps $(A^{\otimes n}, \partial_1) \to (A, \partial_2)$. A twisted ΩBAs-algebra *and a* twisted ΩBAs-morphism *are defined similarly. (Definition 9.3.1 p.163)*

We show that we have in fact defined a twisted ΩBAs-algebra structure on the Morse cochains in Theorem 6.5.1, and a twisted ΩBAs-morphism between two Morse cochains complexes in Theorem 7.4.1. When the manifold M is odd-dimensional, the word *twisted* can moreover be dropped. Our computations are performed using the convenient viewpoint of signed short exact sequences of vector bundles. We finally construct explicit gluing maps for the 1-dimensional moduli spaces of perturbed Morse gradient trees (Section 9.4.3 p.168 and Section 9.5.4 p.173), and prove a key technical lemma on orientation and transversality (Lemma 9.4.4 p.168) which was missing from the proof by Abouzaid of the signs in the A_∞ case in [2, Appendix C].

This article lays the ground for a second article [32] tackling two main problems. Firstly, understand and define a suitable homotopic notion of higher morphisms between A_∞-algebras, which would give a satisfactory description of the *higher algebra of A_∞-algebras*. Secondly, realize these higher morphisms through counts of perturbed Morse trees in order to give a higher categorical meaning to the fact that continuation morphisms in Morse theory are well-defined up to homotopy at the chain level. We explain this problem in Section 7.5 p.154.

Part I: Algebra

1. Operadic algebra

This first section is mostly derived from [24] and [41], and gives a gentle introduction on operadic algebra and the particular case of the operad A_∞. The only original viewpoint that we introduce is to see A_∞-morphisms as being encoded by the operadic bimodule M_∞ (Definition 1.5.6). All the signs will be worked out in Section 4.2, and will temporarily be written $\pm$ in this section.

Notations and terminology We let $\mathcal{C}$ be one of the following two monoidal categories: the category of differential graded $\mathbb{Z}$-modules with cohomological convention $(\texttt{dg-mod}, \otimes)$ or the category $(\texttt{Poly}, \times)$ whose objects are polytopes, which is defined in Definition 2.1.2. We will write $\otimes$ for the tensor product on $\mathcal{C}$, and I for its identity element. We will also use the abbreviation *dg* for "differential graded $\mathbb{Z}$" in the rest of this paper. With this terminology, a *dg module* will in particular exactly be a *cochain complex*.

1.1 Operads

Definition 1.1.1. (i) A *(non-symmetric) $\mathcal{C}$-operad P* consists in the data of a collection of objects $\{P_n\}_{n\geqslant 1}$ of $\mathcal{C}$ together with a unit element $e \in P_1$ and with compositions

$$P_k \otimes P_{i_1} \otimes \cdots \otimes P_{i_k} \underset{c_{i_1,\dots,i_k}}{\longrightarrow} P_{i_1+\cdots+i_k}$$

which are unital and associative.

(ii) Equivalently, an operad is the data of a collection of objects $\{P_n\}_{n\geqslant 1}$ together with a unit element $e \in P_1$ and with partial composition maps

$$\circ_i : P_k \otimes P_h \longrightarrow P_{h+k-1} \ , \ 1 \leqslant i \leqslant k$$

which are unital and associative.

The objects P_n are to be thought as spaces encoding arity n operations while the compositions $c_{i_1,\dots,i_k}$ define how to compose these operations together.

Definition 1.1.2. A *morphism of operads* $P \to Q$ is a sequence of maps $P_n \to Q_n$ compatible with the compositions and preserving the identity.

There is a third equivalent definition of operads using the notion of Schur functors. Call any collection $P = \{P_n\}_{n\geqslant 1}$ of objects of $\mathcal{C}$ a $\mathbb{N}$-*module*. To each $\mathbb{N}$-module one can associate its *Schur functor*, which is the endofunctor $S_P : \mathcal{C} \to \mathcal{C}$ defined as

$$C \longmapsto \bigoplus_{n=1}^{\infty} P_n \otimes C^{\otimes n} \ .$$

Given two $\mathbb{N}$-modules P and Q, composing their Schur functors gives the following formula

$$S_P \circ S_Q : C \longrightarrow \bigoplus_{n=1}^{\infty} \left(\bigoplus_{i_1+\cdots+i_k=n} P_k \otimes Q_{i_1} \otimes \cdots \otimes Q_{i_k} \right) \otimes C^{\otimes n} .$$

In other words, there is a $\mathbb{N}$-module associated to the composition of the Schur functors of two $\mathbb{N}$-modules, and it is given by

$$P \circ Q = \{ \bigoplus_{i_1+\cdots+i_k=n} P_k \otimes Q_{i_1} \otimes \cdots \otimes Q_{i_k} \}_{n \geqslant 1} .$$

The category $(\mathrm{End}(\mathcal{C}), \circ, Id_{\mathcal{C}})$, endowed with composition of endofunctors, is a monoidal category. In particular, there is a well-defined notion of monoid in $\mathrm{End}(\mathcal{C})$. A monoid structure on an endofunctor $F : \mathcal{C} \to \mathcal{C}$ is the data of natural transformations $\mu_F : F \circ F \to F$ and $e : Id_{\mathcal{C}} \to F$, which satisfy the usual commutative diagrams for monoids. This yield the third equivalent definition for the notion of operad:

Definition 1.1.3. A $\mathcal{C}$*-operad* is the data of a $\mathbb{N}$-module $P = \{P_n\}$ of $\mathcal{C}$ together with a monoid structure on its Schur functor S_P.

1.2 P-algebras Let A be a dg module and $n \geqslant 1$. Define the graded module $\mathrm{Hom}(A^{\otimes n}, A)^i$ of i-graded maps $A^{\otimes n} \to A$, and endow it with the differential $[\partial, f] = \partial f - (-1)^{|f|} f \partial$. The $\mathbb{N}$-module $\mathrm{End}_A(n) := \mathrm{Hom}(A^{\otimes n}, A)$ in dg modules can then naturally be endowed with an operad structure, where composition maps are defined as one expects. Let P be a dg operad. A *structure of P-algebra* on A is defined to be the datum of a morphism of operads

$$P \longrightarrow \mathrm{End}_A ,$$

in other words the datum of a way to interpret each operation of P_n in $\mathrm{Hom}(A^{\otimes n}, A)$, such that abstract composition in P coincides with actual composition in End_A.

Definition 1.2.1. A morphism of P-algebras between A and B is a chain map $f : A \to B$ such that for every $m_n \in P_n$,

$$m_n^B \circ f^{\otimes n} = f \circ m_n^A .$$

1.3 Operadic bimodules Let now $(\mathcal{D}, \otimes_{\mathcal{D}}, I)$ be any monoidal category, and (A, μ_A) and (B, μ_B) be two monoids in $\mathcal{D}$. Reproducing the diagrams of usual algebra, one can define the notion of an (A, B)*-bimodule* in $\mathcal{D}$. It is simply the data of an object R of $\mathcal{D}$, together with action maps $\lambda : A \otimes R \to R$ and $\mu : R \otimes B \to R$ which are compatible with the product on A and B, act trivially under their identity elements and satisfy the obvious associativity conditions. A monoid in `dg-mod` is then for instance a unital associative differential graded algebra, and the notion of bimodules in the previous paragraph then coincides with the usual notion of bimodules over dg algebras.

Definition 1.3.1. Given P and Q two operads seen as their Schur functors S_P and S_Q, let $R = \{R_n\}$ be a $\mathbb{N}$-module of $\mathcal{C}$ seen as its Schur functor S_R. A (P, Q)*-operadic bimodule structure* on R is a (S_P, S_Q)-bimodule structure $\lambda : S_P \circ S_R \to S_R$ and $\mu : S_R \circ S_Q \to S_R$ on S_R in $(\mathrm{End}(\mathcal{C}), \circ, Id_{\mathcal{C}})$.

This definition is of course of no use for actual computations. Unraveling the definitions, we get an equivalent definition for (P, Q)-operadic bimodules.

Definition 1.3.2. (i) A (P, Q)-*operadic bimodule structure* on R corresponds to the data of action-composition maps

$$R_k \otimes Q_{i_1} \otimes \cdots \otimes Q_{i_k} \underset{\mu_{i_1,\dots,i_k}}{\longrightarrow} R_{i_1+\cdots+i_k} \ ,$$
$$P_h \otimes R_{j_1} \otimes \cdots \otimes R_{j_h} \underset{\lambda_{j_1,\dots,j_h}}{\longrightarrow} R_{j_1+\cdots+j_h} \ ,$$

which are compatible with one another, with identities, and with compositions in P and Q.

(ii) Equivalently, the action of Q on R can be reduced to partial action-composition maps

$$\circ_i : R_k \otimes Q_h \longrightarrow R_{h+k-1} \quad 1 \leqslant i \leqslant k \ .$$

We point out that the action of P on R cannot be reduced to partial action-composition maps, as R does not necessarily have an identity.

Let A and B be two dg modules. We have seen that they each determine an operad, End_A and End_B respectively:

Definition 1.3.3. The operadic bimodule $\mathrm{Hom}(A, B)$ is defined to be the $\mathbb{N}$-module in dg modules $\mathrm{Hom}(A, B) := \{\mathrm{Hom}(A^{\otimes n}, B)\}_{n \geqslant 1}$ endowed with its $(\mathrm{End}_B, \mathrm{End}_A)$-operadic bimodule structure, where the action-composition maps are defined as one could expect.

1.4 The operad A_∞

1.4.1 A_∞-algebras

Definition 1.4.1. Let A be a graded module. We define sA to be the graded module $(sA)^i := A^{i-1}$. In other words, $|sa| = |a| - 1$.

Definition 1.4.2. Let A be a dg module with differential m_1. A structure of A_∞-algebra on A is the data of a collection of degree $2 - n$ maps

$$m_n : A^{\otimes n} \longrightarrow A \ , \ n \geqslant 1,$$

extending m_1 and which satisfy the following equations, called the A_∞-equations

$$[m_1, m_n] = \sum_{\substack{i_1+i_2+i_3=n \\ 2 \leqslant i_2 \leqslant n-1}} \pm m_{i_1+1+i_3}(\mathrm{id}^{\otimes i_1} \otimes m_{i_2} \otimes \mathrm{id}^{\otimes i_3}).$$

We refer to Section 4.2.4 for the signs $\pm$. Representing m_n as  a corolla of arity n, these equations can be written as

$[m_1,$ 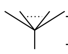 $] = \sum_{\substack{i_1+i_2+i_3=n \\ 2 \leqslant i_2 \leqslant n-1}} \pm$ 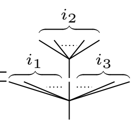 .

We have in particular that

$$[m_1, m_2] = 0 \ ,$$
$$[m_1, m_3] = m_2(\mathrm{id} \otimes m_2 - m_2 \otimes \mathrm{id}) \ .$$

Defining $H^*(A)$ to be the cohomology of A relative to m_1, the last two equations show that m_2 descends to an associative product on $H^*(A)$. An A_∞-algebra is simply a correct notion of a dg algebra whose product is associative up to homotopy, where the operations m_n for $n \geqslant 4$ are the higher homotopies keeping track of the homotopy associativity of m_2.

1.4.2 The operad A_∞

The A_∞-algebra structure defined previously is actually governed by the following operad:

Definition 1.4.3. The *operad* A_∞ is the quasi-free dg operad generated in arity $n \geqslant 2$ by one operation m_n of degree $2 - n$ and whose differential is defined by

$$\partial(m_n) = \sum_{\substack{i_1+i_2+i_3=n \\ 2 \leqslant i_2 \leqslant n-1}} \pm m_{i_1+1+i_3}(\mathrm{id}^{\otimes i_1} \otimes m_{i_2} \otimes \mathrm{id}^{\otimes i_3}) \ .$$

This is often written as $A_\infty = \mathcal{F}($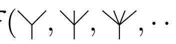$)$ where

$$\partial(\text{}$$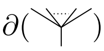$$) = \sum_{\substack{i_1+i_2+i_3=n \\ 2 \leqslant i_2 \leqslant n-1}} \pm$$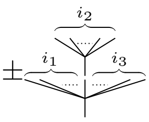

.

Recall that quasi-free means that the operad is freely generated by the operations  as a graded object, with the additional datum of a differential on its generating operations that is non-canonical. We then check that an A_∞-algebra structure on a dg module A amounts simply to a morphism of operads $A_\infty \to \mathrm{End}_A$.

1.4.3 The bar construction viewpoint

Definition 1.4.4. The (reduced) *bar construction* of a graded module V is defined to be the graded module

$$\overline{T}V := V \oplus V^{\otimes 2} \oplus \cdots$$

endowed with the coassociative comultiplication

$$\Delta_{\overline{T}V}(v_1 \dots v_n) := \sum_{i=1}^{n-1} v_1 \dots v_i \otimes v_{i+1} \dots v_n \ .$$

Lemma 1.4.5. *There is a correspondence*

$$\left\{ \begin{matrix} \textit{collections of morphisms of degree } 2-n \\ m_n : A^{\otimes n} \to A \ , \ n \geqslant 1 \end{matrix} \right\} \leftrightarrow \left\{ \begin{matrix} \textit{collections of morphisms of degree } +1 \\ b_n : (sA)^{\otimes n} \to sA \ , \ n \geqslant 1 \end{matrix} \right\}$$
$$\updownarrow$$
$$\left\{ \textit{coderivations } D \textit{ of degree } +1 \textit{ of } \overline{T}(sA) \right\} ,$$

and a correspondence

$$\left\{ \begin{matrix} \textit{collections of morphisms of degree } 2-n \\ m_n : A^{\otimes n} \to A \ , \ n \geqslant 1, \\ \textit{satisfying the } A_\infty\textit{-equations} \end{matrix} \right\} \leftrightarrow \left\{ \begin{matrix} \textit{coderivations } D \textit{ of degree } +1 \textit{ of} \\ \overline{T}(sA) \textit{ such that } D^2 = 0 \end{matrix} \right\} .$$

Proof. The first correspondence results from the universal property of the bar construction and the observation that the datum of a degree $2-n$ map $A^{\otimes n} \to A$ is equivalent to the datum of a degree $+1$ map $(sA)^{\otimes n} \to sA$. The second correspondence results from the fact that the coderivation $D : \overline{T}(sA) \to \overline{T}(sA)$ associated to the family of maps $b_n : (sA)^{\otimes n} \to sA$, has restriction to the summand $(sA)^{\otimes n}$ of $\overline{T}(sA)$ given by

$$\sum_{i_1+i_2+i_3=n} \pm \mathrm{id}^{\otimes i_1} \otimes b_{i_2} \otimes \mathrm{id}^{\otimes i_3} .$$

The A_∞-equations are then easily seen to be equivalent to the equation $D^2 = 0$. □

Hence, the following equivalent definition for the notion of A_∞-algebra:

Definition 1.4.6. An A_∞-algebra structure on a graded module A is a coderivation $D : \overline{T}(sA) \to \overline{T}(sA)$ of degree $+1$ which squares to 0.

1.5 A_∞-morphisms Using Definition 1.2.1, a morphism between two A_∞-algebras A and B is simply a chain map $f : A \to B$ which is compatible with all the m_n. This notion of morphism is however not satisfactory from an homotopy-theoretic point of view. Indeed, an A_∞-algebra being an algebra whose product is associative up to homotopy, the correct homotopy notion of a morphism between two A_∞-algebras would be that of a map which preserves the product m_2 up to homotopy, i.e. of a chain map $f_1 : A \to B$ together with higher coherent homotopies, the first one satisfying

$$[\partial, f_2] = f_1 m_2^A - m_2^B (f_1 \otimes f_1) .$$

1.5.1 A_∞-morphisms

Definition 1.5.1. An *A_∞-morphism* between two A_∞-algebras A and B is a dg coalgebra morphism $F : (\overline{T}(sA), D_A) \to (\overline{T}(sB), D_B)$ between their bar constructions.

Lemma 1.5.2. *There is a one-to-one correspondence*

$$\left\{ \begin{array}{c} \textit{collections of morphisms of degree } 1-n \\ f_n : A^{\otimes n} \to B \ , \ n \geqslant 1, \end{array} \right\} \longleftrightarrow \left\{ \begin{array}{c} \textit{morphisms of graded coalgebras} \\ F : \overline{T}(sA) \to \overline{T}(sB) \end{array} \right\} .$$

Proof. The proof is similar to the proof of Lemma 1.4.5. The component of F mapping $(sA)^{\otimes n}$ to $(sB)^{\otimes s}$ is given by

$$\sum_{i_1+\cdots+i_s=n} \pm f_{i_1} \otimes \cdots \otimes f_{i_s} .$$ □

A coalgebra morphism preserves the differentials if and only if for all $n \geqslant 1$,

$$\sum_{i_1+i_2+i_3=n} \pm f_{i_1+1+i_3} (\mathrm{id}^{\otimes i_1} \otimes m_{i_2}^A \otimes \mathrm{id}^{\otimes i_3}) = \sum_{i_1+\cdots+i_s=n} \pm m_s^B (f_{i_1} \otimes \cdots \otimes f_{i_s}) . \qquad (\star)$$

These equations can be rewritten as

$$[m_1, f_n] = \sum_{\substack{i_1+i_2+i_3=n \\ i_2 \geqslant 2}} \pm f_{i_1+1+i_3} (\mathrm{id}^{\otimes i_1} \otimes m_{i_2}^A \otimes \mathrm{id}^{\otimes i_3}) + \sum_{\substack{i_1+\cdots+i_s=n \\ s \geqslant 2}} \pm m_s^B (f_{i_1} \otimes \cdots \otimes f_{i_s}) . \qquad (\star)$$

This yields the following equivalent definition:

Definition 1.5.3. An A_∞-*morphism* between two A_∞-algebras A and B is a family of maps $f_n : A^{\otimes n} \to B$ of degree $1-n$ satisfying Equation ($\star$).

The signs $\pm$ are made explicit in Section 4.2.4. We check that we recover in particular

$$[m_1, f_1] = 0 \ ,$$
$$[m_1, f_2] = f_1 m_2^A - m_2^B (f_1 \otimes f_1) \ .$$

As a result, an A_∞-morphism of A_∞-algebras induces a morphism of associative algebras on the level of cohomology.

Definition 1.5.4. An A_∞-*quasi-isomorphism* is defined to be an A_∞-morphism inducing an isomorphism in cohomology.

1.5.2 Composing A_∞-morphisms

Given two coalgebra morphisms $F : \overline{T}V \to \overline{T}W$ and $G : \overline{T}W \to \overline{T}Z$, the family of morphisms associated to $G \circ F$ is

$$(G \circ F)_n := \sum_{i_1 + \cdots + i_s = n} \pm g_s (f_{i_1} \otimes \cdots \otimes f_{i_s}) \ ,$$

where the signs $\pm$ are given in Section 4.2.4.

Definition 1.5.5. (i) The composition of two A_∞-morphisms $f : A \to B$ and $g : B \to C$ is defined to be

$$(g \circ f)_n := \sum_{i_1 + \cdots + i_s = n} \pm g_s (f_{i_1} \otimes \cdots \otimes f_{i_s}) \ .$$

(ii) The category $\mathtt{A}_\infty - \mathtt{alg}$ is defined to be the category whose objects are A_∞-algebras and morphisms the A_∞-morphisms between them, where composition is defined by the previous formula.

1.5.3 The (A_∞,A_∞)-operadic bimodule encoding A_∞-morphisms

Definition 1.5.6. The operadic bimodule M_∞ is the quasi-free (A_∞, A_∞)-operadic bimodule generated in arity $n \geqslant 1$ by one operation f_n of degree $1-n$ and whose differential is defined by

$$\partial(f_n) = \sum_{\substack{i_1 + i_2 + i_3 = n \\ i_2 \geqslant 2}} \pm f_{i_1 + 1 + i_3} (\mathrm{id}^{\otimes i_1} \otimes m_{i_2} \otimes \mathrm{id}^{\otimes i_3}) + \sum_{\substack{i_1 + \cdots + i_s = n \\ s \geqslant 2}} \pm m_s (f_{i_1} \otimes \cdots \otimes f_{i_s}) \ .$$

Representing the generating operations of the operad A_∞ acting on the right in blue (thick line)  and the ones of the operad A_∞ acting on the left in red (thin line) , we represent f_n by 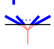. This operadic bimodule can then be written as

$M_\infty = \mathcal{F}^{A_\infty, A_\infty}($ 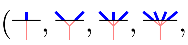 $, \cdots) \ ,$

with differential defined as

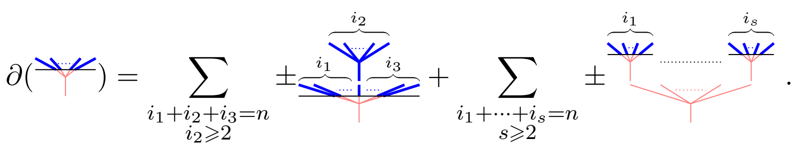

Consider A and B two A_∞-algebras, which we can see as two morphisms of operads $A_\infty \to \mathrm{End}_A$ and $A_\infty \to \mathrm{End}_B$. Recall from Definition 1.3.3 that $\mathrm{Hom}(A, B)$ is a $(\mathrm{End}_B, \mathrm{End}_A)$-operadic bimodule. The previous two morphisms of operads make $\mathrm{Hom}(A, B)$ into an $(A_\infty$,$A_\infty)$-operadic bimodule. An A_∞-morphism between A and B is then simply a morphism of $(A_\infty$,$A_\infty)$-operadic bimodules

$$M_\infty \longrightarrow \mathrm{Hom}(A, B) \ .$$

It is in that sense that M_∞ is the $(A_\infty$,$A_\infty)$-operadic bimodule encoding the notion of A_∞-morphisms of A_∞-algebras.

1.5.4 The framework of 2-colored operads

In fact, our choice of notation 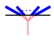 reveals that the operad A_∞ and the operadic bimodule M_∞ naturally define a 2-colored operad:

Definition 1.5.7. The 2-colored operad A^2_∞ is the quasi-free 2-colored operad

$$A^2_\infty := \mathcal{F}(\ \cdots\ ) \ ,$$

whose differential on the generating operations is given by the previous formulae for the operad A_∞ and the operadic bimodule M_∞.

A 2-colored operad can be roughly defined as an operad whose operations have entries and output labeled either in red or in blue, and whose operations can only be composed along the same color. See [43] for a complete definition.

1.6 Homotopy theory of A_∞-algebras A_∞-algebras with A_∞-morphisms between them provide a suitable framework to study homotopy theory of dg algebras. Following [26], this stems from the fact that the 2-colored operad A^2_∞ is a resolution

$$A^2_\infty \xrightarrow{\sim} As^2 \ ,$$

of the 2-colored operad encoding associative algebras with morphisms of algebras, and a fibrant-cofibrant object in the model category of 2-colored operads in dg modules. We illustrate these statements with two fundamental theorems. We refer moreover to [27] for a more general version of Theorem 1.6.1.

Theorem 1.6.1 (Homotopy transfer theorem, [19])**.** *Let (A, ∂_A) and (H, ∂_H) be two dg modules. Suppose that H is a* deformation retract *of A, that is that they fit into a diagram*

$$h \circlearrowright (A, \partial_A) \underset{i}{\overset{p}{\rightleftarrows}} (H, \partial_H) \ ,$$

where $\mathrm{id}_A - ip = [\partial, h]$. Then if (A, ∂_A) is endowed with an associative algebra structure, H can be made into an A_∞-algebra such that i and p extend to A_∞-morphisms.

Theorem 1.6.2 (Fundamental theorem of A_∞-quasi-isomorphisms, [22])**.** *Let $f : A \to B$ be an A_∞-quasi-isomorphism. Then there exists an A_∞-quasi-isomorphism $B \to A$ which inverts f on the level of cohomology.*

2. Associahedra and multiplihedra

We recall in the first section the monoidal category `Poly` defined in [29], which yields a good framework to handle operadic calculus in a category whose objects are polytopes. We then introduce in Sections 2.2 and 2.3 the two main combinatorial objects of this article: the *associahedra* and the *multiplihedra*, which are polytopes that respectively encode the notions of A_∞-algebras and A_∞-morphisms between them.

2.1 Three monoidal categories and their operadic algebra

2.1.1 The monoidal categories `dg-mod`, `CW` and `Poly`

Definition 2.1.1. (i) We define `dg-mod` to be the category whose objects are differential graded $\mathbb{Z}$-modules with cohomological convention, and morphisms the morphisms of dg modules. It is a monoidal category with the classical tensor product of dg modules and unit the ring $\mathbb{Z}$ seen as a dg module concentrated in degree 0.

(ii) We define `CW` to be the category whose objects are finite CW-complexes and whose morphisms are CW-maps between CW-complexes. This category is again a monoidal category with product the usual cartesian product and unit the point $*$.

The cellular chain functor $C_*^{cell} : \mathtt{CW} \to \mathtt{dg\text{-}mod}$ is then strong monoidal. To be consistent with the cohomological degree convention on A_∞-algebras, we will actually work with the strong monoidal functor $C_{-*}^{cell} : \mathtt{CW} \longrightarrow \mathtt{dg\text{-}mod}$, where $C_{-*}^{cell}(P)$ is simply the dg module $C_*^{cell}(P)$ taken with its opposite grading.

Definition 2.1.2. The category `Poly` is the category whose objects are polytopes and whose morphisms are continuous maps $f : P \to Q$ which are homeomorphisms $P \to |\mathcal{D}|$ where $\mathcal{D}$ is a polytopal subcomplex of Q and $f^{-1}(\mathcal{D})$ is a polytopal subdivision of P. Its morphisms will be called *polytopal maps*. It is a monoidal category with product the usual cartesian product and unit the polytope reduced to a point $*$. It is moreover a monoidal subcategory of `CW`.

A *polytope* is here simply defined to be the convex hull of a finite number of points in a Euclidean space $\mathbb{R}^n$, while we refer to [29, Section 1.3] for more details on the notions of *polytopal complex* and *polytopal subdivision*. We also refer to Remark 2.2.2 for an explanation on the definition of the morphisms of the category `Poly`.

2.1.2 From operadic algebra in `Poly` to operadic algebra in `dg-mod`

Let $\{X_n\}$ be a `Poly`-operad, that is a collection of polytopes X_n together with polytopal maps

$$\circ_i : X_k \times X_h \longrightarrow X_{h+k-1} \ ,$$

satisfying the compatibility conditions of partial compositions. The functor C_{-*}^{cell} being strong monoidal, it yields a new dg operad $\{P_n\}$ defined by $P_n := C_{-*}^{cell}(X_n)$ and whose partial compositions are

$$\circ_i : C_{-*}^{cell}(X_k) \otimes C_{-*}^{cell}(X_h) \xrightarrow{\sim} C_{-*}^{cell}(X_k \times X_h) \underset{C_{-*}^{cell}(\circ_i)}{\longrightarrow} C_{-*}^{cell}(X_{h+k-1}) \ .$$

Similarly, an operadic bimodule in `Poly` is sent to a dg operadic bimodule under the strong monoidal functor C_{-*}^{cell}.

2.2 The associahedra A_∞-structures were introduced for the first time in two seminal papers by Stasheff on homotopy associative H-spaces [39]. In the first paper of the series, he defined cell complexes $K_n \subset I^{n-2}$ called *associahedra*, which govern A_n-structures on topological spaces. The associahedra were later realized as polytopes by Haiman in [16], Lee in [21] or Loday in [23]. They were recently endowed with an operad structure in the category `Poly` by Masuda, Thomas, Tonks and Vallette in [29], using the notion of weighted Loday realizations.

Theorem 2.2.1 ([29]). *There exists realizations of the associahedra as polytopes, which can be endowed with a structure of operad in the category* `Poly` *and whose image under the functor* C_{-*}^{cell} *yields the operad* A_∞.

We refer to Section 4.3 in the appendix for a complete description of the associahedra of [29] as well as a proof that $A_\infty(n) = C_{-*}^{cell}(K_n)$. The fact that the Loday associahedra form an operad in `Poly` is moreover already proven in [29]. The first three associahedra K_2, K_3 and K_4 are represented in Figure 2.1, labeling their cells by the operations they define in A_∞ when seen in $C_{-*}^{cell}(K_n)$.

Remark 2.2.2. The assumptions in the definition of the morphisms of the category `Poly` was motivated in [29] by Theorem 2.2.1: they are the minimal assumptions to be required in order for the realizations K_n to carry the structure of an operad in `Poly`.

These polytopes are in fact constructed such that the boundary of K_n is exactly

$$\partial K_n = \bigcup_{\substack{i_1+i_2+i_3=n \\ 2\leqslant i_2 \leqslant n-1}} K_{i_1+1+i_3} \times K_{i_2} \ ,$$

and such that partial compositions are then simply polytopal inclusions of $K_k \times K_h$ in the boundary of K_{h+k-1}.

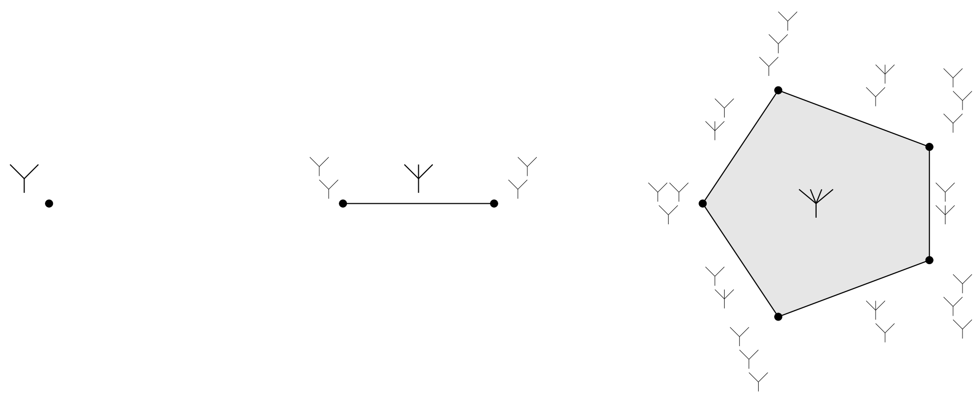

Figure 2.1: The associahedra K_2, K_3 and K_4

2.3 The multiplihedra Just like the operad A_∞, the dg operadic bimodule M_∞ is the image under the functor C_{-*}^{cell} of an operadic bimodule in `Poly`, called the *multiplihedra*. Iwase and Mimura realized the multiplihedra as cell complexes in [18] following the hints of Stasheff in [39]. The multiplihedra were later realized as polytopes in [12]. They were finally adapted by Laplante-Anfossi and the author in [20], by using again the notion of weighted Loday realizations in order to prove the following theorem:

Theorem 2.3.1 ([20]). *There exists realizations of the multiplihedra as polytopes, which can be endowed with an operadic bimodule structure over the associahedra of Theorem 2.2.1, i.e. with polytopal action-composition maps*

$$K_s \times J_{i_1} \times \cdots \times J_{i_s} \xrightarrow{\mu} J_{i_1+\cdots+i_s} \ , \qquad J_k \times K_h \xrightarrow[\circ_i]{} J_{h+k-1} \ ,$$

and whose image under the functor C_{-*}^{cell} yields the dg operadic bimodule M_∞.

We refer this time to Section 4.4 for a complete definition of the realizations J_n as well as a proof that $M_\infty(n) = C_{-*}^{cell}(J_n)$. We simply point out that these realizations have the following properties

(i) the boundary of J_n is exactly

$$\partial J_n = \bigcup_{\substack{i_1+i_2+i_3=n \\ i_2 \geqslant 2}} J_{i_1+1+i_3} \times K_{i_2} \cup \bigcup_{\substack{i_1+\cdots+i_s=n \\ s \geqslant 2}} K_s \times J_{i_1} \times \cdots \times J_{i_s} \ ,$$

(ii) action-compositions are polytopal inclusions of faces in the boundary of J_n.

The first three polytopes J_1, J_2 and J_3 are represented in Figure 2.2, labeling their cells by the operations they define in M_∞.

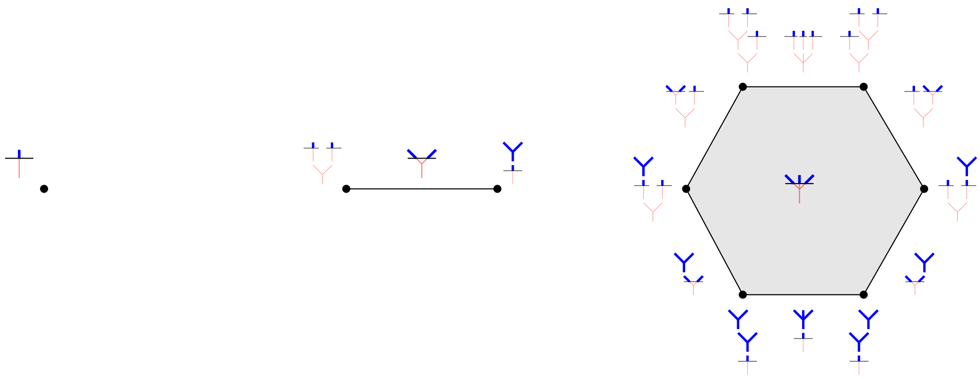

Figure 2.2: The multiplihedra J_1, J_2 and J_3

3. Moduli spaces of metric trees

3.1 The associahedra and metric ribbon trees

Sections 3.1.1 and 3.1.2 are inspired from [3, Section 7].

3.1.1 Stable metric ribbon trees

Definition 3.1.1. (i) A *(rooted) ribbon tree*, is the data of a tree together with a cyclic ordering on the edges at each vertex of the tree and a distinguished vertex adjacent to an external edge called the *root*. This external edge is then called the *outgoing edge*, while all the other external edges are called the *incoming edges*. For a ribbon tree t, we will write $E(t)$ for the set of its internal edges, $\overline{E}(t)$ for the set of all its edges, and $e(t)$ for its number of internal edges.

(ii) A *metric ribbon tree* is the data of a ribbon tree, together with a length $l_e \in]0, +\infty[$ for each of its internal edge e. The external edges are thought as having length equal to $+\infty$.

(iii) A ribbon tree is called *stable* if all its inner vertices are at least trivalent. It is called *binary* if all its inner vertices are trivalent. We denote SRT_n the set of all stable ribbon trees of arity n, and BRT_n the set of all binary ribbon trees. Note in particular that for a binary tree $t \in BRT_n$ we have that $e(t) = n - 2$.

The best way to understand this definition is with the examples depicted in Figure 3.1.

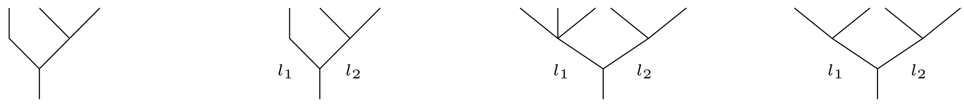

A ribbon tree | A metric ribbon tree | A stable metric ribbon tree | A binary metric ribbon tree

Figure 3.1

Definition 3.1.2. (i) A *broken ribbon tree* corresponds to the data of a ribbon tree together with a distinguished subset of internal edges which are labeled as *broken*.

(ii) A broken ribbon tree is said to be *stable* if its underlying ribbon tree is stable.

(iii) A *broken metric ribbon tree* corresponds to the data of a broken ribbon tree together with a length $l_e \in]0, +\infty[$ for each of its unbroken internal edge e. A broken internal edge e is moreover considered to have length $l_e = +\infty$.

The best way to understand this definition is again with the examples depicted in Figure 3.2.

A stable broken ribbon tree | A stable broken metric ribbon tree

Figure 3.2

3.1.2 Moduli spaces of stable metric ribbon trees

Definition 3.1.3. We define $\mathcal{T}_n$ to be *moduli space of stable metric ribbon trees* with n incoming edges. For each stable ribbon tree type t, we define moreover $\mathcal{T}_n(t) \subset \mathcal{T}_n$ to be the moduli space

$$\mathcal{T}_n(t) := \{\text{stable metric ribbon trees of type } t\} .$$

We then have that

$$\mathcal{T}_n = \bigcup_{t \in SRT_n} \mathcal{T}_n(t) .$$

Recalling that $e(t)$ denotes the number of internal edges for a ribbon tree of type t, each $\mathcal{T}_n(t)$ is naturally topologized as $]0, +\infty[^{e(t)}$, and they form a stratification of $\mathcal{T}_n$. This is illustrated in Figures 3.3 and 3.4. Interpreting a length in $]0, +\infty[^{e(t)}$ which goes towards 0 as the contraction of the corresponding edge of t, the strata $\mathcal{T}_n(t)$ can in fact be consistently glued together. With this observation, one can prove that the space $\mathcal{T}_n$ is in fact itself homeomorphic to $\mathbb{R}^{n-2}$.

Definition 3.1.4. We define $\overline{\mathcal{T}}_n$ to be the compactification of the moduli space $\mathcal{T}_n$, by allowing lengths of internal edges to go to $+\infty$.

The compactified moduli space $\overline{\mathcal{T}}_n$ can then be seen a $(n-2)$-dimensional CW-complex , where $\mathcal{T}_n$ is seen as its unique $(n-2)$-dimensional stratum and whose codimension 1 strata are given by

$$\bigcup_{\substack{i_1+i_2+i_3=n \\ 2\leqslant i_2 \leqslant n-1}} \mathcal{T}_{i_1+1+i_3} \times \mathcal{T}_{i_2} \ .$$

They correspond to metric trees with one broken edge. More generally, the codimension m strata are given by metric trees with m broken edges.

Definition 3.1.5. This cell decomposition of $\overline{\mathcal{T}}_n$ will be called its A_∞*-cell decomposition*. We will denote it as $(\overline{\mathcal{T}}_n)_{A_\infty}$

Theorem 3.1.6 ([6, Section 1.4], [24, Appendix C.2])**.** *The compactified moduli space* $(\overline{\mathcal{T}}_n)_{A_\infty}$ *is isomorphic as a CW-complex to the associahedron* K_n*.*

Theorem 3.1.6 is illustrated in Figure 3.4.

3.1.3 The ΩBAs -cell decomposition of $\overline{\mathcal{T}}_n$

The compactifications of the moduli spaces $\mathcal{T}_n$ of Definition 3.1.4 can in fact be obtained by first compactifying each stratum $\mathcal{T}_n(t)$ individually and then gluing consistently all compactifications together. For $t \in SRT_n$, the stratum $\mathcal{T}_n(t)$ is homeomorphic to $]0,+\infty[^{e(t)}$ and its compactification $\overline{\mathcal{T}}_n(t) \subset \overline{\mathcal{T}}_n$ is homeomorphic to $[0,+\infty]^{e(t)}$. A length equal to 0 simply corresponds to collapsing one edge of t and a length equal to $+\infty$ is interpreted as breaking this edge. This is illustrated in the instance of a cell of the moduli space $\mathcal{T}_4$ in Figure 3.3.

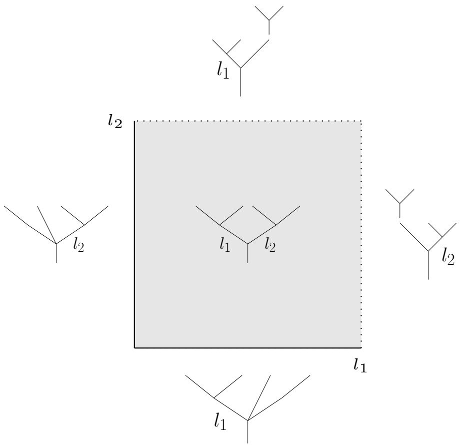

Figure 3.3: Compactification of a stratum of $\mathcal{T}_4$. The solide edges are inner strata of $\mathcal{T}_4$ labeled by stable ribbon trees, while the dotted edges are the outer strata obtained by allowing lengths to go to $+\infty$ and are labeled by broken stable ribbon trees.

The viewpoint introduced in the previous paragraph yields a new cell decomposition of $\overline{\mathcal{T}}_n$, two examples of which are given in Figure 3.4. Its strata are indexed by broken stable ribbon trees, a broken stable ribbon tree with i finite internal edges labeling an i-dimensional stratum.

Definition 3.1.7. The cell decomposition of $\overline{\mathcal{T}}_n$ by broken stable ribbon tree type will be called its ΩBAs*-cell decomposition*. We will denote it as $(\overline{\mathcal{T}}_n)_{\Omega BAs}$.

Strata of $(\overline{\mathcal{T}}_n)_{\Omega BAs}$ labeled by unbroken trees are then called *internal* i.e. are lying in the interior of $(\overline{\mathcal{T}}_n)_{A_\infty}$, while strata labeled by broken trees are called *external* i.e. lie in the boundary of $(\overline{\mathcal{T}}_n)_{A_\infty}$. It is moreover clear that the ΩBAs-cell decomposition on $\overline{\mathcal{T}}_n$ refines its A_∞-cell decomposition.

Proposition 3.1.8. *The compactified moduli spaces $(\overline{\mathcal{T}}_n)_{\Omega BAs}$ form an operad in* `CW`*.*

Proof. Endowing the $\overline{\mathcal{T}}_n$ with their ΩBAs-cell decomposition, it is clear that the obvious maps

$$(\overline{\mathcal{T}}_k)_{\Omega BAs} \times (\overline{\mathcal{T}}_h)_{\Omega BAs} \underset{\circ_i}{\longrightarrow} (\overline{\mathcal{T}}_{h+k-1})_{\Omega BAs}$$

are then cellular maps and satisfy the axioms of the partial compositions of an operad in `CW`. □

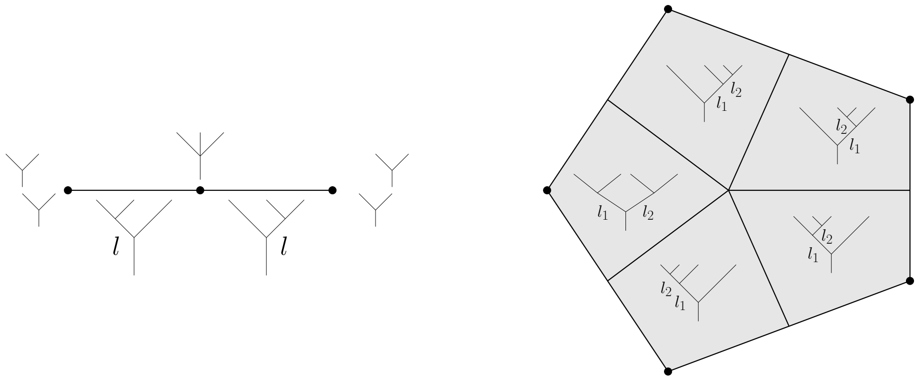

Figure 3.4: The compactified moduli spaces $(\overline{\mathcal{T}}_3)_{\Omega BAs}$ and $(\overline{\mathcal{T}}_4)_{\Omega BAs}$

3.1.4 The operad ΩBAs

Definition 3.1.9 (Definition 5.1.2)**.** The *operad* ΩBAs is the quasi-free operad generated by the set of stable ribbon trees, where a stable ribbon tree t has degree $|t| := -e(t)$. Its differential on a stable ribbon tree t is given by the signed sum of all stable ribbon trees obtained from t by breaking or collapsing exactly one of its internal edges.

We will denote this operad as

$\Omega BAs := \mathcal{F}($ 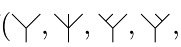 $, \cdots , SRT_n, \cdots)$,

and refer to Definition 5.1.2 for a complete description of this operad and its sign conventions.

Example 3.1.10. We have for instance that

$|$ 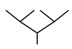 $| = -2$,

$\partial($ 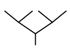 $) = \pm$ 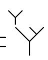 $\pm$ 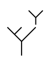 $\pm$  $\pm$  .

Proposition 3.1.11. *The functor C_{-*}^{cell} maps the operad $(\overline{\mathcal{T}}_n)_{\Omega BAs}$ to the operad ΩBAs.*

Proof. See Section 5.1.3. □

Remark 3.1.12. As explained in [24, Section 6.5], the dg operad ΩBAs is in fact the bar-cobar construction of the operad As encoding associative algebras.

3.1.5 From the operad A_∞ to the operad ΩBAs

The ΩBAs-cell decomposition on the compactified moduli spaces $\overline{\mathcal{T}}_n$ can in fact be described explicitly under the isomorphism of Theorem 3.1.6:

Lemma 3.1.13 ([24, Appendix C.2],[31, Section 2]). *The compactified moduli space $(\overline{\mathcal{T}}_n)_{\Omega BAs}$ is isomorphic as a CW complex to the associahedron K_n endowed with its dual subdivision.*

REMARK 3.1.14. The associahedron K_n is a simple polytope: its dual subdivision is thereby often referred to as its *cubical subdivision*. The open cubes forming this cubical subdivision are then exactly the strata of $(\overline{\mathcal{T}}_n)_{\Omega BAs}$.

This is illustrated in Figure 3.4. We will prove that Lemma 3.1.13 implies that the dg operads A_∞ and ΩBAs are related by an explicit morphism of operads:

Proposition 3.1.15 ([28]). *There exists a morphism of operads $A_\infty \to \Omega BAs$ given on the generating operations of A_∞ by*

$$m_n \longmapsto \sum_{t \in BRT_n} \pm m_t \ .$$

Proof. We compute the explicit signs in Section 5.1.4 and prove that this morphism between dg operads stems from the image under the functor C_{-*}^{cell} of the identity map $\mathrm{id} : (\overline{\mathcal{T}}_n)_{A_\infty} \to (\overline{\mathcal{T}}_n)_{\Omega BAs}$ refining the cell decomposition on $\overline{\mathcal{T}}_n$. The formula for m_n then simply corresponds to associating to the $(n-2)$-dimensional cell of $(\overline{\mathcal{T}}_n)_{A_\infty}$, the signed sum of all $n-2$-dimensional cells of $(\overline{\mathcal{T}}_n)_{\Omega BAs}$. □

This geometric construction of the morphism $A_\infty \to \Omega BAs$ is an adaptation of the algebraic construction by Markl and Shnider in [28]. Proposition 3.1.15 dates in fact back to [15], and is built in the theory of Koszul duality, as explained in [24, Sections 7 and 9]. It implies moreover in particular that in order to construct a structure of A_∞-algebra on a dg module, it is enough to endow it with a structure of ΩBAs-algebra.

3.2 The multiplihedra and 2-colored metric ribbon trees

3.2.1 2-colored metric ribbon trees

Definition 3.2.1. (i) *A 2-colored ribbon tree* is defined to be a ribbon tree together with a distinguished subset of inner vertices $E_{col}(T)$ called the *colored vertices*. This set is such that, either there is exactly one colored vertex in every non-self crossing path from an incoming edge to the root and none in the path from the outgoing edge to the root, or there is no colored vertex in any non-self crossing path from an incoming edge to the root and exactly one in the path from the outgoing edge to the root.

(ii) A *2-colored metric ribbon tree* is the data of a length for all internal edges $l_e \in]0, +\infty[$, such that the lengths of all non self-crossing paths from a colored vertex to the root are equal.

Definition 3.2.2. A *gauged metric ribbon tree* is defined to be a metric ribbon tree together with a length $\lambda \in \mathbb{R}$. This length is to be thought of as a *gauge* (a dividing line) drawn over the metric tree, at distance λ from its root, where the positive direction is pointing down.

We illustrate the following lemma in Figure 3.5.

Lemma 3.2.3. *The datum of a 2-colored metric ribbon tree is equivalent to the datum of a gauged metric ribbon tree.*

Proof. Given a 2-colored metric ribbon tree $T_c := (t_c, \{l_e\}_{e\in E(t_c)})$, denote L the length of any non-self crossing path from a colored vertex to the root. We form a metric ribbon tree T from T_c by forgetting the colored vertices as follows:

(i) If the colored vertex v is bivalent, we delete v and form a new edge connecting the two non-colored vertices adjacent to v. The length of this edge is set to be the sum of the lengths of the two edges adjacent to v. If v is adjacent to an external edge, this newly obtained edge has length $+\infty$, i.e. is an external edge.

(ii) If the colored vertex v is at least trivalent, we do not delete it and simply forget the fact that it is colored.

The gauged metric tree associated to T_c is then the metric tree T endowed with a gauge:

(i) At distance $\lambda := L$ from its root if the 2-colored tree t_c has a unique colored vertex which is bivalent and located below the root.

(ii) At distance $\lambda := -L$ from its root otherwise.

Conversely, consider a gauged metric ribbon tree (T, λ). We form a 2-colored ribbon tree t_c from the ribbon tree t, by defining the set of colored vertices to be the set of intersection points between the gauge and the tree t. This set is made of the vertices of t that are intersected by the gauge λ, as well as new bivalent colored vertices, corresponding to the intersection of the gauge with the edges of t. The lengths of the internal edges of the 2-colored tree t_c are then defined to be the unique lengths such that the method of the previous paragraph recovers exactly the metric gauged tree (T, λ). □

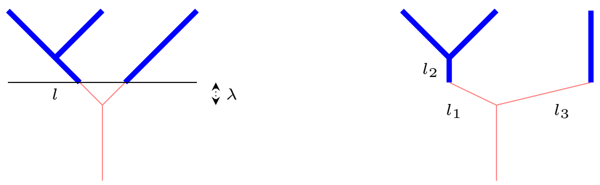

Figure 3.5: An example of a stable 2-colored metric ribbon tree with the two definitions: here $0 < -\lambda < l$, $l_1 = l_3 = -\lambda$ and $l = l_1 + l_2$

Following Lemma 3.2.3, a 2-colored ribbon tree can thereby equivalently be seen as a ribbon tree together with a gauge drawn over it, where the intersection points between the gauge and the tree are exactly the 2-colored vertices. The gauge divides the tree into two parts, each of which we think of as being colored in a different color (*colored vertices* should then be thought as being *2-colored*, as they mark the limit between the two colors).

Remark 3.2.4. The *gauge* of a 2-colored ribbon tree is called a *cut* in [20, Section 1.1.1].

Definition 3.2.5. (i) A 2-colored ribbon tree t_c is *stable* if all its inner non-colored vertices are at least trivalent and all its colored vertices are at least bivalent. We denote $SCRT_n$ the set of all stable 2-colored ribbon trees.

(ii) We also denote $CBRT_n$ to be the set of all *2-colored binary ribbon trees*, i.e. of 2-colored ribbon trees all of whose non-colored vertices are trivalent and all of whose colored vertices are bivalent.

For a stable 2-colored ribbon tree t_c, we will denote t the underlying stable ribbon tree obtained by forgetting the colored vertices as in the proof of Lemma 3.2.3.

EXAMPLE 3.2.6. The underlying stable ribbon tree of 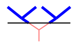 is 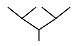 .

3.2.2 Moduli spaces of stable 2-colored metric ribbon trees

This section is inspired from [31, Section 7] (in which the two authors refer to stable 2-colored metric ribbon trees as *stable colored rooted metric ribbon trees*).

Definition 3.2.7. For $n \geqslant 2$, we define $\mathcal{CT}_n$ to be the *moduli space of stable 2-colored metric ribbon trees* of arity n. We also denote $\mathcal{CT}_1 := \{+\}$ the singleton space whose only element is the unique 2-colored ribbon tree of arity 1.

The space $\mathcal{CT}_n$ is homeomorphic to $\mathbb{R}^{n-1}$: the moduli space $\mathcal{T}_n$ is homeomorphic to $\mathbb{R}^{n-2}$ and using Lemma 3.2.3 we have that $\mathcal{CT}_n \simeq \mathbb{R} \times \mathcal{T}_n$, as the datum of a gauge on a stable metric ribbon tree adds a factor $\mathbb{R}$. Allowing internal edges of 2-colored metric trees to go to $+\infty$, the moduli space $\mathcal{CT}_n$ can be compactified into a $(n-1)$-dimensional CW-complex whose $n-1$ dimensional stratum is given by $\mathcal{CT}_n$.

Definition 3.2.8. We define $\overline{\mathcal{CT}}_n$ to be the compactication of the moduli space $\mathcal{CT}_n$ under the previous rule.

Two sequences of stable 2-colored metric ribbon trees converging in the compactification $\overline{\mathcal{CT}}_3$ are represented in Figure 3.6. The codimension 1 strata of the compactification $\overline{\mathcal{CT}}_n$ are moreover given by the union

$$\bigcup_{i_1+\cdots+i_s=n} \mathcal{T}_s \times \mathcal{CT}_{i_1} \times \cdots \times \mathcal{CT}_{i_s} \cup \bigcup_{i_1+i_2+i_3=n} \mathcal{CT}_{i_1+1+i_3} \times \mathcal{T}_{i_2} \ .$$

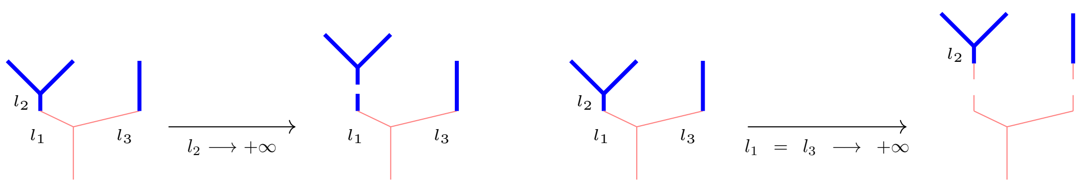

Figure 3.6: Two sequences of stable 2-colored metric ribbon trees converging in the compactification $\overline{\mathcal{CT}}_3$

Definition 3.2.9. This cell decomposition of $\overline{\mathcal{CT}}_n$ will be called its *A_∞-cell decomposition*. We will denote it as $(\overline{\mathcal{CT}}_n)_{A_\infty}$.

Theorem 3.2.10 ([31]). *The compactified moduli space $(\overline{\mathcal{CT}}_n)_{A_\infty}$ is isomorphic as a CW-complex to the multiplihedron J_n.*

Theorem 3.2.10 is illustrated in Figure 3.8.

3.2.3 Broken 2-colored ribbon trees

Definition 3.2.11. (i) A *broken 2-colored ribbon tree* corresponds to the data of a 2-colored ribbon tree together with a distinguished subset of internal edges which are labeled as *broken*. This subset is such that if the gauge of the 2-colored ribbon tree is above the root, either no internal edge below the gauge is broken or there is at least one internal edge below the gauge which is broken in each non-self crossing path from an incoming edge to the root.

(ii) A broken 2-colored ribbon tree is said to be *stable* if its underlying 2-colored ribbon tree is stable.

We will write $t_{br,c}$ for a broken 2-colored stable ribbon tree and t_c for an (unbroken) 2-colored stable ribbon tree.

Example 3.2.12. The following two broken 2-colored ribbon trees are stable: 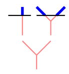 and 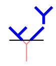 .

Definition 3.2.13. Let t_c be a stable 2-colored ribbon tree. We introduce four tree transformations:

(i) The gauge moves to cross exactly one additional vertex of the underlying stable ribbon tree t of t_c (gauge-vertex).

(ii) An internal edge located above the gauge or intersecting it breaks or, when the gauge is below the root, the outgoing edge breaks between the gauge and the root (above-break).

(iii) Edges (internal or incoming) that are possibly intersecting the gauge of t_c, break below it, such that there is exactly one edge breaking in each non-self crossing path from an incoming edge to the root (below-break).

(iv) An internal edge that does not intersect the gauge collapses (int-collapse).

Example 3.2.14. The broken 2-colored trees resulting from the transformations of Definition 3.2.13 for the stable 2-colored ribbon tree 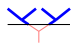 read as

(i) The gauge moves to cross exactly one vertex of 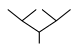 : 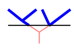 , 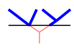 and 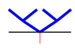 .

(ii) An internal edge breaks above the gauge: 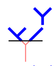 and 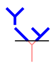 .

(iii) Both internal edges break below the gauge: 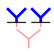 .

We point out that no internal edge can collapse in this example.

3.2.4 The moduli spaces $\mathcal{CT}_n(t_c)$

Definition 3.2.15. Given a stable 2-colored ribbon tree t_c of arity n, we define $\mathcal{CT}_n(t_c)$ to be the moduli space of stable 2-colored metric ribbon trees modeled on t_c.

We refer to Definition 5.2.5 for an explicit description of the moduli spaces $\mathcal{CT}_n(t_c)$ using the viewpoint of Lemma 3.2.3. We will prove in Section 5.2.2 that for a 2-colored stable ribbon tree t_c, writing again $e(t)$ for the number of internal edges of the underlying stable ribbon tree t, the stratum $\mathcal{CT}_n(t_c)$ is a polyhedral cone in $\mathbb{R}^{e(t)+1}$: denoting j the number of vertices v of t crossed by the gauge as depicted below

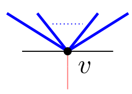

,

the polyhedral cone $\mathcal{CT}_n(t_c)$ has dimension $e(t) + 1 - j$.

Example 3.2.16. Applying Definition 5.2.5, we have for instance that

$\mathcal{CT}_4($ 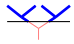 $) = \{(\lambda, l_1, l_2),\ 0 < -\lambda < l_1, l_2\} \subset \mathbb{R}\times]0, +\infty[^2$.

The moduli space $\mathcal{CT}_n$ then has a cell decomposition by stable 2-colored ribbon tree type,

$$\mathcal{CT}_n = \bigcup_{t_c \in SCRT_n} \mathcal{CT}_n(t_c) .$$

See also Remark 5.2.13.

3.2.5 The ΩBAs-cell decomposition of $\overline{\mathcal{CT}}_n$

The stratum $\mathcal{CT}_n(t_c)$ can be compactified by allowing lengths of internal edges to go towards 0 or $+\infty$, with combinatorics induced by the equalities defined by the colored vertices. The codimension 1 strata of its compactification are then labeled by the broken 2-colored trees obtained under the tree transformations of Definition 3.2.13 (see also Section 5.2.3). The compactification $\overline{\mathcal{CT}}_n$ is simply obtained by gluing these compactifications. This yields a new cell decomposition of $\overline{\mathcal{CT}}_n$, where each stratum is labeled by a broken 2-colored stable ribbon tree.

Definition 3.2.17. The cell decomposition of $\overline{\mathcal{CT}}_n$ by broken stable 2-colored ribbon tree type will be called its *ΩBAs-cell decomposition*. We will denote it as $(\overline{\mathcal{CT}}_n)_{\Omega BAs}$.

Again, strata of $(\overline{\mathcal{CT}}_n)_{\Omega BAs}$ labeled by unbroken 2-colored trees are called *internal*, while strata labeled by broken 2-colored trees are called *external*. The cell decompositions for $(\overline{\mathcal{CT}}_2)_{\Omega BAs}$ and $(\overline{\mathcal{CT}}_3)_{\Omega BAs}$ are represented in Figure 3.8. The compactification of

$\mathcal{CT}_3($  $) = \{(\lambda, l) \text{ such that } l > 0\ ;\ -\lambda > l\}$

is moreover illustrated in Figure 3.7. The solide edges are inner strata of $\mathcal{CT}_3$ labeled by stable 2-colored trees, while the dotted edges are outer strata obtained by allowing lengths to go to $+\infty$ and are labeled by broken stable 2-colored trees.

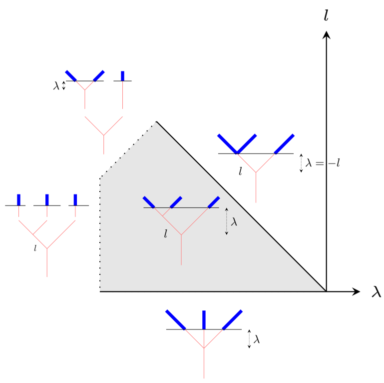

Figure 3.7: Compactification of a stratum of $\mathcal{CT}_3$

Proposition 3.2.18. *The compactified moduli spaces $(\overline{\mathcal{CT}}_n)_{\Omega BAs}$ form an operadic bimodule over the operad $(\overline{\mathcal{T}}_n)_{\Omega BAs}$ in* `CW`.

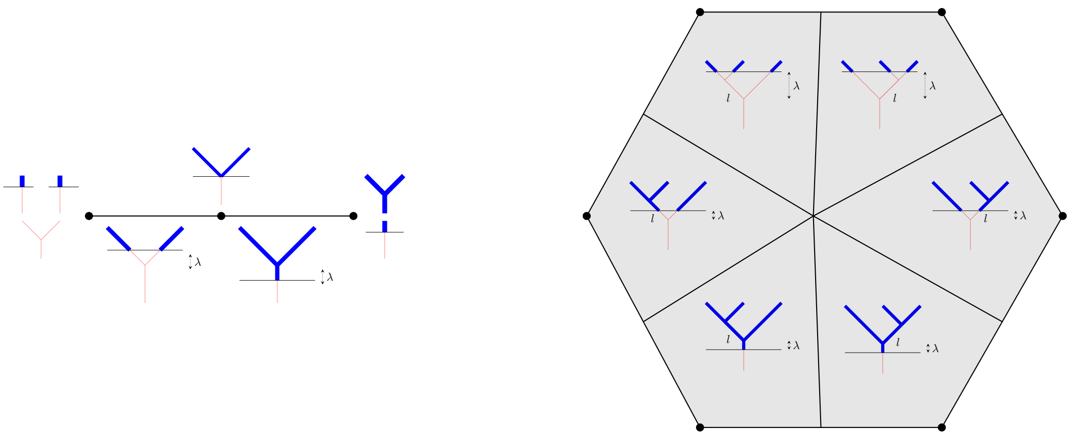

Figure 3.8: The compactified moduli spaces $\overline{\mathcal{CT}}_2$ and $\overline{\mathcal{CT}}_3$ with their cell decomposition by broken stable 2-colored ribbon tree type

Proof. Endowing the compactified moduli spaces $\overline{\mathcal{T}}_n$ and $\overline{\mathcal{CT}}_n$ with their ΩBAs-cell decomposition, it is again straightforward that the obvious maps

$$\overline{\mathcal{T}}_s \times \overline{\mathcal{CT}}_{i_1} \times \cdots \times \overline{\mathcal{CT}}_{i_s} \longrightarrow \overline{\mathcal{CT}}_{i_1+\cdots+i_s} \ ,$$
$$\overline{\mathcal{CT}}_k \times \overline{\mathcal{T}}_h \underset{\circ_i}{\longrightarrow} \overline{\mathcal{CT}}_{h+k-1} \ ,$$

are cellular and satisfy the axioms of Item (ii) in Definition 1.3.2 for the action-composition maps of an operadic bimodule structure on $\overline{\mathcal{CT}}_n$. □

3.2.6 The operadic bimodule $M_{\Omega BAs}$

Definition 3.2.19. We define $M_{\Omega BAs}$ to be the $(\Omega BAs, \Omega BAs)$-operadic bimodule obtained by applying the functor C_{-*}^{cell} to the operadic bimodule $(\overline{\mathcal{CT}}_n)_{\Omega BAs}$.

We point out that we used Proposition 3.1.11 to define the operadic bimodule $M_{\Omega BAs}$.

Proposition 3.2.20. *The operadic bimodule $M_{\Omega BAs}$ is the quasi-free $(\Omega BAs, \Omega BAs)$-operadic bimodule generated by the set of stable 2-colored ribbon trees. A 2-colored stable ribbon tree t_c with $e(t)$ internal edges and whose gauge crosses j vertices has degree $|t_c| := j - e(t) - 1$. The differential of a stable 2-colored ribbon tree t_c is given by the signed sum of all stable 2-colored ribbon trees obtained from t_c under the four tree transformations of Definition 3.2.13.*

Proof. The description of $M_{\Omega BAs}$ as the quasi-free operadic bimodule generated by the set of stable 2-colored ribbon trees is straightforward from Section 3.2.5. We refer to Lemmas 5.3.1 and 5.3.3 for a complete proof of this proposition and explicit sign computations. □

In other words, we defined the quasi-free $(\Omega BAs, \Omega BAs)$-operadic bimodule

$$M_{\Omega BAs} := \mathcal{F}^{\Omega BAs, \Omega BAs}(\ \ , \ \ , \ \ , \ \ , \cdots , SCRT_n, \cdots) \ .$$

We point out that the symbol used here is the same as the one used for the only arity 2 generating operation of M_∞. It will however be clear from the context what stands for in the rest of this paper.

Example 3.2.21. We compute for instance that

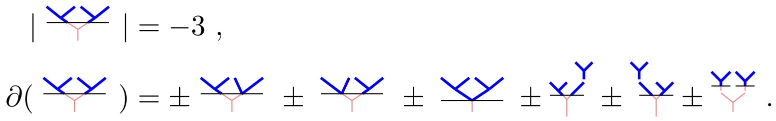

Remark 3.2.22. We expect in fact that the operadic bimodule $M_{\Omega BAs}$ should appear as a bar-cobar construction of the (As, As)-operadic bimodule M_{As} encoding morphisms of associative algebras. See for instance [9] for notions of bar and cobar constructions of operadic bimodules.

3.2.7 From the operadic bimodule M_∞ to the operadic bimodule $M_{\Omega BAs}$

Lemma 3.2.23 ([12, Section 5],[31, Section 7]). *The compactified moduli space $(\overline{\mathcal{CT}}_n)_{\Omega BAs}$ is isomorphic as a CW complex to the multiplihedron endowed with its dual subdivision.*

Lemma 3.2.23 is illustrated in Figure 3.8.

Remark 3.2.24. The multiplihedron J_n is not a simple polytope in general: see for instance J_4 in Figure 4.2, which has four edges connecting at a vertex. We can thereby not speak about a cubical subdivision of the multiplihedron, unlike in Remark 3.1.14.

We now point out that the morphism of operads $A_\infty \to \Omega BAs$ makes the $(\Omega BAs, \Omega BAs)$-operadic bimodule $M_{\Omega BAs}$ into an (A_∞, A_∞)-operadic bimodule. Lemma 3.2.23 then implies the following result:

Proposition 3.2.25. *There exists a morphism of (A_∞, A_∞)-operadic bimodules $M_\infty \to M_{\Omega BAs}$ given on the generating operations of M_∞ by*

$$f_n \longmapsto \sum_{t_c \in CBRT_n} \pm f_{t_c} \ .$$

Proof. We refer to Section 5.3.3 for a complete proof as well as the explicit signs. As for Proposition 3.1.15, this morphism will stem from the image under the functor C_{-*}^{cell} of the identity $\mathrm{id} : (\overline{\mathcal{CT}}_n)_{A_\infty} \to (\overline{\mathcal{CT}}_n)_{\Omega BAs}$ refining the cell decomposition on $\overline{\mathcal{CT}}_n$. □

As a result, in order to construct an A_∞-morphism between two A_∞-algebras whose A_∞-algebra structure comes from an ΩBAs-algebra structure, it is enough to construct an ΩBAs-morphism between them.

3.2.8 The 2-colored operad ΩBAs^2

As explained in Section 1.6, it follows from [26] that since the 2-colored operad A_∞^2 is a fibrant-cofibrant replacement of As^2 in the model category of 2-colored dg operads, the category of A_∞-algebras with A_∞-morphisms between them yields a nice homotopic framework to study the notion of homotopy associative dg algebras. In fact, most classical theorems for A_∞-algebras can be proven using the machinery of model categories on the model category of 2-colored dg operads. We can thus similarly introduce the 2-colored operad ΩBAs^2, which is again a fibrant-cofibrant replacement of As^2 in the model category of 2-colored operads. The notions of ΩBAs-algebras with ΩBAs-morphisms between them then yield another satisfactory homotopic framework to study homotopy associative dg algebras, in which most classical theorems for A_∞-algebras still hold. We point out however that we did not define a *category* of ΩBAs-algebras, as we did not define a way to compose ΩBAs-morphisms. See [33, Section III.1.1.1] for a discussion of that matter.

4. Signs and polytopes for A_∞-algebras and A_∞-morphisms

The goal of this section is twofold: work out all the signs written as $\pm$ in the A_∞-equations in Section 1 and complete the proofs of Theorems 2.2.1 and 2.3.1 by proving that the Loday realizations of the associahedra of [29] and the Forcey–Loday realizations of the multiplihedra of [20] determine indeed our sign conventions for A_∞-algebras and A_∞-morphisms.

4.1 Basic conventions for signs and orientations

4.1.1 Koszul sign rule

All the formulae in this section will be written using the Koszul sign rule that we briefly recall. We will work exclusively with cohomological conventions.

Given A and B two dg modules, the differential on $A \otimes B$ is defined as

$$\partial_{A\otimes B}(a \otimes b) = \partial_A a \otimes b + (-1)^{|a|} a \otimes \partial_B b \ .$$

Given A and B two dg modules, we consider the graded module $\mathrm{Hom}(A, B)$ whose degree r component is given by all maps $A \to B$ of degree r. We endow it with the differential

$$\partial_{\mathrm{Hom}(A,B)}(f) := \partial_B \circ f - (-1)^{|f|} f \circ \partial_A =: [\partial, f] \ .$$

Given $f : A \to A'$ and $g : B \to B'$ two graded maps between dg modules, we set

$$(f \otimes g)(a \otimes b) = (-1)^{|g||a|} f(a) \otimes g(b) \ .$$

Finally, given $f : A \to A'$, $f' : A' \to A''$, $g : B \to B'$ and $g' : B' \to B''$, we define

$$(f' \otimes g') \circ (f \otimes g) = (-1)^{|g'||f|} (f' \circ f) \otimes (g' \circ g) \ .$$

We check in particular that with this sign rule, the differential on a tensor product $A_1 \otimes \cdots \otimes A_n$ is given by

$$\partial_{A_1 \otimes \cdots \otimes A_n} = \sum_{i=1}^{n} \mathrm{id}_{A_1} \otimes \cdots \otimes \partial_{A_i} \otimes \cdots \otimes \mathrm{id}_{A_n} \ .$$

4.1.2 Orientation of the boundary of a manifold with boundary

Let $(M, \partial M)$ be an oriented n-manifold with boundary. We choose to orient its boundary ∂M as follows: given $x \in \partial M$, a basis $e_1, \ldots, e_{n-1}$ of $T_x(\partial M)$, and an outward pointing vector $\nu \in T_x M$, the basis $e_1, \ldots, e_{n-1}$ is positively oriented if and only if the basis $\nu, e_1, \ldots, e_{n-1}$ is a positively oriented basis of $T_x M$. Note that in the particular case when the manifold with boundary is a half-space inside the Euclidean space $\mathbb{R}^n$, defined by an inequality

$$\sum_{i=1}^{n} a_i x_i \leqslant C \ ,$$

the vector $(a_1, \ldots, a_n)$ is outward-pointing.

Example 4.1.1. We recover for instance the classical singular differential under this convention. Take X a topological space. Given a singular simplex $\sigma : \Delta^n \to X$, its differential is classically defined as

$$\partial_{sing}(\sigma) := \sum_{i=0}^{n} (-1)^i \sigma_i \ ,$$

where σ_i stands for the restriction $[0 < \cdots < \hat{i} < \cdots < n] \hookrightarrow \Delta^n \to X$. Realizing Δ^n as a polytope in $\mathbb{R}^n$ and orienting it with the canonical orientation of $\mathbb{R}^n$, we check that its boundary reads exactly as

$$\partial \Delta^n = \bigcup_{i=0}^{n} (-1)^i \Delta_i^{n-1} \ ,$$

where Δ_i^{n-1} is the $(n-1)$-simplex corresponding to the face $[0 < \cdots < \hat{i} < \cdots < n]$. The sign $(-1)^i$ means that the orientation of Δ_i^{n-1} induced by its canonical identification with Δ^{n-1} and its orientation as the boundary of Δ^n, differ by a $(-1)^i$ sign.

4.1.3 Coorientations

Our convention for orienting the boundary of an oriented manifold with boundary $(M, \partial M)$ can in fact be rephrased as follows: *the boundary ∂M is cooriented by the outward pointing vector field ν.* More generally consider an oriented manifold N and a submanifold $S \subset N$.

Definition 4.1.2. A *coorientation* of S is defined to be an orientation of the normal bundle to S.

Given any complement bundle ν_S to TS in $TN|_S$,

$$TN|_S = \nu_S \oplus TS \ ,$$

this orientation induces in turn an orientation on ν_S, the normal bundle being canonically isomorphic to ν_S. The manifold S is then orientable if and only if it is coorientable. This can be proven using the first Stiefel-Whitney class for instance.

Definition 4.1.3. Given a coorientation for S, *the induced orientation on S* is set to be the one whose concatenation with that of ν_S, in the order (ν_S, TS), gives the orientation on $TN|_S$.

4.2 Signs for A_∞-algebras and A_∞-morphisms using the bar construction There exist various conventions on signs for A_∞-algebras and A_∞-morphisms between them, which can seem inexplicable when met out of context. The goal of this section is to give a comprehensive account of the two sign conventions coming from the bar construction, and to state our choice of signs for the rest of the paper (Section 4.2.4).

4.2.1 A_∞-algebras

We will first be interested in the following two sign conventions for A_∞-algebras:

$$[m_1, m_n] = - \sum_{\substack{i_1+i_2+i_3=n \\ 2 \leqslant i_2 \leqslant n-1}} (-1)^{i_1 i_2 + i_3} m_{i_1+1+i_3} (\mathrm{id}^{\otimes i_1} \otimes m_{i_2} \otimes \mathrm{id}^{\otimes i_3}) \ , \tag{A}$$

$$[m_1, m_n] = - \sum_{\substack{i_1+i_2+i_3=n \\ 2 \leqslant i_2 \leqslant n-1}} (-1)^{i_1 + i_2 i_3} m_{i_1+1+i_3} (\mathrm{id}^{\otimes i_1} \otimes m_{i_2} \otimes \mathrm{id}^{\otimes i_3}) \ , \tag{B}$$

which can be rewritten as

$$\sum_{i_1+i_2+i_3=n} (-1)^{i_1 i_2 + i_3} m_{i_1+1+i_3} (\mathrm{id}^{\otimes i_1} \otimes m_{i_2} \otimes \mathrm{id}^{\otimes i_3}) = 0 \ , \tag{A}$$

$$\sum_{i_1+i_2+i_3=n} (-1)^{i_1 + i_2 i_3} m_{i_1+1+i_3} (\mathrm{id}^{\otimes i_1} \otimes m_{i_2} \otimes \mathrm{id}^{\otimes i_3}) = 0 \ . \tag{B}$$

Remark 4.2.1. Conventions (A) are for instance used in [39], while conventions (B) are used in [22].

First, note that these two sign conventions are equivalent in the following sense: given a sequence of operations $m_n : A^{\otimes n} \to A$ satisfying equations (A), we check that the operations $m'_n := (-1)^{\binom{n}{2}} m_n$ satisfy equations (B). This sign change does not come out of the blue, and appears in the following proof that these equations come from the bar construction. We introduce the suspension and desuspension maps

$$\begin{aligned} s : A &\longrightarrow sA & \qquad w : sA &\to A \\ a &\longmapsto sa & sa &\longmapsto a \ , \end{aligned}$$

which are respectively of degree -1 and $+1$. We check that with the Koszul sign rule,

$$w^{\otimes n} \circ s^{\otimes n} = (-1)^{\binom{n}{2}} \mathrm{id}_{A^{\otimes n}} \ .$$

We note that a degree $2-n$ map $m_n : A^{\otimes n} \to A$ yields a degree $+1$ map $b_n := s m_n w^{\otimes n} : (sA)^{\otimes n} \to sA$. Consider now a collection of degree $2-n$ maps $m_n : A^{\otimes n} \to A$, and the associated degree $+1$ maps $b_n : (sA)^{\otimes n} \to sA$. Denoting D the unique coderivation on $\overline{T}(sA)$ associated to the b_n, the equation $D^2 = 0$ is then equivalent to the equations

$$\sum_{i_1+i_2+i_3=n} b_{i_1+1+i_3}(\mathrm{id}^{\otimes i_1} \otimes b_{i_2} \otimes \mathrm{id}^{\otimes i_3}) = 0 \ .$$

There are now two ways to unravel the signs from these equations.

The first way consists in simply replacing the b_i by their definition. It leads to the (A) sign conventions:

$$\begin{aligned} &\sum_{i_1+i_2+i_3=n} b_{i_1+1+i_3}(\mathrm{id}^{\otimes i_1} \otimes b_{i_2} \otimes \mathrm{id}^{\otimes i_3}) \\ =&\sum_{i_1+i_2+i_3=n} s m_{i_1+1+i_3}(w^{\otimes i_1} \otimes w \otimes w^{\otimes i_3})(\mathrm{id}^{\otimes i_1} \otimes s m_{i_2} w^{\otimes i_2} \otimes \mathrm{id}^{\otimes i_3}) \\ =&\sum_{i_1+i_2+i_3=n} (-1)^{i_3} s m_{i_1+1+i_3}(w^{\otimes i_1} \otimes m_{i_2} w^{\otimes i_2} \otimes w^{\otimes i_3}) \\ =&\sum_{i_1+i_2+i_3=n} (-1)^{i_3+i_1 i_2} s m_{i_1+1+i_3}(\mathrm{id}^{\otimes i_1} \otimes m_{i_2} \otimes \mathrm{id}^{\otimes i_3})(w^{\otimes i_1} \otimes w^{\otimes i_2} \otimes w^{\otimes i_3}) \\ =&s\left(\sum_{i_1+i_2+i_3=n} (-1)^{i_1 i_2+i_3} m_{i_1+1+i_3}(\mathrm{id}^{\otimes i_1} \otimes m_{i_2} \otimes \mathrm{id}^{\otimes i_3})\right) w^{\otimes n} \ . \end{aligned}$$

The second way consists in first composing and post-composing by w and $s^{\otimes n}$ and then replacing the b_i by their definition. It leads to the (B) sign conventions and makes the $(-1)^{\binom{n}{2}}$ sign change appear:

$$\begin{aligned}
&\sum_{i_1+i_2+i_3=n} wb_{i_1+1+i_3}(\mathrm{id}^{\otimes i_1}\otimes b_{i_2}\otimes \mathrm{id}^{\otimes i_3})s^{\otimes n}\\
=&\sum_{i_1+i_2+i_3=n} wb_{i_1+1+i_3}(\mathrm{id}^{\otimes i_1}\otimes b_{i_2}\otimes \mathrm{id}^{\otimes i_3})(s^{\otimes i_1}\otimes s^{\otimes i_2}\otimes s^{\otimes i_3})\\
=&\sum_{i_1+i_2+i_3=n} (-1)^{i_1} wb_{i_1+1+i_3}(s^{\otimes i_1}\otimes b_{i_2}s^{\otimes i_2}\otimes s^{\otimes i_3})\\
=&\sum_{i_1+i_2+i_3=n} (-1)^{i_1} wsm_{i_1+1+i_3}w^{\otimes i_1+1+i_3}(s^{\otimes i_1}\otimes sm_{i_2}w^{\otimes i_2}s^{\otimes i_2}\otimes s^{\otimes i_3})\\
=&\sum_{i_1+i_2+i_3=n} (-1)^{i_1} m_{i_1+1+i_3}w^{\otimes i_1+1+i_3}(s^{\otimes i_1}\otimes (-1)^{\binom{i_2}{2}}sm_{i_2}\otimes s^{\otimes i_3})\\
=&\sum_{i_1+i_2+i_3=n} (-1)^{i_1+i_2i_3} m_{i_1+1+i_3}w^{\otimes i_1+1+i_3}s^{\otimes i_1+1+i_3}(\mathrm{id}^{\otimes i_1}\otimes (-1)^{\binom{i_2}{2}}m_{i_2}\otimes \mathrm{id}^{\otimes i_3})\\
=&\sum_{i_1+i_2+i_3=n} (-1)^{i_1+i_2i_3}(-1)^{\binom{i_1+1+i_3}{2}} m_{i_1+1+i_3}(\mathrm{id}^{\otimes i_1}\otimes (-1)^{\binom{i_2}{2}}m_{i_2}\otimes \mathrm{id}^{\otimes i_3})\ .
\end{aligned}$$

4.2.2 A_∞-morphisms

We now delve into the two sign conventions for A_∞-morphisms that are coming with the bar construction viewpoint. They are as follows:

$$\begin{aligned}
[m_1,f_n] =& \sum_{\substack{i_1+i_2+i_3=n\\ i_2\geqslant 2}} (-1)^{i_1i_2+i_3} f_{i_1+1+i_3}(\mathrm{id}^{\otimes i_1}\otimes m_{i_2}\otimes \mathrm{id}^{\otimes i_3}) && \text{(A)}\\
&- \sum_{\substack{i_1+\cdots+i_s=n\\ s\geqslant 2}} (-1)^{\epsilon_A} m_s(f_{i_1}\otimes\cdots\otimes f_{i_s})\ ,\\
[m_1,f_n] =& \sum_{\substack{i_1+i_2+i_3=n\\ i_2\geqslant 2}} (-1)^{i_1+i_2i_3} f_{i_1+1+i_3}(\mathrm{id}^{\otimes i_1}\otimes m_{i_2}\otimes \mathrm{id}^{\otimes i_3}) && \text{(B)}\\
&- \sum_{\substack{i_1+\cdots+i_s=n\\ s\geqslant 2}} (-1)^{\epsilon_B} m_s(f_{i_1}\otimes\cdots\otimes f_{i_s})\ ,
\end{aligned}$$

which can we rewritten as

$$\sum_{i_1+i_2+i_3=n} (-1)^{i_1i_2+i_3} f_{i_1+1+i_3}(\mathrm{id}^{\otimes i_1}\otimes m_{i_2}\otimes \mathrm{id}^{\otimes i_3}) = \sum_{i_1+\cdots+i_s=n} (-1)^{\epsilon_A} m_s(f_{i_1}\otimes\cdots\otimes f_{i_s})\ , \quad \text{(A)}$$

$$\sum_{i_1+i_2+i_3=n} (-1)^{i_1+i_2i_3} f_{i_1+1+i_3}(\mathrm{id}^{\otimes i_1}\otimes m_{i_2}\otimes \mathrm{id}^{\otimes i_3}) = \sum_{i_1+\cdots+i_s=n} (-1)^{\epsilon_B} m_s(f_{i_1}\otimes\cdots\otimes f_{i_s})\ , \quad \text{(B)}$$

where

$$\epsilon_A = \sum_{u=1}^{s} i_u\left(\sum_{u<t\leqslant s}(1-i_t)\right)\ , \qquad \epsilon_B = \sum_{u=1}^{s}(s-u)(1-i_u)\ .$$

These two sign conventions are again equivalent: given a sequence of operations m_n and f_n satisfying equations (A), we check that the operations $m'_n := (-1)^{\binom{n}{2}}m_n$ and $f'_n := (-1)^{\binom{n}{2}}f_n$ satisfy equations (B). The $(-1)^{\binom{n}{2}}$ twist comes again from the formula $w^{\otimes n}\circ s^{\otimes n} = (-1)^{\binom{n}{2}}\mathrm{id}_{A^{\otimes n}}$.

Consider now two dg modules A and B, together with a collection of degree $2-n$ maps $m_n : A^{\otimes n}\to A$ and $m_n : B^{\otimes n}\to B$ (we use the same notation for sake of readability), and a collection of degree $1-n$ maps $f_n : A^{\otimes n} \to B$. We associate again to the m_n the degree $+1$ maps b_n, and also associate to the f_n the degree 0 maps $F_n := sf_n w^{\otimes n} : (sA)^{\otimes n} \to sB$. We denote D_A and D_B the unique coderivations acting respectively on $\overline{T}(sA)$ and $\overline{T}(sB)$, and $F : \overline{T}(sA) \to \overline{T}(sB)$ the unique coalgebra morphism associated to the F_n. The equation $FD_A = D_B F$ is then equivalent to the equations

$$\sum_{i_1+i_2+i_3=n} F_{i_1+1+i_3}(\mathrm{id}^{\otimes i_1} \otimes b_{i_2} \otimes \mathrm{id}^{\otimes i_3}) = \sum_{i_1+\cdots+i_s=n} b_s(F_{i_1} \otimes \cdots \otimes F_{i_s}) \ .$$

There are again two ways to unravel the signs from these equations, which will lead to conventions (A) and (B). The proofs proceed exactly as in Section 4.2.1.

4.2.3 Composition of A_∞-morphisms

Let $f_n : A^{\otimes n} \to B$ and $g_n : B^{\otimes n} \to C$ be two A_∞-morphisms under conventions (A). The arity n component of their composition $g \circ f$ is defined as

$$\sum_{i_1+\cdots+i_s=n} (-1)^{\epsilon_A} g_s(f_{i_1} \otimes \cdots \otimes f_{i_s}) \ , \tag{A}$$

where ϵ_A is as previously.

Let $f_n : A^{\otimes n} \to B$ and $g_n : B^{\otimes n} \to C$ be two A_∞-morphisms under conventions (B). The arity n component of their composition $g \circ f$ is this time defined as

$$\sum_{i_1+\cdots+i_s=n} (-1)^{\epsilon_B} g_s(f_{i_1} \otimes \cdots \otimes f_{i_s}) \ , \tag{B}$$

where ϵ_B is as previously.

We check that in each case, this newly defined morphism satisfies the A_∞-equations, respectively under the sign conventions (A) and (B). This can again be proven using the bar construction and applying the previous transformations.

4.2.4 Choice of convention in this paper

We will work in the rest of this paper under the set of conventions (B). This choice of conventions will be accounted for in Sections 4.3 and 4.4: the signs are the ones which arise naturally from the realizations of the associahedra and the multiplihedra à la Loday. The operations m_n of an A_∞-algebra will satisfy equations

$$[m_1, m_n] = -\sum_{\substack{i_1+i_2+i_3=n \\ 2 \leqslant i_2 \leqslant n-1}} (-1)^{i_1+i_2 i_3} m_{i_1+1+i_3}(\mathrm{id}^{\otimes i_1} \otimes m_{i_2} \otimes \mathrm{id}^{\otimes i_3}) \ ,$$

an A_∞-morphism between two A_∞-algebras will satisfy equations

$$[m_1, f_n] = \sum_{\substack{i_1+i_2+i_3=n \\ i_2 \geqslant 2}} (-1)^{i_1+i_2 i_3} f_{i_1+1+i_3}(\mathrm{id}^{\otimes i_1} \otimes m_{i_2} \otimes \mathrm{id}^{\otimes i_3}) - \sum_{\substack{i_1+\cdots+i_s=n \\ s \geqslant 2}} (-1)^{\epsilon_B} m_s(f_{i_1} \otimes \cdots \otimes f_{i_s}) \ ,$$

and two A_∞-morphisms will be composed as

$$\sum_{i_1+\cdots+i_s=n} (-1)^{\epsilon_B} g_s(f_{i_1} \otimes \cdots \otimes f_{i_s}) \ ,$$

where $\epsilon_B = \sum_{u=1}^{s} (s-u)(1-i_u)$.

4.3 Loday associahedra and signs We recall now the definition of the weighted Loday realizations of the associahedra in [29], and use them to prove the second part of Theorem 2.2.1.

Definition 4.3.1 ([29])**.** Given $n \geqslant 1$, define a weight ω to be a list of n positive integers $(\omega_1, \ldots, \omega_n)$. The *Loday realization of weight* ω of K_n is defined to be the intersection in $\mathbb{R}^{n-1}$ of the hyperplane of equation

$$H_\omega : \sum_{i=1}^{n-1} x_i = \sum_{1 \leqslant k < l \leqslant n} \omega_k \omega_l$$

and of the half-spaces of equation

$$D_{i_1,i_2,i_3} : x_{i_1+1} + \cdots + x_{i_1+i_2-1} \geqslant \sum_{i_1+1 \leqslant k < l \leqslant i_1+i_2} \omega_k \omega_l \ ,$$

for all $i_1 + i_2 + i_3 = n$ and $2 \leqslant i_2 \leqslant n-1$. This polytope is denoted K_ω.

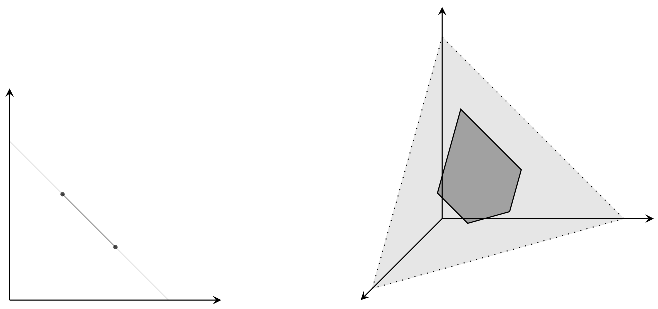

Figure 4.1: The Loday realizations K_3 and K_4: the lighter grey depicts H_ω, while the darker grey stands for K_ω.

For the weight $\mathbf{1}_n$ of length n whose entries are all equal to 1, we will denote $K_n := K_{\mathbf{1}_n}$. The Loday realizations K_3 and K_4 are represented in Figure 4.1. Our goal is now to prove the second part of Theorem 2.2.1:

Theorem 2.2.1. *The Loday associahedra K_n form an operad in* `Poly` *whose image under the functor C_{-*}^{cell} is the operad A_∞.*

Proof. We have to prove that after choosing an orientation for each polytope K_n, their boundary reads as

$$\partial K_n = - \bigcup_{\substack{i_1+i_2+i_3=n \\ 2 \leqslant i_2 \leqslant n-1}} (-1)^{i_1+i_2 i_3} K_{i_1+1+i_3} \times K_{i_2} \ ,$$

where $K_{i_1+1+i_3} \times K_{i_2}$ is sent to $m_{i_1+1+i_3}(\mathrm{id}^{\otimes i_1} \otimes m_{i_2} \otimes \mathrm{id}^{\otimes i_3})$ under the functor C_{-*}^{cell}. The signs mean that after comparing the product orientation on $K_{i_1+1+i_3} \times K_{i_2}$ induced by the orientations of $K_{i_1+1+i_3}$ and K_{i_2}, to the orientation of the boundary of K_n, they differ by the sign $-(-1)^{i_1+i_2 i_3}$.

Step 1 We begin by explaining how to obtain the set-theoretic decomposition of the boundary

$$\partial K_n = \bigcup_{\substack{i_1+i_2+i_3=n \\ 2 \leqslant i_2 \leqslant n-1}} K_{i_1+1+i_3} \times K_{i_2} \ .$$

The top dimensional strata in the boundary of some K_ω are obtained by allowing exactly one of the inequalities

$$x_{i_1+1} + \cdots + x_{i_1+i_2-1} \geqslant \sum_{i_1+1\leqslant k<l\leqslant i_1+i_2} \omega_k\omega_l \ ,$$

to become an equality. We write H_{i_1,i_2,i_3} for these hyperplanes. Defining two new weights

$$\overline{\omega} := (\omega_1, \dots, \omega_{i_1}, \omega_{i_1+1} + \cdots + \omega_{i_1+i_2}, \omega_{i_1+i_2+1}, \dots, \omega_n) \ ,$$
$$\widetilde{\omega} := (\omega_{i_1+1}, \dots, \omega_{i_1+i_2}) \ ,$$

the map

$$\theta : \mathbb{R}^{i_1+i_3} \times \mathbb{R}^{i_2-1} \longrightarrow \mathbb{R}^{n-1}$$
$$(x_1, \dots, x_{i_1+i_3}) \times (y_1, \dots, y_{i_2-1}) \longmapsto (x_1, \dots, x_{i_1}, y_1, \dots, y_{i_2-1}, x_{i_1+1}, \dots, x_{i_1+i_3})$$

induces a bijection between $K_{\overline{\omega}} \times K_{\widetilde{\omega}}$ and the codimension 1 face of K_ω corresponding to the intersection with H_{i_1,i_2,i_3}.

Step 2 The directing hyperplane $\overline{H}_\omega$ of the affine hyperplane H_ω has basis

$$e_j^\omega = (1, 0, \cdots, 0, -1_{j+1}, 0, \cdots, 0) \ ,$$

where -1 is in the $j+1$-th spot, and we add a superscript ω for later use. We choose this basis as a positively oriented basis for $\overline{H}_\omega$: this defines our orientation of K_ω. Choosing any $(a_1, \dots, a_{n-1}) \in H_\omega$, the basis e_j^ω parametrizes H_ω under the map

$$(y_1, \dots, y_{n-2}) \longmapsto (\sum_{j=1}^{n-2} y_j + a_1, -y_1 + a_2, \dots, -y_{n-2} + a_{n-1}) \ .$$

Hence in the coordinates of the basis e_j^ω, the half-space $H_\omega \cap D_{i_1,i_2,i_3}$ reads as

$$\text{when } i_1 = 0\text{: } -y_{i_2-1} - \cdots - y_{n-2} \leqslant C \ ,$$
$$\text{when } i_1 \geqslant 1\text{: } y_{i_1} + \cdots + y_{i_1+i_2-2} \leqslant C \ ,$$

where C denotes some constant that we are not interested in. Hence, in the basis e_j^ω, an outward pointing vector for the boundary $H_\omega \cap H_{i_1,i_2,i_3}$ is

$$\text{when } i_1 = 0\text{: } \nu := (0, \dots, 0, -1_{i_2-1}, \dots, -1_{n-2}) \ ,$$
$$\text{when } i_1 \geqslant 1\text{: } \nu := (0, \dots, 0, 1_{i_1}, \dots, 1_{i_1+i_2-2}, 0, \dots, 0) \ .$$

We have chosen orienting bases for the directing hyperplanes $\overline{H}_\omega$, and computed all outward pointing vectors for the boundaries in these bases. It only remains to study the image of these bases under the maps θ. We write $e_j^{\overline{\omega}}$ for the orienting basis of $K_{\overline{\omega}}$ and $e_j^{\widetilde{\omega}}$ for the one of $K_{\widetilde{\omega}}$. We distinguish two cases.

When $i_1 = 0$, the map θ reads as

$$\theta(x_1, \dots, x_{i_3}, y_1, \dots, y_{i_2-1}) = (y_1, \dots, y_{i_2-1}, x_1, \dots, x_{i_3}) \ ,$$

and we compute that:

$$\theta(e_j^{\overline{\omega}}) = -e_{i_2-1}^\omega + e_{j+i_2-1}^\omega \qquad\qquad \theta(e_j^{\widetilde{\omega}}) = e_j^\omega \ .$$

The determinant then has value

$$\det_{e_j^\omega}\left(\nu, \theta(e_j^{\overline{\omega}}), \theta(e_j^{\widetilde{\omega}})\right) = -i_3(-1)^{i_2 i_3} \ .$$

Thus, we recover the $-(-1)^{i_1+i_2i_3} K_{i_1+1+i_3} \times K_{i_2}$ oriented component of the boundary.

When $i_1 \geqslant 1$, the map θ now reads as

$$\theta(x_1, \dots, x_{i_3}, y_1, \dots, y_{i_2-1}) = (x_1, \dots, x_{i_1}, y_1, \dots, y_{i_2-1}, x_{i_1+1}, \dots, x_{i_1+i_3}) \ ,$$

and we compute that:

$$j \leqslant i_1 - 1 \ , \ \theta(e_j^{\overline{\omega}}) = e_j^\omega \qquad j \geqslant i_1 \ , \ \theta(e_j^{\overline{\omega}}) = e_{j+i_2-1}^\omega \qquad \theta(e_j^{\widetilde{\omega}}) = e_{j+i_1}^\omega - e_{i_1}^\omega \ .$$

This time,

$$\det_{e_j^\omega}\left(\nu, \theta(e_j^{\overline{\omega}}), \theta(e_j^{\widetilde{\omega}})\right) = -(i_2-1)(-1)^{i_1+i_2 i_3} \ .$$

We find again the $-(-1)^{i_1+i_2i_3} K_{i_1+1+i_3} \times K_{i_2}$ oriented component of the boundary, which concludes the proof of Theorem 2.2.1. □

4.4 Forcey–Loday multiplihedra and signs We now define the weighted Forcey–Loday realizations of the multiplihedra of [20] and prove the second part of Theorem 2.3.1.

Definition 4.4.1 ([20]). Given $n \geqslant 1$, choose a weight $\omega = (\omega_1, \dots, \omega_n)$. The *Forcey–Loday realization* of weight ω of J_n is defined as the intersection in $\mathbb{R}^{n-1}$ of the half-spaces of equation

$$D_{i_1,i_2,i_3} : x_{i_1+1} + \cdots + x_{i_1+i_2-1} \geqslant \sum_{i_1+1 \leqslant k < l \leqslant i_1+i_2} \omega_k \omega_l \ ,$$

for all $i_1 + i_2 + i_3 = n$ and $i_2 \geqslant 2$, with the half-spaces of equation

$$D^{i_1,\dots,i_s} : x_{i_1} + x_{i_1+i_2} + \cdots + x_{i_1+\cdots+i_{s-1}} \leqslant 2 \sum_{1 \leqslant t < u \leqslant s} \Omega_t \Omega_u$$

for all $i_1 + \cdots + i_s = n$, with each $i_t \geqslant 1$ and $s \geqslant 2$, and where $\Omega_t := \sum_{a=1}^{i_t} \omega_{i_1+\cdots+i_{t-1}+a}$. This polytope is denoted J_ω.

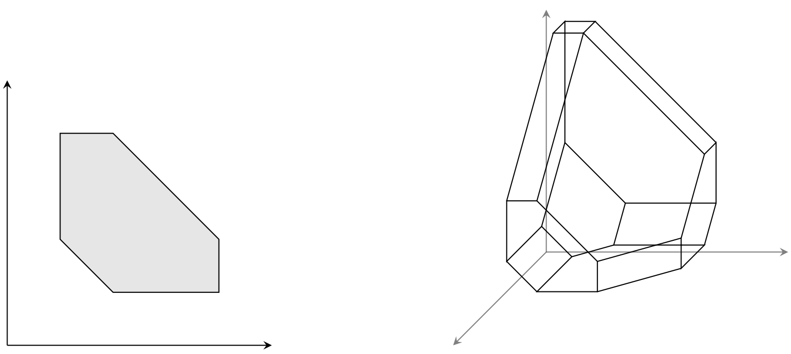

Figure 4.2: The Forcey–Loday realizations J_3 and J_4

For the weight $\mathbf{1}_n$ of length n whose entries are all equal to 1, we write again $J_n := J_{\mathbf{1}_n}$. The Forcey–Loday realizations J_3 and J_4 are represented in Figure 4.2. We can now prove the second part of Theorem 2.3.1:

Theorem 2.3.1. *The Forcey–Loday multiplihedra J_n form an operadic bimodule in* `Poly` *whose image under the functor C^{cell}_{-*} is the operadic bimodule M_∞.*

Proof. Our goal is to prove that, after orienting the K_n as before and choosing an orientation for the J_n, the boundary of J_n reads as

$$\partial J_n = \bigcup_{\substack{i_1+i_2+i_3=n \\ i_2 \geqslant 2}} (-1)^{i_1+i_2 i_3} J_{i_1+1+i_3} \times K_{i_2} \cup - \bigcup_{\substack{i_1+\cdots+i_s=n \\ s \geqslant 2}} (-1)^{\epsilon_B} K_s \times J_{i_1} \times \cdots \times J_{i_s} \ ,$$

where ϵ_B is as in Section 4.2.4 ; $K_{i_1+1+i_3} \times K_{i_2}$ is sent to $f_{i_1+1+i_3}(\mathrm{id}^{\otimes i_1} \otimes m_{i_2} \otimes \mathrm{id}^{\otimes i_3})$ while $K_s \times J_{i_1} \times \cdots \times J_{i_s}$ is sent to $m_s(f_{i_1} \otimes \cdots \otimes f_{i_s})$ by the functor C^{cell}_{-*}.

Step 1 We first explain how to obtain the set-theoretic equality for the boundary

$$\partial J_n = \bigcup_{\substack{i_1+i_2+i_3=n \\ i_2 \geqslant 2}} J_{i_1+1+i_3} \times K_{i_2} \cup \bigcup_{\substack{i_1+\cdots+i_s=n \\ s \geqslant 2}} K_s \times J_{i_1} \times \cdots \times J_{i_s} \ .$$

The top dimensional strata in the boundary of a J_ω are obtained by allowing exactly one of the inequalities

$$x_{i_1+1} + \cdots + x_{i_1+i_2-1} \geqslant \sum_{i_1+1 \leqslant k < l \leqslant i_1+i_2} \omega_k \omega_l \ ,$$
$$x_{i_1} + x_{i_1+i_2} + \cdots + x_{i_1+\cdots+i_{s-1}} \leqslant 2 \sum_{1 \leqslant t < u \leqslant s} \Omega_t \Omega_u \ ,$$

to become an equality. We write H_{i_1,i_2,i_3} and $H^{i_1,\ldots,i_s}$ for these hyperplanes.

Begin with the H_{i_1,i_2,i_3} component. Defining two new weights

$$\overline{\omega} := (\omega_1, \ldots, \omega_{i_1}, \omega_{i_1+1} + \cdots + \omega_{i_1+i_2}, \omega_{i_1+i_2+1}, \ldots, \omega_n) \ ,$$
$$\widetilde{\omega} := (\omega_{i_1+1}, \ldots, \omega_{i_1+i_2}) \ ,$$

the map

$$\theta : \mathbb{R}^{i_1+i_3} \times \mathbb{R}^{i_2-1} \longrightarrow \mathbb{R}^{n-1}$$
$$(x_1, \ldots, x_{i_1+i_3}) \times (y_1, \ldots, y_{i_2-1}) \longmapsto (x_1, \ldots, x_{i_1}, y_1, \ldots, y_{i_2-1}, x_{i_1+1}, \ldots, x_{i_1+i_3})$$

induces a bijection between $J_{\overline{\omega}} \times K_{\widetilde{\omega}}$ and the codimension 1 face of J_ω corresponding to the intersection with H_{i_1,i_2,i_3}.

In the case of the $H^{i_1,\ldots,i_s}$ component, we define the weights

$$\overline{\omega} := (\sqrt{2}\Omega_1, \ldots, \sqrt{2}\Omega_s) \ ,$$
$$\widetilde{\omega}_t := (\omega_{i_1+\cdots+i_{t-1}+1}, \ldots, \omega_{i_1+\cdots+i_{t-1}+i_t}) \ , \ 1 \leqslant t \leqslant s \ .$$

This time, the map

$$\theta : \mathbb{R}^{s-1} \times \mathbb{R}^{i_1-1} \times \cdots \times \mathbb{R}^{i_s-1} \longrightarrow \mathbb{R}^{n-1}$$

sends an element $(x_1, \ldots, x_{s-1}) \times (y^1_1, \ldots, y^1_{i_1-1}) \times \cdots \times (y^s_1, \ldots, y^s_{i_s-1})$ to

$$(y^1_1, \ldots, y^1_{i_1-1}, x_1, y^2_1, \ldots, y^2_{i_2-1}, x_2, y^3_1, \ldots, x_{s-1}, y^s_1, \ldots, y^s_{i_s-1}) \ .$$

It induces a bijection between $K_{\overline{\omega}} \times J_{\widetilde{\omega}_1} \times \cdots \times J_{\widetilde{\omega}_s}$ and the codimension 1 face of J_ω corresponding to the intersection with $H^{i_1,\ldots,i_s}$.

Step 2 We set the orientation on $\mathbb{R}^{n-1}$, and hence on J_ω, to be such that the vectors

$$f_j^\omega := (0, 0, \cdots, 0, -1_j, 0, \cdots, 0) \ ,$$

define a positively oriented basis of $\mathbb{R}^{n-1}$. In the coordinates of the basis f_j^ω, the half-space D_{i_1,i_2,i_3} reads as

$$z_{i_1+1} + \cdots + z_{i_1+i_2-1} \leqslant - \sum_{i_1+1 \leqslant k < l \leqslant i_1+i_2} \omega_k \omega_l \ ,$$

and the half-space $D^{i_1,\dots,i_s}$ as

$$-z_{i_1} - z_{i_1+i_2} - \cdots - z_{i_1+\cdots+i_{s-1}} \leqslant 2 \sum_{1 \leqslant t < u \leqslant s} \Omega_t \Omega_u$$

In this basis, an outward pointing vector for the boundary H_{i_1,i_2,i_3} is then

$$\nu := (0, \dots, 0, 1_{i_1+1}, \dots, 1_{i_1+i_2-1}, 0, \dots, 0) \ ,$$

while an outward pointing vector for the boundary $H^{i_1,\cdots,i_s}$ is

$$\nu := (0, \dots, 0, -1_{i_1}, 0, \dots, 0, -1_{i_1+i_2}, 0, \dots\dots, 0, -1_{i_1+i_2+\cdots+i_{s-1}}, 0, \dots, 0) \ .$$

Now that we have chosen positively oriented bases for the J_ω, and chosen outward pointing vectors for each component of their boundaries, we conclude again by computing the image of these bases under the maps θ.

In the case of a boundary component H_{i_1,i_2,i_3},

$$j \leqslant i_1 \ , \ \theta(f_j^{\overline{\omega}}) = f_j^\omega \qquad j \geqslant i_1 + 1 \ , \ \theta(f_j^{\overline{\omega}}) = f_{j+i_2-1}^\omega \qquad \theta(e_j^{\widetilde{\omega}}) = -f_{i_1+1}^\omega + f_{i_1+j+1}^\omega \ .$$

The determinant against the basis f_j^ω then has value

$$\det_{f_j^\omega}\left(\nu, \theta(f_j^{\overline{\omega}}), \theta(e_j^{\widetilde{\omega}})\right) = (i_2 - 1)(-1)^{i_1+i_2 i_3} \ .$$

Thus, we recover the $(-1)^{i_1+i_2i_3} J_{i_1+1+i_3} \times K_{i_2}$ oriented component of the boundary.

Finally, in the case of a boundary component $H^{i_1,\dots,i_s}$, we compute that

$$\theta(e_j^{\overline{\omega}}) = -f_{i_1}^\omega + f_{i_1+\cdots+i_{j+1}}^\omega \qquad\qquad \theta(f_j^{\widetilde{\omega}_t}) = f_{j+i_1+\cdots+i_{t-1}}^\omega \ .$$

This time,

$$\det_{f_j^\omega}\left(\nu, \theta(e_j^{\overline{\omega}}), \theta(f_j^{\widetilde{\omega}_1}), \dots, \theta(f_j^{\widetilde{\omega}_s})\right) = -(s-1)(-1)^{\epsilon_B} \ .$$

We find again the $-(-1)^{\epsilon_B} K_s \times J_{i_1} \times \cdots \times J_{i_s}$ oriented component of the boundary, which concludes the proof of the theorem. □

5. Signs and moduli spaces for ΩBAs-algebras and ΩBAs-morphisms

5.1 The operad ΩBAs

5.1.1 Definition of the operad ΩBAs

The definition of the operad ΩBAs that we now lay out is the one given by Markl and Shnider in [28]. We only expose the material necessary to our construction, and refer to their paper for further details and proofs. In the rest of the section, the notation t stands for a stable ribbon tree, and the notation t_{br} denotes a broken stable ribbon tree. Observe that a stable ribbon tree is a broken stable ribbon tree with 0 broken edge. As a result, all constructions performed for broken stable ribbon trees in the upcoming sections will hold in particular for stable ribbon trees.

Definition 5.1.1 ([28]). Given a broken stable ribbon tree t_{br}, an *ordering* of t_{br} is defined to be an ordering of its i finite internal edges $e_1, \dots, e_i$. Two orderings are said to be *equivalent* if one passes from one ordering to the other by an even permutation. An *orientation* of t_{br} is then defined to be an equivalence class of orderings, and written $\omega := e_1 \wedge \cdots \wedge e_i$. Each tree t_{br} has exactly two orientations. Given an orientation ω of t_{br} we will write $-\omega$ for the second orientation on t_{br}, called its *opposite orientation*.

Definition 5.1.2 ([28]). The operad ΩBAs is defined as follows. Consider the $\mathbb{Z}$-module freely generated by the pairs (t_{br}, ω) where t_{br} is a broken stable ribbon tree and ω an orientation of t_{br}. We define the arity n space of operations $\Omega BAs(n)_*$ to be the quotient of this $\mathbb{Z}$-module under the relation

$$(t_{br}, -\omega) = -(t_{br}, \omega) \ .$$

A pair (t_{br}, ω) where t_{br} has i finite internal edges, is defined to have degree $-i$. The partial compositions are then

$$(t_{br}, \omega) \circ_k (t'_{br}, \omega') = (t_{br} \circ_k t'_{br}, \omega \wedge \omega') \ ,$$

where the tree $t_{br} \circ_k t'_{br}$ is the broken ribbon tree obtained by grafting t'_{br} to the k-th incoming edge of t_{br}, and the edge resulting from the grafting is broken. The differential $\partial_{\Omega BAs}$ on $\Omega BAs(n)_*$ is finally set to send an element $(t_{br}, e_1 \wedge \cdots \wedge e_i)$ to

$$\sum_{j=1}^{i} (-1)^j \left((t_{br}/e_j, e_1 \wedge \cdots \wedge \hat{e_j} \wedge \cdots \wedge e_i) - ((t_{br})_j, e_1 \wedge \cdots \wedge \hat{e_j} \wedge \cdots \wedge e_i) \right) \ ,$$

where t_{br}/e_j is the tree obtained from t by collapsing the edge e_j and $(t_{br})_j$ is the tree obtained from t_{br} by breaking the edge e_j.

Choosing a distinguished orientation for every stable ribbon tree $t \in SRT$, this definition of the operad ΩBAs yields the definition as the quasi-free operad

$$\mathcal{F}(\curlyvee, \curlyvee, \curlyvee, \curlyvee, \cdots, SRT_n, \cdots) \ ,$$

given in Section 3.1.4. Albeit Definition 5.1.2 is more tedious at first sight, it allows for easier computations of signs.

5.1.2 Canonical orientations for the binary ribbon trees ([28])

For a fixed $n \geqslant 2$, the set of binary ribbon trees BRT_n can be endowed with a partial order that Tamari introduced in his thesis [40].

Definition 5.1.3. The *Tamari order* on BRT_n is the partial order generated by the covering relations

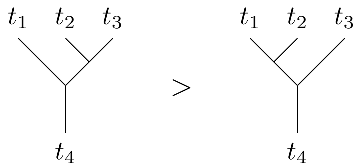

where t_1, t_2, t_3 and t_4 are binary ribbon trees.

The left-hand side in the above covering relation will be called a *right-leaning configuration*, and the right-hand side a *left-leaning configuration*. Hence given two trees t and t' in BRT_n, the inequality $t \geqslant t'$ holds if and only one can pass from t to t' by successive transformations of a right-leaning configuration into a left-leaning configuration.

For example in the case of BRT_4, we obtain the Hasse diagram in Figure 5.1. The Tamari poset is moreover a lattice, hence has a unique maximal element and a unique minimal element, respectively given by the right-leaning and left-leaning combs and denoted t_{max} and t_{min}. Given moreover a binary ribbon tree t, its immediate neighbours are by definition the trees obtained from t by either transforming exactly one right-leaning configuration of t into a left-leaning configuration, or transforming exactly one left-leaning configuration of t into a right-leaning configuration.

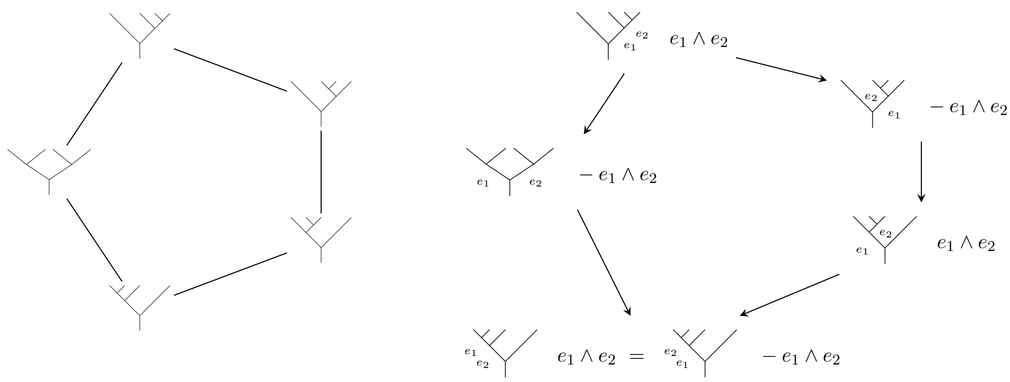

Figure 5.1: On the left, the Hasse diagram of the Tamari poset, where the maximal element is written at the top. On the right, all the canonical orientations for BRT_4 computed going down the Tamari poset.

The canonical orientation on the maximal binary tree is defined as

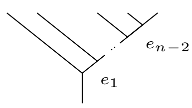

$$\omega_{can} := e_1 \wedge \cdots \wedge e_{n-2} \ .$$

Using the Tamari order, we can now build inductively canonical orientations on all binary trees.

We start at the maximal binary ribbon tree, and use the following rule on the covering relations

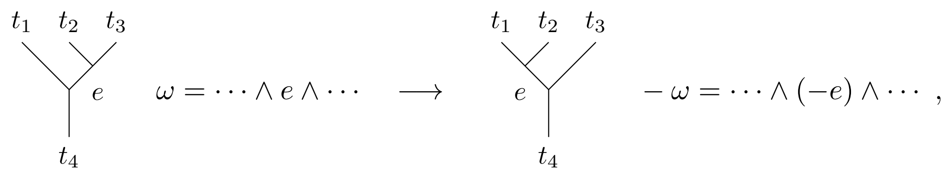

to define the orientations of its immediate neighbours. We then repeat this rule while going down the Tamari poset until the minimal binary tree is reached.

Lemma 5.1.4 ([28]). *This process is consistent: it does not depend on the path taken in the Tamari poset from the maximal binary tree to the binary tree whose orientation is being defined.*

Definition 5.1.5 ([28]). The well-defined orientations obtained under this process are called the *canonical orientations* and written ω_{can}.

5.1.3 Proof of Proposition 3.1.11

Consider a cell $\overline{\mathcal{T}}_n(t_{br}) \subset (\overline{\mathcal{T}}_n)_{\Omega BAs}$, where t_{br} is a broken stable ribbon tree. An ordering of its finite internal edges $e_1, \dots, e_i$ induces an isomorphism

$$\overline{\mathcal{T}}_n(t_{br}) \xrightarrow{\sim} [0, +\infty]^i ,$$

where the length l_{e_j} is seen as the j-th coordinate in $[0, +\infty]^i$. This ordering induces in particular an orientation on $\mathcal{T}_n(t_{br})$, by taking the image of the canonical orientation of $]0, +\infty[^i$ under the isomorphism. We check that two orderings of t_{br} define the same orientation on $\mathcal{T}_n(t_{br})$ if and only if they are equivalent: in other words, an orientation of t_{br} amounts to an orientation of $\mathcal{T}_n(t_{br})$.

Consider now the $\mathbb{Z}$-module freely generated by the pairs

$$(\overline{\mathcal{T}}_n(t_{br}), \text{choice of orientation } \omega \text{ on the cell } \overline{\mathcal{T}}_n(t_{br})) ,$$

where t_{br} is a broken stable ribbon tree. The complex $C_{-*}^{cell}(\overline{\mathcal{T}}_n)$ is exactly defined to be the quotient of this $\mathbb{Z}$-module under the relation

$$-(\overline{\mathcal{T}}_n(t_{br}), \omega) = (\overline{\mathcal{T}}_n(t_{br}), -\omega) .$$

The differential of an element $(\overline{\mathcal{T}}_n(t_{br}), \omega)$ is moreover given by the classical cubical differential on $[0, +\infty]^i$. Defining the cell chain complex in this way, the result of Proposition 3.1.11 becomes tautological.

5.1.4 Proof of Proposition 3.1.15

We now have all the necessary material to prove Proposition 3.1.15: our goal is to show that the obvious map $\mathrm{id} : (\overline{\mathcal{T}}_n)_{A_\infty} \to (\overline{\mathcal{T}}_n)_{\Omega BAs}$ is sent under the functor C_{-*}^{cell} to the morphism of operads $A_\infty \to \Omega BAs$ of [28] acting as

$$m_n \longmapsto \sum_{t \in BRT_n} (t, \omega_{can}) .$$

Beware however that we do not construct a morphism of operads $K_n \to (\overline{\mathcal{T}}_n)_{\Omega BAs}$ (see Remark 5.1.6). For this purpose, we will work with the Loday realizations of the associahedra and use Lemma 3.1.13: we will prove that taking the restriction of the orientation of K_n chosen in Section 4.3 to the top dimensional cells of its dual subdivision, yields the canonical orientations on these cells under the identification $(\overline{\mathcal{T}}_n)_{\Omega BAs} \simeq (K_n)_{dual}$.

We begin by proving this statement for the cell labeled by the right-leaning comb t_{max}. Consider the orientation on the cell $\overline{\mathcal{T}}_n(t_{max})$ induced by the canonical ordering $e_1, \dots, e_{n-2}$ under the isomorphism

$$\overline{\mathcal{T}}_n(t_{max}) \xrightarrow{\sim} [0, +\infty]^{n-2} .$$

The face of $\overline{\mathcal{T}}_n(t_{max})$ associated to the breaking of the i-th edge corresponds to the face $H_{i,n-i,0}$ when seen in the Loday polytope. An outward-pointing vector for the face $H_{i,n-i,0}$ is moreover

$$\nu_i := (0, \dots, 0, 1_i, \dots, 1_{n-2}) ,$$

where coordinates are taken in the basis e_j^ω. The orientation defined by the canonical basis of $[0, +\infty]^{n-2}$ being exactly the one defined by the ordered list of the outwarding-point vectors to the $+\infty$ boundary, it is sent to the orientation of the basis $(\nu_1, \dots, \nu_{n-2})$ in the Loday polytope. We then check that

$$\det_{e_j^\omega}(\nu_j) = 1 .$$

Hence the orientation of K_n and the one induced by the canonical orientation are the same for the cell $\overline{\mathcal{T}}_n(t_{max})$.

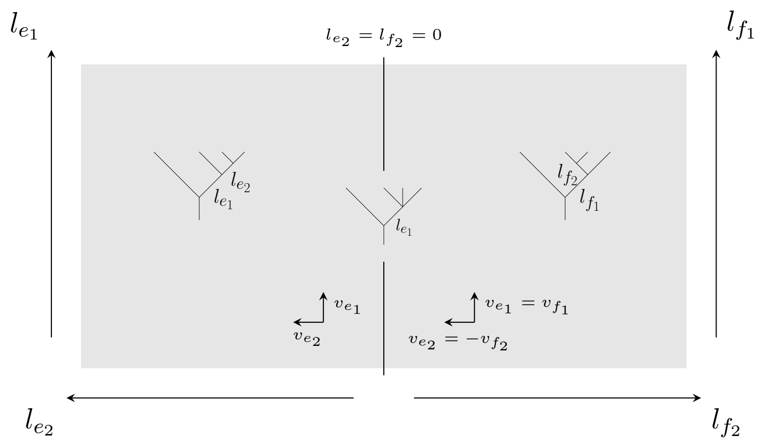

Figure 5.2: Gluing the cells $\overline{\mathcal{T}}_n(t_{max})$ and $\overline{\mathcal{T}}_n(t)$ along their common boundary: on this diagram, a vector of the form v_e is the vector orienting the axis associated to the length l_e

It can easily be seen from Definition 5.1.3 that the cells labeled by the immediate neighbours of the right-leaning comb t_{max} in the Tamari order are exactly the cells having a codimension 1 stratum in common with this cell. Choose an immediate neighbour t, and write e for the edge that has been collapsed to obtain the common codimension 1 stratum. The method to obtain the induced orientation on $\overline{\mathcal{T}}_n(t)$ follows Figure 5.2. Gluing the cells $\overline{\mathcal{T}}_n(t_{max})$ and $\overline{\mathcal{T}}_n(t)$ along their common boundary, we obtain a new copy of $[0, +\infty]^{n-2}$ which can be divided into two halves t_{max} and t. We then orient the total space $[0, +\infty]^{n-2}$ as the t_{max} half. Reading the induced orientation on the t half, it is the one obtained from the t_{max} half by reversing the axis associated to the edge e. By construction, this orientation is exactly the one obtained by restricting the global orientation on K_n to an orientation on $\mathcal{T}_n(t)$. Finally, going down the Tamari order, we can read the induced orientation on the top dimensional cells one immediate neighbour after another. And the rule to do this step-by-step process is exactly the one given in Section 5.1.2 on the covering relations. Hence, by construction, the global orientation on K_n restricts to the canonical orientations on binary trees, which concludes the proof of Proposition 3.1.15.

Remark 5.1.6. The operad $(\overline{\mathcal{T}}_n)_{\Omega BAs}$ is in fact naturally isomorphic to the W-construction $WAss$ of the standard associative operad Ass, as explained in [6]. It is unclear to the author whether explicit morphisms of topological operads $K \to WAss$ or $WAss \to K$ were already constructed in the litterature or not - where K denotes any topological operad isomorphic to the Loday associahedra operad. We should however mention in this regard that in [5, Theorem 1.4.10] Barber constructs an explicit isomorphism of topological operads $WK \tilde{\to} K$.

5.2 The moduli spaces $\mathcal{CT}_n(t_{br,c})$ The goal of this section is two-fold: complete the definition of the moduli spaces $\mathcal{CT}_n(t_c)$ introduced in Definition 3.2.15 and compute the signs appearing in the codimension 1 strata of their compactification in order to complete the definition of the differential on the operadic bimodule $M_{\Omega BAs}$ (Definition 3.2.15) in Lemma 5.3.3 of Section 5.3.1.

5.2.1 Definition of the moduli spaces $\mathcal{CT}_n(t_{br,c})$

We will write $t_{br,c}$ for a broken 2-colored stable ribbon tree (Definition 3.2.11) and t_c for an (unbroken) 2-colored stable ribbon tree. We will moreover call the unique stable 2-colored tree of arity 1 the *trivial 2-colored tree.*

Definition 5.2.1. We define the *underlying broken stable ribbon tree* t_{br} of a broken 2-colored stable ribbon tree $t_{br,c}$ to be the broken stable ribbon tree obtained by first deleting all the in $t_{br,c}$, and then forgetting all the remaining gauges of $t_{br,c}$. We then refer to a gauge in $t_{br,c}$ which is associated to a non-trivial gauged tree as a *non-trivial gauge* of $t_{br,c}$.

We refer to Figure 5.3 for an instance of association $t_{br,c} \mapsto t_{br}$. We now define the moduli spaces $\mathcal{CT}_n(t_{br,c})$ in Definition 5.2.5 following a step-by-step approach in Steps 5.2.2 to 5.2.4.

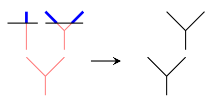

Figure 5.3: An instance of association $t_{br,c} \mapsto t_{br}$, where $t_{br,c}$ has one trivial gauge and one non-trivial gauge

Step 5.2.2. Consider a 2-colored stable ribbon tree t_c whose gauge does not intersect any of its vertices. Locally at any vertex directly adjacent to the gauge, the intersection between the gauge and the edges of t corresponds to one of the following two cases

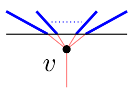

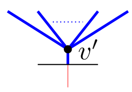

.

Write r for the root, the unique vertex adjacent to the outgoing edge. For a vertex v, we denote $d(r, v)$ the distance separating it from the root: the sum of the lengths of the edges appearing in the unique non self-crossing path going from r to v. Associating lengths $l_e > 0$ to all edges of t, we then associate the following inequalities to the two above cases

$$-\lambda > d(r, v) \qquad\qquad -\lambda < d(r, v') \ .$$

Note that this set of inequalities amounts to seeing the gauge as going towards $-\infty$ when going up, and towards $+\infty$ as going down. The moduli space $\mathcal{CT}_n(t_c)$ is then defined as

$$\mathcal{CT}_n(t_c) := \left\{(\lambda, \{l_e\}_{e \in E(t)}) \ , \ \lambda \in \mathbb{R}, \ l_e > 0, \ -\lambda > d(r,v), \ -\lambda < d(r,v')\right\} \ ,$$

where the set of inequalities on λ is prescribed by the 2-colored tree t_c.

Step 5.2.3. Consider now a 2-colored stable ribbon tree t_c whose gauge may intersect some of its vertices. To the two local pictures of Step 5.2.2, one has to add the case

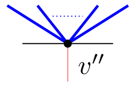

to which we associate the equality

$$-\lambda = d(r, v'') \ .$$

The moduli space $\mathcal{CT}_n(t_c)$ is this time defined as

$$\mathcal{CT}_n(t_c) := \left\{(\lambda, \{l_e\}_{e \in E(t)}) \ , \ \lambda \in \mathbb{R}, \ l_e > 0, \ -\lambda > d(r,v), \ -\lambda < d(r,v'), \ -\lambda = d(r,v'')\right\} \ ,$$

where the set of equalities and inequalities on λ is prescribed by the 2-colored tree t_c.

Step 5.2.4. Finally, consider a 2-colored broken stable ribbon tree $t_{br,c}$, whose gauges may intersect some of its vertices. We order the non-trivial unbroken 2-colored ribbon trees appearing in $t_{br,c}$ from left to right, as

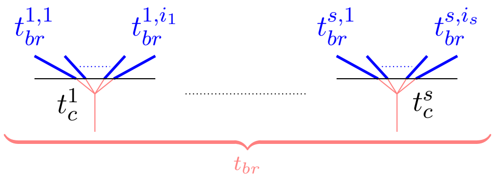

where $t_{br}^{1,1}, \dots, t_{br}^{1,i_1}, \dots, t_{br}^{s,1}, \dots, t_{br}^{s,i_s}$ and t_{br} are broken stable ribbon trees, and the non-trivial unbroken 2-colored ribbon trees are represented in the picture as 2-colored corollae $t_c^1, \dots, t_c^s$ for the sake of readability. We write moreover $r_1, \dots, r_s$ and $\lambda_1, \dots, \lambda_s$ for their respective roots and gauges.

Definition 5.2.5. Given a 2-colored broken stable ribbon tree $t_{br,c}$, we define the moduli space

$$\mathcal{CT}_n(t_{br,c}) := \left\{ \begin{array}{c} (\lambda_1, \dots, \lambda_s, \{l_e\}_{e \in E(t_{br})}) \ , \ \lambda_i \in \mathbb{R}, \ l_e > 0, \\ -\lambda_i > d(r_i, v), \ -\lambda_i < d(r_i, v'), \ -\lambda_i = d(r_i, v'') \end{array} \right\} \ ,$$

where the set of equalities and inequalities on λ_i is prescribed by the unbroken 2-colored tree t_c^i as in Steps 5.2.2 to 5.2.4.

Example 5.2.6. We consider the unbroken 2-colored trees t_c^1 and t_c^2 and the broken 2-colored tree t_c^3 defined as follows

$t_c^1 :=$ 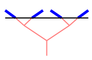 $\quad t_c^2 :=$ 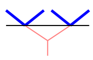 $\quad t_c^3 :=$ 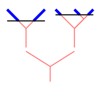 .

Applying Definition 5.2.5 we have that

$$\begin{aligned} \mathcal{CT}_4(t_c^1) &= \{(\lambda, \{l_1, l_2\}), -\lambda > l_1, l_2 \text{ and } l_1, l_2 > 0\} \ , \\ \mathcal{CT}_4(t_c^2) &= \{(\lambda, \{l_1, l_2\}), -\lambda = l_1 = l_2 > 0\} \subset \mathcal{CT}_4(t_c^1) \ , \\ \mathcal{CT}_4(t_c^3) &= \{(\lambda_1, \lambda_2, l), \lambda_1 < 0, -\lambda_2 > l > 0\} \ . \end{aligned}$$

5.2.2 Orienting the moduli spaces $\mathcal{CT}_n(t_{br,c})$

Definition 5.2.7. We define an *ordering/orientation* on a broken 2-colored stable ribbon tree $t_{br,c}$, to be an ordering/orientation on the broken ribbon tree t_{br} (Definition 5.1.1).

We will denote orderings on trees with the symbol Ω and orientations on trees with the symbol ω. We now explain how to orient the moduli spaces $\mathcal{CT}_n(t_{br,c})$ in Definition 5.2.11, following the step-by-step approach adopted in the previous section in Steps 5.2.8 to 5.2.10.

Step 5.2.8. Begin with a 2-colored stable ribbon tree t_c whose gauge does not intersect any of its vertices. An ordering Ω on t_c identifies $\mathcal{CT}_n(t_c)$ with a polyhedral cone

$$\mathcal{CT}_n(t_c) \subset]-\infty,+\infty[\times]0,+\infty[^{e(t)} ,$$

defined by the inequalities $-\lambda > d(r,v)$ and $-\lambda < d(r,v')$. This polyhedral cone has dimension $e(t)+1$, and we choose to orient it as an open subset of $]-\infty,+\infty[\times]0,+\infty[^{e(t)}$ endowed with its canonical orientation.

Step 5.2.9. Consider now a 2-colored stable ribbon tree t_c whose gauge may intersect some of its vertices. This time, an ordering Ω on t_c identifies $\mathcal{CT}_n(t_c)$ with a polyhedral cone

$$\mathcal{CT}_n(t_c) \subset]-\infty,+\infty[\times]0,+\infty[^{e(t)} ,$$

defined by the inequalities $-\lambda > d(r,v)$ and $-\lambda < d(r,v')$, to which we add the equalities $-\lambda = d(r,v'')$. If there are exactly j gauge-vertex intersections in the gauged tree t_c, this polyhedral cone has codimension j in $]-\infty,+\infty[\times]0,+\infty[^{e(t)}$ (it is given by j equalities $-\lambda = d(r,v'')$), hence has dimension $e(t)+1-j$.

Order now the j intersections from left to right

and consider the tree t'_c obtained by replacing these intersections by

One can see t_c as lying in the boundary of t'_c, by allowing the inequalities $-\lambda > d(r,v_k)$ to become equalities $-\lambda = d(r,v_k)$ for $k = 1,\dots,j$. This determines in particular j vectors ν_k corresponding to the outwarding-pointing vectors to the boundary of the half-space $-\lambda \geqslant d(r,v_k)$. We finally choose to coorient (and hence orient) $\mathcal{CT}_n(t_c)$ inside $]-\infty,+\infty[\times]0,+\infty[^{e(t)}$ with the vectors $(\nu_1,\dots,\nu_j)$.

Step 5.2.10. Lastly, consider a 2-colored broken stable ribbon tree $t_{br,c}$, whose gauges may intersect some of its vertices. Suppose there are exactly s non-trivial unbroken 2-colored trees $t_c^1,\dots,t_c^s$ appearing in $t_{br,c}$, which are ordered from left to right as previously. Suppose also that in each tree t_c^i, there are j_i gauge-vertex intersections. An ordering Ω on $t_{br,c}$ identifies $\mathcal{CT}_n(t_{br,c})$ with a polyhedral cone

$$\mathcal{CT}_n(t_{br,c}) \subset]-\infty,+\infty[^s\times]0,+\infty[^{e(t_{br})} ,$$

defined by the set of equalities and inequalities on the λ_i, and where the factor $]-\infty,+\infty[^s$ corresponds to $(\lambda_1,\dots,\lambda_s)$. This polyhedral cone has dimension $e(t_{br})+s-\sum_{i=1}^s j_i$. Now, as in

Step 5.2.9, order all gauge-vertex intersections from left to right in every tree t_c^i, and construct a new tree $t'_{br,c}$. Seeing $\mathcal{CT}_n(t_{br,c})$ as lying in the boundary of $\mathcal{CT}_n(t'_{br,c})$, this determines again a collection of outward-pointing vectors $\nu_{i,1}, \dots, \nu_{i,j_i}$ for $i = 1, \dots, s$. We then coorient $\mathcal{CT}_n(t_{br,c})$ inside $]-\infty, +\infty[^s \times]0, +\infty[^{e(t_{br})}$ with the vectors $(\nu_{1,1}, \dots, \nu_{1,j_1}, \dots, \nu_{s,1}, \dots, \nu_{s,j_s})$.

Definition 5.2.11. Given a 2-colored broken stable ribbon tree $t_{br,c}$ together with an ordering Ω, we define $\mathcal{CT}_n(t_{br,c}, \Omega)$ to be the moduli space $\mathcal{CT}_n(t_{br,c})$ endowed with the orientation described in Steps 5.2.8 to 5.2.10.

For two equivalent orderings Ω_1 and Ω_2 on $t_{br,c}$, the oriented space $\mathcal{CT}_n(t_{br,c}, \Omega_1)$ and the oriented space $\mathcal{CT}_n(t_{br,c}, \Omega_2)$ are then naturally isomorphic as oriented spaces.

Example 5.2.12. We keep the notations t_c^1 and t_c^2 of Example 5.2.6 and order the edges of t_c^1 and t_c^2 from left to right. We then have that the moduli space $\mathcal{CT}_4(t_c^1)$ is oriented as an open subset of $]-\infty, +\infty[\times]0, +\infty[^2$ and that the moduli space $\mathcal{CT}_4(t_c^2) \subset \mathcal{CT}_4(t_c^1)$ is cooriented in $\mathcal{CT}_4(t_c^1) \subset]-\infty, +\infty[\times]0, +\infty[^2$ by the vectors $(1, 1, 0)$ and $(1, 0, 1)$.

Remark 5.2.13. We point out that for a fixed broken stable ribbon tree type t_{br} together with an ordering, all 2-colored trees $t_{br,c}$ whose underlying ribbon tree is t_{br} determine a partition of $]-\infty, +\infty[^s \times]0, +\infty[^{e(t_{br})}$ in polyhedral cones. This is illustrated in Figure 5.4.

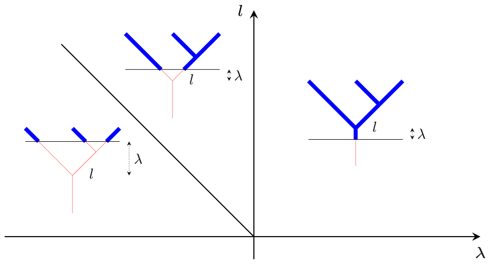

Figure 5.4

5.2.3 Codimension 1 strata of the compactification $\overline{\mathcal{CT}}_n(t_c)$

For a 2-colored stable ribbon tree t_c, the compactified moduli space $\overline{\mathcal{CT}}_n(t_c)$ has codimension 1 strata given by the four components introduced in Definition 3.2.13: (int-collapse), (gauge-vertex), (above-break) and (below-break). Choose an ordering Ω for t_c. We will now compute the signs appearing in the boundary of the compactification of the oriented moduli space $\mathcal{CT}_n(t_c, \Omega)$ in Sections 5.2.4 to 5.2.7.

5.2.4 The (int-collapse) boundary component

Consider a 2-colored stable ribbon tree t_c. The (int-collapse) boundary corresponds to the collapsing of an internal edge that does not intersect the gauge of the tree t. Choosing an ordering $\Omega = e_1, \dots, e_i$, suppose that it is the p-th edge of t which collapses. Write moreover $(t/e_p)_c$ for the resulting 2-colored tree, and $\Omega_p := e_1, \dots, \widehat{e_p}, \dots, e_i$ for the induced ordering on the edges of t/e_p.

Proposition 5.2.14 ((int-collapse) sign)**.** *For a 2-colored stable ribbon tree t_c whose gauge intersects j of its vertices, the boundary component $\mathcal{CT}_n((t/e_p)_c, \Omega_p)$ corresponding to the collapsing of the p-th edge of t bears a $(-1)^{p+1+j}$ sign in the boundary of $\overline{\mathcal{CT}}_n(t_c, \Omega)$.*

Proof. Case 1. We begin by considering the case of a 2-colored tree t_c whose gauge does not intersect any of its vertices. Suppose first that the collapsing edge is located above the gauge. A neighborhood of the boundary can then be parametrized as

$$\begin{aligned} \Phi :] - 1, 0] \times \mathcal{CT}_n((t/e_p)_c, \Omega_p) &\longrightarrow \overline{\mathcal{CT}}_n(t_c, \Omega) \\ (\delta, \lambda, l_1, \dots, \widehat{l_p}, \dots, l_i) &\longmapsto (\lambda, l_1, \dots, l_p := -\delta, \dots, l_i) \ . \end{aligned}$$

This map has sign $(-1)^{p+1}$, and the component $\mathcal{CT}_n((t/e_p)_c, \Omega_p)$ consequently bears a $(-1)^{p+1}$ sign in the boundary of $\overline{\mathcal{CT}}_n(t_c, \Omega)$.

Case 2. Suppose next that the collapsing edge is located below the gauge. We define a parametrization of a neighborhood of the boundary

$$] - 1, 0] \times \mathcal{CT}_n((t/e_p)_c, \Omega_p) \longrightarrow \overline{\mathcal{CT}}_n(t_c, \Omega)$$

as follows: λ is sent to $\lambda + \delta$; if the edge e_q is located directly below a gauge-edge intersection

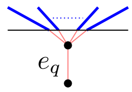

,

then we send l_q to $l_q - \delta$; for all the other edges e_q of (t/e_p), we send l_q to l_q ; finally, we set $l_p := -\delta$. We check again that this map has sign $(-1)^{p+1}$. Hence, in general, for a 2-colored tree t_c whose gauge does not intersect any of its vertices, the component $\mathcal{CT}_n((t/e_p)_c, \Omega_p)$ bears a $(-1)^{p+1}$ sign in the boundary of $\overline{\mathcal{CT}}_n(t_c, \Omega)$.

Case 3. Move on to the case of a 2-colored stable ribbon tree t_c whose gauge may intersect some of its vertices. Order the j gauge-vertex intersections from left to right as depicted in Section 5.2.2. We are going to distinguish three cases, but will eventually end up with the same sign in each case. Suppose to begin with that the collapsing edge e_p is located above the gauge, and is not adjacent to a gauge-vertex intersection. Then, denoting $(t/e_p)'_c$ the tree obtained via the same process as t'_c, we check that parametrization introduced in (Case 1)

$$\Phi :] - 1, 0] \times \mathcal{CT}_n((t/e_p)'_c, \Omega_p) \longrightarrow \overline{\mathcal{CT}}_n(t'_c, \Omega) \ ,$$

restricts to a parametrization of a neighborhood of the boundary

$$\phi :] - 1, 0] \times \mathcal{CT}_n((t/e_p)_c, \Omega_p) \longrightarrow \overline{\mathcal{CT}}_n(t_c, \Omega) \ .$$

We also check that Φ sends the outward-pointing vectors $\nu_k^{(t/e_p)}$ associated to the gauge-vertex intersections in $(t/e_p)_c$, to the outward-pointing vectors ν_k^t associated to the gauge-vertex intersections in t_c. Computing the sign of ϕ amounts to computing the sign of Φ and then exchanging the direction δ with the outward-pointing vectors $\nu_1^t, \dots, \nu_j^t$. The total sign is hence $(-1)^{p+1+j}$.

Case 4. Suppose, as second case, that the collapsing edge e_p is located above the gauge, and directly adjacent to a gauge-vertex intersection.

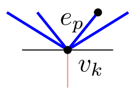

.

We cannot use the trees $(t/e_p)'_c$ and t'_c as in the last paragraph, as the gauge would then cut the edge e_p in the 2-colored tree t'_c. A small change is required. We form the tree t''_c as the tree t'_c, but instead of moving the gauge up at the vertex v_k, we move it down. The tree $(t/e_p)''_c$ is defined similarly. Applying the same argument as previously, we compute again a $(-1)^{p+1+j}$ sign for the boundary.

Case 5. Finally, suppose that the collapsing edge e_p is located below the gauge. It may this time be directly adjacent to a gauge-vertex intersection. Introducing again the trees $(t/e_p)'_c$ and t'_c, and using this time the parametrization of (Case 2), we find a $(-1)^{p+1+j}$ sign for the boundary. Note that there is a small adjustment to make in the proof for the outward-pointing vectors. Indeed, the outward-pointing vector $\nu_k^{(t/e_p)}$ gets again sent to the outward-pointing vector ν_k^t, except if the edge e_p is located in the non-self crossing path going from the vertex v_k intersected by the gauge to the root. For such an intersection, the vector $\nu_k^{(t/e_p)}$ is sent to $\nu_k^t - e_p$ by the map Φ, where e_p is the positive direction for the length l_p. Though the vector $\nu_k^t - e_p$ is not equal to ν_k^t, it is still outward-pointing to the half-space $-\lambda \geqslant d(r, v_k)$. As a result, $\Phi(\nu_1^{(t/e_p)}), \dots, \Phi(\nu_j^{(t/e_p)})$ defines indeed the same coorientation of $\mathcal{CT}_n(t_c, \Omega)$ as $\nu_1^t, \dots, \nu_j^t$. $\square$

5.2.5 The (gauge-vertex) boundary component

Consider a 2-colored stable ribbon tree t_c whose gauge may intersect some of its vertices. We order the gauge-vertex intersections from left to right as depicted in Section 5.2.2. The (gauge-vertex) boundary corresponds to the gauge crossing exactly one additional vertex of t. We suppose that this intersection takes place between the k-th and $k+1$-th intersections of t_c. We write moreover t_c^0 for the resulting 2-colored tree, and introduce again the tree t'_c of Section 5.2.2.

Proposition 5.2.15 ((gauge-vertex) sign)**.** *Suppose the crossing results from a move*

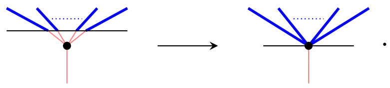

Then the boundary component $\mathcal{CT}_n(t_c^0, \Omega)$ has sign $(-1)^{j+k}$ in the boundary of $\overline{\mathcal{CT}}_n(t_c, \Omega)$.

Proof. Indeed the orientation induced on $\mathcal{CT}_n(t_c^0, \Omega)$ in the boundary of $\overline{\mathcal{CT}}_n(t_c, \Omega)$, is defined by the coorientation $(\nu_1, \dots, \nu_k, \widehat{\nu}, \nu_{k+1}, \dots, \nu_j, \nu)$ inside $\mathcal{CT}_n(t'_c, \Omega)$. The orientation defined by Ω on $\mathcal{CT}_n(t_c^0, \Omega)$, is the one defined by the coorientation $(\nu_1, \dots, \nu_k, \nu, \nu_{k+1}, \dots, \nu_j)$ inside $\mathcal{CT}_n(t'_c, \Omega)$. Hence, these two orientations differ by a $(-1)^{j+k}$ sign. $\square$

Proposition 5.2.16 ((gauge-vertex) sign)**.** *Suppose the crossing results from a move*

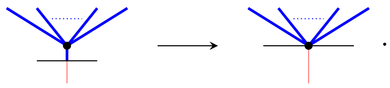

Then the boundary component $\mathcal{CT}_n(t_c^0, \Omega)$ has sign $(-1)^{j+k+1}$ in the boundary of $\overline{\mathcal{CT}}_n(t_c, \Omega)$.

Proof. Again the orientation induced on $\mathcal{CT}_n(t_c^0, \Omega)$ in the boundary of $\overline{\mathcal{CT}}_n(t_c, \Omega)$, is defined by the coorientation $(\nu_1, \dots, \nu_k, \widehat{\nu}, \nu_{k+1}, \dots, \nu_j, -\nu)$ inside $\mathcal{CT}_n(t'_c, \Omega)$. The orientation defined by Ω on $\mathcal{CT}_n(t_c^0, \Omega)$, is the one defined by the coorientation $(\nu_1, \dots, \nu_k, \nu, \nu_{k+1}, \dots, \nu_j)$ inside $\mathcal{CT}_n(t'_c, \Omega)$. Hence, these two orientations differ by a $(-1)^{j+k+1}$ sign. $\square$

5.2.6 The (above-break) boundary component

The (above-break) boundary corresponds either to the breaking of an internal edge of t, that is located above the gauge or intersects the gauge, or, when the gauge is below the root, to the outgoing edge breaking between the gauge and the root. Choosing an ordering $\Omega = e_1, \dots, e_i$, suppose that it is the p-th edge of t which breaks and write moreover $(t_p)_c$ for the resulting broken 2-colored tree.

Proposition 5.2.17 ((above-break) sign)**.** *For a 2-colored stable ribbon tree t_c whose gauge intersects j vertices, the boundary component $\mathcal{CT}_n((t_p)_c, \Omega_p)$ corresponding to the breaking of the p-th edge of t bears a $(-1)^{p+j}$ sign in the boundary of $\overline{\mathcal{CT}}_n(t_c, \Omega)$, where we set e_0 for the outgoing edge of t.*

Proof. Case 1. We begin by considering the case of a 2-colored tree t_c whose gauge does not intersect any of its vertices. Suppose first that the breaking edge does not intersect the gauge. A neighborhood of the boundary can then be parametrized as

$$
\begin{aligned}
]0,+\infty] \times \mathcal{CT}_n((t_p)_c, \Omega_p) &\longrightarrow \overline{\mathcal{CT}}_n(t_c, \Omega) \\
(\delta, \lambda, l_1, \dots, \widehat{l_p}, \dots, l_i) &\longmapsto (\lambda, l_1, \dots, l_p := \delta, \dots, l_i) \ .
\end{aligned}
$$

This map has sign $(-1)^p$. In the case when the breaking edge does intersect the gauge, a neighbordhood of the boundary can be parametrized as

$$
\begin{aligned}
]0,+\infty] \times \mathcal{CT}_n((t_p)_c, \Omega_p) &\longrightarrow \overline{\mathcal{CT}}_n(t_c, \Omega) \\
(\delta, \lambda, l_1, \dots, \widehat{l_p}, \dots, l_i) &\longmapsto (\lambda, l_1, \dots, l_p := \delta - \lambda, \dots, l_i) \ ,
\end{aligned}
$$

where we set this time $l_p := \delta - \lambda$ in order for the inequality $-\lambda < d(r, v')$ to hold in this case. This parametrization again has sign $(-1)^p$.

Case 2. The case of a 2-colored tree t_c whose gauge may intersect some of its vertices is treated as in Section 5.2.4. We check again that the parametrization maps Φ introduced in the previous paragraph, restrict to parametrizations of a neighborhood of the boundary

$$
]0,+\infty] \times \mathcal{CT}_n((t_p)_c, \Omega_p) \longrightarrow \overline{\mathcal{CT}}_n(t_c, \Omega) \ ,
$$

and that Φ sends moreover the coorientation of $\mathcal{CT}_n((t_p)_c, \Omega_p)$ to the coorientation of $\mathcal{CT}_n(t_c, \Omega)$. These coorientations introduce as previously an additional $(-1)^j$ sign.

Case 3. Finally, suppose that the gauge of t_c intersects its outgoing edge and compute the sign of the (above-break) boundary component corresponding to the gauge going towards $+\infty$. A parametrization of a neighborhood of the boundary is simply given by

$$
\begin{aligned}
]0,+\infty] \times \mathcal{CT}_n((t_0)_c, \Omega_p) &\longrightarrow \overline{\mathcal{CT}}_n(t_c, \Omega) \\
(\delta, l_1, \dots, l_i) &\longmapsto (\lambda := \delta, l_1, \dots, l_i) \ .
\end{aligned}
$$

This map has sign 1. □

5.2.7 The (below-break) boundary component

The (below-break) boundary finally corresponds to the breaking of edges of t that are located below the gauge or intersect it, such that there is exactly one edge breaking in each non-self crossing path from an incoming edge to the root. Write $(t_{br})_c$ for the resulting broken 2-colored tree. Consider now an ordering $\Omega = e_1, \dots, e_i$ of t_c. We order again from left to right the s non-trivial unbroken 2-colored trees $t_c^1, \dots, t_c^s$ of $(t_{br})_c$, and denote moreover $e_{j_1}, \dots, e_{j_s}$ the internal edges of t whose breaking produce the trees $t_c^1, \dots, t_c^s$. Beware that we do not necessarily have that $j_1 < \dots < j_s$. We denote $\varepsilon(j_1, \dots, j_s; \Omega)$ the sign obtained after modifying Ω by moving e_{j_k} to the k-th spot in Ω, and write Ω_0 for the newly obtained ordering on t_c. Twisting the orientation on $\mathcal{CT}_n(t_c, \Omega)$ by $(-1)^{\varepsilon(j_1, \dots, j_s; \Omega)}$ amounts to identifying it with $\mathcal{CT}_n(t_c, \Omega_0)$.

Proposition 5.2.18 ((below-break) sign). *For a 2-colored stable ribbon tree t_c whose gauge intersects j vertices, the boundary component $\mathcal{CT}_n((t_{br})_c, \Omega_{br})$ corresponding to the breaking of the internal edges $e_{j_1}, \dots, e_{j_s}$ of t bears a $(-1)^{\varepsilon(j_1,\dots,j_s;\Omega)+1+j}$ sign in the boundary of $\overline{\mathcal{CT}}_n(t_c, \Omega)$.*

Proof. We begin by assuming that $j_1 = 1, \dots, j_s = s$, and will explain how to deal with the general case at the end of the proof. We set to this extent $\Omega_{br} := e_{s+1}, \dots, e_i$. We moreover introduce two more pieces of notation. We will denote $\mathcal{E}_\infty$ the set of incoming edges of t which are crossed by the gauge and correspond to the trivial 2-colored trees in $(t_{br})_c$. In other words, the set of edges which are breaking in the (below-break) boundary component associated to $(t_{br})_c$ is $\mathcal{E}_\infty \cup \{e_{j_1}, \dots, e_{j_s}\}$. For an edge e, internal or external, we will moreover write w_e for the vertex adjacent to e which is closest to the root r of t, and set $w_u := w_{e_u}$ for $u = 1, \dots, s$.

Case 1. Start by considering the case of a 2-colored tree t_c whose gauge does not intersect any of its vertices. Suppose first that among the breaking internal edges, none of them intersects the gauge. We define a parametrization of a neighbourhood of the boundary

$$]0, +\infty] \times \mathcal{CT}_n((t_{br})_c, \Omega_{br}) \longrightarrow \overline{\mathcal{CT}}_n(t_c, \Omega)$$

by sending $(\delta, \lambda_1, \dots, \lambda_s, l_{s+1}, \dots, l_i)$ to the element of $\mathcal{CT}_n(t_c, \Omega)$ whose entries are defined as

$$\begin{aligned}
\lambda &:= -\delta + \sum_{u=1}^{s} (\lambda_u - d(r, w_u)) - \sum_{e \in \mathcal{E}_\infty} d(r, w_e) \ , & \\
l_v &:= \delta + \sum_{\substack{u=1,\dots,s \\ u \neq v}} (-\lambda_u + d(r, w_u)) + \sum_{e \in \mathcal{E}_\infty} d(r, w_e) & \text{for } v = e_1, \dots, e_s \ , \\
l_k &:= l_k & \text{for } k = s+1, \dots, i \ .
\end{aligned}$$

We compute that this map has sign -1.

Case 2. Suppose now that among the breaking internal edges of t_c, some of them may intersect the gauge. We denote $\mathcal{N}_\cap \subset \{1, \dots, s\}$ for the set of indices corresponding to the breaking internal edges which intersect the gauge, and $\mathcal{N}_\emptyset \subset \{1, \dots, s\}$ for the set of indices corresponding to the breaking of internal edges which do not intersect the gauge. We define this time a parametrization of a neighbourhood of the boundary

$$]0, +\infty] \times \mathcal{CT}_n((t_{br})_c, \Omega_{br}) \longrightarrow \overline{\mathcal{CT}}_n(t_c, \Omega)$$

by sending $(\delta, \lambda_1, \dots, \lambda_s, l_{s+1}, \dots, l_i)$ to the element of $\mathcal{CT}_n(t_c, \Omega)$ whose entries are set to be

$$\begin{aligned}
\lambda &:= -\delta + \sum_{u \in \mathcal{N}_\emptyset} (\lambda_u - d(r, w_u)) - \sum_{u \in \mathcal{N}_\cap} d(r, w_u) - \sum_{e \in \mathcal{E}_\infty} d(r, w_e) \ , & \\
l_v &:= \delta + \sum_{\substack{u \in \mathcal{N}_\emptyset \\ u \neq v}} (-\lambda_u + d(r, w_u)) + \sum_{u \in \mathcal{N}_\cap} d(r, w_u) + \sum_{e \in \mathcal{E}_\infty} d(r, w_e) & \text{for } v \in \mathcal{N}_\emptyset \ , \\
l_v &:= \delta + \lambda_v + \sum_{u \in \mathcal{N}_\emptyset} (-\lambda_u + d(r, w_u)) + \sum_{\substack{u \in \mathcal{N}_\cap \\ u \neq v}} d(r, w_u) + \sum_{e \in \mathcal{E}_\infty} d(r, w_e) & \text{for } v \in \mathcal{N}_\cap \ , \\
l_k &:= l_k & \text{for } k = s+1, \dots, i \ .
\end{aligned}$$

We compute that this map has again sign -1.

Case 3. Consider now the case of a 2-colored tree t_c whose gauge intersects j of its vertices. We check as in the previous proofs that the parametrization maps introduced in the previous paragraphs, restrict to parametrizations of a neighborhood of the boundary

$$]0,+\infty] \times \mathcal{CT}_n((t_{br})_c, \Omega_{br}) \longrightarrow \overline{\mathcal{CT}}_n(t_c, \Omega) \ ,$$

and that these maps send moreover the coorientation of $\mathcal{CT}_n((t_{br})_c, \Omega_{br})$ to the coorientation of $\mathcal{CT}_n(t_c, \Omega)$. These coorientations introduce an additional $(-1)^j$ sign.

General case. We have thus computed the sign of the (below-break) boundary when $j_1 = 1, \dots, j_s = s$. Now, consider the general case where we dot no necessarily have that $j_1 = 1, \dots, j_s = s$. We can apply the previous constructions and find the desired sign for the associated (below-break) component. □

5.3 The operadic bimodule $M_{\Omega BAs}$

5.3.1 Proof of Proposition 3.2.20

We use the formalism of orientations on 2-colored trees in this proof, so that our description of the operadic bimodule $M_{\Omega BAs}$ be compatible with the definition of [28] for the operad ΩBAs. As before, $t_{br,c}$ will stand for a broken 2-colored stable ribbon tree, while t_c will denote an unbroken 2-colored stable ribbon tree. We also respectively write t_{br} and t for their underlying stable ribbon trees.

Lemma 5.3.1. *Consider the $\mathbb{Z}$-module freely generated by the pairs $(t_{br,c}, \omega)$. The arity n space of operations $M_{\Omega BAs}(n)_*$ is the quotient of this $\mathbb{Z}$-module under the relation*

$$(t_{br,c}, -\omega) = -(t_{br,c}, \omega) \ .$$

An element $(t_{br,c}, \omega)$ where $t_{br,c}$ has $e(t_{br})$ finite internal edges and g non-trivial gauges which intersect j vertices of t_{br} has degree $j - (e(t_{br}) + g)$. The operad ΩBAs then acts on $M_{\Omega BAs}$ as follows

$$(t_{br,c}, \omega) \circ_i (t'_{br}, \omega') = (t_{br,c} \circ_i t'_{br}, \omega \wedge \omega') \ ,$$
$$\mu((t_{br}, \omega), (t^1_{br,c}, \omega_1), \dots, (t^s_{br,c}, \omega_s)) = (-1)^\dagger (\mu(t_{br}, t^1_{br,c} \dots, t^s_{br,c}), \omega \wedge \omega_1 \wedge \dots \wedge \omega_s) \ ,$$

where the tree $t_{br,c} \circ_i t'_{br}$ is the 2-colored broken ribbon tree obtained by grafting t'_{br} to the i-th incoming edge of $t_{br,c}$ and $\mu(t_{br}, t^1_{br,c} \dots, t^s_{br,c})$ is the 2-colored broken ribbon tree defined by grafting each $t^j_{br,c}$ to the j-th incoming edge of t_{br}. Writing g_i for the number of non-trivial gauges and j_i for the number of gauge-vertex intersections of $t^i_{br,c}$, $i = 1, \dots, s$, and setting $t^0_{br} := t_{br}$ and $g_0 = j_0 = 0$,

$$\dagger := \sum_{i=1}^{s} g_i \sum_{l=0}^{i-1} e(t^l_{br}) + \sum_{i=1}^{s} j_i \sum_{l=0}^{i-1} (e(t^l_{br}) + g_l - j_l) \ .$$

Proof. The description of $M_{\Omega BAs}(n)_*$ as a graded $\mathbb{Z}$-module stems from the same arguments used in the proof of Proposition 3.1.11 in Section 5.1.3. It remains to check that the signs for the action-composition maps are indeed the ones determined by the compactified moduli spaces $(\overline{\mathcal{CT}}_n)_{\Omega BAs}$. The computation for $\circ_i$ is straighforward. Consider now the map

$$\mu : \mathcal{T}(t_{br}, \Omega) \times \mathcal{CT}(t^1_{br,c}, \Omega_1) \times \dots \times \mathcal{CT}(t^s_{br,c}, \Omega_s) \longrightarrow \mathcal{CT}(\mu(t_{br}, t^1_{br,c} \dots, t^s_{br,c}), \Omega \cdot \Omega_1 \cdot \dots \cdot \Omega_s)$$
$$(L_\Omega, (\Lambda_1, L_{\Omega_1}), \dots, (\Lambda_s, L_{\Omega_s})) \longmapsto (\Lambda_1, \dots, \Lambda_s, L_\Omega, L_{\Omega_1}, \dots, L_{\Omega_s}) \ ,$$

where L_{Ω_i} stands for the list of lengths of t^i_{br} according to the ordering Ω_i, $\Omega \cdot \Omega_1 \cdot \cdots \cdot \Omega_s$ is the concatenation of the orderings $\Omega, \Omega_1, \ldots, \Omega_s$ and $\Lambda_i := (\lambda_{i,1}, \ldots, \lambda_{i,g_i})$ stands for the list of non-trivial gauges of $t^i_{br,c}$. We compute that, in the absence of gauge vertex intersections, this map has sign

$$(-1)^{\sum_{i=1}^{s} g_i \sum_{l=0}^{i-1} e(t^l_{br})} .$$

Assuming that there are some gauge-vertex intersections, the combinatorics of coorientations introduce an additional sign

$$(-1)^{\sum_{i=1}^{s} j_i \sum_{l=0}^{i-1} (e(t^l_{br}) + g_l - j_l)} .$$

In total, we recover the sign $(-1)^{\dagger}$, which concludes the proof. □

Choosing a distinguished orientation for every 2-colored stable ribbon tree $t_c \in SCRT$, this definition of the operadic bimodule $M_{\Omega BAs}$ amounts to defining it as the free operadic bimodule in graded modules

$\mathcal{F}^{\Omega BAs, \Omega BAs}($ 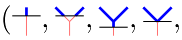 $, \cdots , SCRT_n, \cdots)$.

Remark 5.3.2. We point out that a second formula for $\dagger$ is

$$\dagger = \sum_{i=1}^{s} g_i \left(|t_{br}| + \sum_{l=1}^{i-1} |t^l_{br}| \right) + \sum_{i=1}^{s} j_i \left(|t_{br}| + \sum_{l=1}^{i-1} |t^l_{br,c}| \right) .$$

Lemma 5.3.3. *The differential of a 2-colored stable ribbon tree (t_c, ω) is the signed sum of all codimension 1 contributions*

$$\partial(t_c, \omega) = \sum \pm (int - collapse) + \sum \pm (gauge - vertex) + \sum \pm (above - break) + \sum \pm (below - break) ,$$

where our choice of notation for the terms of the sums is as in Definition 3.2.13 and where the signs are as computed in Propositions 5.2.14 to 5.2.18.

Example 5.3.4. We compute for instance that after choosing the orientation $e_1 \wedge e_2$ on

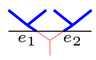

,

the signs in Example 3.2.21 are

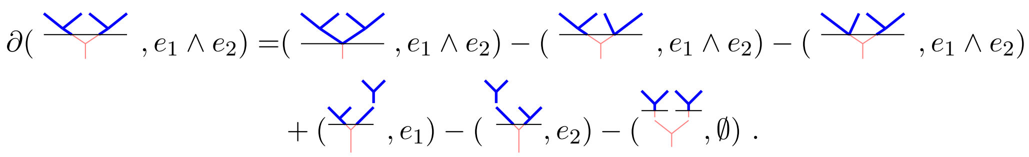

5.3.2 Canonical orientations for 2-colored binary ribbon trees

For a fixed $n \geqslant 2$, the set of 2-colored binary ribbon trees $CBRT_n$ can be endowed with a partial order, inspired by the Tamari order on BRT_n. It is introduced in [20].

Definition 5.3.5 ([20]). The *Tamari order on $CBRT_n$* is the partial order generated by the covering relations

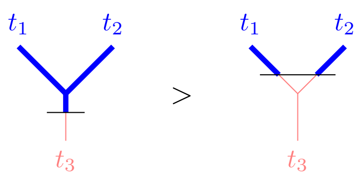

(A)

where t_1, t_2 and t_3 are binary ribbon trees,

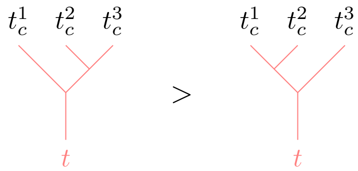

(B.1)

where t_c^1, t_c^2, t_c^3 are 2-colored binary ribbon trees and t is a binary ribbon tree, and

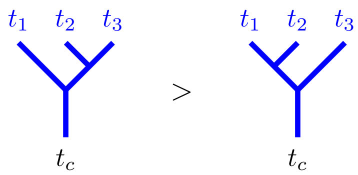

(B.2)

where t_1, t_2, t_3 are binary ribbon trees and t_c is a 2-colored binary ribbon tree.

For example in the case of $CBRT_4$, we obtain the Hasse diagram in Figure 5.5. This Tamari-like poset has a unique maximal element and a unique minimal element, respectively given by the right-leaning comb whose gauge intersects the outgoing edge, and the left-leaning comb whose gauge intersects all incoming edges.

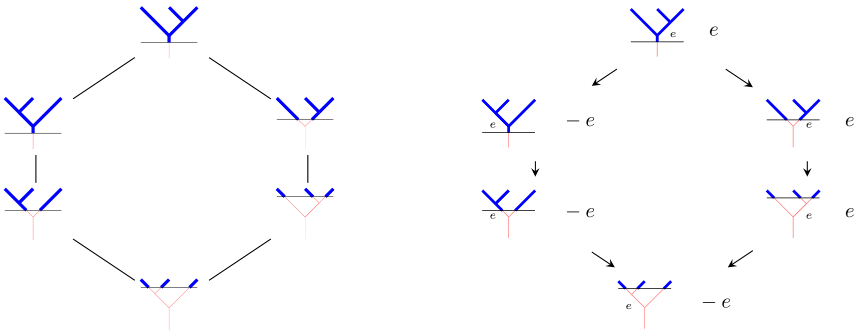

Figure 5.5: On the left, the Hasse diagram of the poset $CBRT_3$, where the maximal element is written at the top. On the right, all the canonical orientations for $CBRT_3$ computed going down the poset.

The canonical orientation on the maximal 2-colored binary tree is defined as

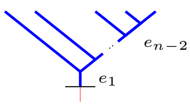

$$\omega_{can} := e_1 \wedge \cdots \wedge e_{n-2} \ .$$

Using this Tamari-like order, we can now build inductively canonical orientations on all 2-colored binary trees. We start at the maximal 2-colored binary tree, and transport the orientation ω_{can} to its immediate neighbours as follows: the immediate neighbours of t_c^{max} obtained under the covering relation (A) are endowed with the orientation ω_{can}, while the ones obtained under the covering relations (B) are endowed with the orientation $-\omega_{can}$. We then repeat this operation while going down the poset until the minimal 2-colored binary tree is reached.

Lemma 5.3.6. *This process is consistent, it does not depend on the path taken in the poset from t_c^{max} to the 2-colored binary tree whose orientation is being defined.*

Proof. An adapatation of the proof of Lemma 5.1.4 in [28] shows that it is enough to prove that the diagrams described by K_4 and J_3 commute in order to conclude. This is proven in Figures 5.1 and 5.5. □

Definition 5.3.7. These well-defined orientations will again be called the *canonical orientations* and written ω_{can}.

It is in fact straighforward to check that they coincide with the canonical orientations on the underlying binary trees.

Remark 5.3.8. Lemmas 5.1.4 and 5.3.6 are MacLane's coherence type lemmas. A heuristic explanation for Lemma 5.1.4 can be given as follows. A path between two trees t and t' in the Tamari poset corresponds to a path in the 1-skeleton of K_n. The faces of the 2-skeleton of K_n consist moreover of the products

$$K_2 \times \cdots \times K_2 \times K_3 \times K_2 \times \cdots \times K_2 \times K_3 \times K_2 \times \cdots \times K_2 \ ,$$
$$K_2 \times \cdots \times K_2 \times K_4 \times K_2 \times \cdots \times K_2 \ .$$

The first type of face corresponds to a square diagram that tautologically commutes, while the second type of face corresponds to the K_4 diagram. Given now two paths from t to t', they delineate a family of faces in the 2-skeleton of K_n. Translating this into algebra, as all faces translate into commuting diagrams, the two paths produce the same orientation. See also [10].

5.3.3 Proof of Proposition 3.2.25

We can now show that the map $\mathrm{id} : (\overline{\mathcal{CT}}_n)_{A_\infty} \to (\overline{\mathcal{CT}}_n)_{\Omega BAs}$ is sent under the functor C^{cell}_{-*} to a morphism of operadic bimodules $M_\infty \to M_{\Omega BAs}$ acting as

$$f_n \longmapsto \sum_{t_c \in CBRT_n} (t_c, \omega_{can}) \ .$$

Beware that we do not construct a morphism of operadic bimodules $J_n \to (\overline{\mathcal{CT}}_n)_{\Omega BAs}$. We will work with the Forcey–Loday realizations of the multiplihedra J_n and use Lemma 3.2.23, to prove that taking the restriction of the orientation of J_n chosen in Section 4.4 to the top dimensional cells of its dual subdivision yields the canonical orientations on these cells in the $\overline{\mathcal{CT}}_n$ viewpoint. We follow in this regard the exact same line of proof as in Section 5.1.4.

This statement is at first shown for the maximal 2-colored binary tree t_c^{max}, the right-leaning comb whose gauge crosses the outgoing edge. The orientation on the cell $\overline{\mathcal{CT}}_n(t_c^{max})$ induced by the canonical ordering $e_1, \cdots, e_{n-2}$ defines an isomorphism

$$\overline{\mathcal{CT}}_n(t_c^{max}) \xrightarrow{\sim} [0, +\infty] \times [0, +\infty]^{n-2} \ ,$$

where the factor $[0, +\infty]$ corresponds to the gauge λ, and the factor $[0, +\infty]^{n-2}$ to the lengths of the inner edges. The face of $\overline{\mathcal{CT}}_n(t_c^{max})$ associated to the gauge going to $+\infty$ corresponds to the face $H_{0,n,0}$ when seen in the Forcey–Loday polytope, while the face associated to the breaking of the i-th edge corresponds to the face $H_{i,n-i,0}$. An outward-pointing vector for the face $H_{i,n-i,0}$ is moreover

$$\nu_i := (0, \dots, 0, 1_{i+1}, \dots, 1_{n-1}) \ ,$$

where coordinates are taken in the basis f_j^{ω}. The orientation defined by the canonical basis of $[0, +\infty] \times [0, +\infty]^{n-2}$ is exactly the one defined by the ordered list of the outward-pointing vectors to the $+\infty$ boundary. This orientation is thus sent to the orientation defined by the basis $(\nu_0, \ldots, \nu_{n-2})$ in the Forcey–Loday polytope. It remains to check that

$$\det_{f_j^\omega}(\nu_j) = 1 \ .$$

As a result, the orientation induced by J_n and the one defined by the canonical orientation coincide for the cell $\overline{\mathcal{CT}}_n(t_c^{max})$.

The rest of the proof is a mere adaptation of the proof of Section 5.1.4. The cells labeled by the 2-colored binary trees which are immediate neighbours of the maximal 2-colored binary tree, are exactly the ones having a codimension 1 stratum in common with $\overline{\mathcal{CT}}_n(t_c^{max})$. Choosing one such tree t_c, and gluing the cells $\overline{\mathcal{CT}}_n(t_c)$ and $\overline{\mathcal{CT}}_n(t_c^{max})$ along their common boundary, one can read the induced orientation on $\overline{\mathcal{CT}}_n(t_c)$. In the case when the immediate neighbour t_c is obtained under the covering relation (A), the cells $\mathcal{CT}_n(t_c)$ and $\mathcal{CT}_n(t_c^{max})$ are in fact both oriented as subspaces of $]-\infty, +\infty[\times]0, +\infty[^{n-2}$. In the case when the immediate neighbour t_c is obtained under the covering relations (B), we send the reader back to Section 5.1.4 for explanations on why a -1 twist of the orientation has to be introduced. In each case, the induced orientation is exactly the canonical orientation on $\overline{\mathcal{CT}}_n(t_c)$. This argument can now be repeated going down the poset, and the induced orientation will always coincide with the canonical orientation on the cell, which concludes the proof of the theorem.

Part II: Geometry

6. A_∞ and ΩBAs-algebra structures on the Morse cochains

Let M be an oriented closed Riemannian manifold endowed with a Morse function f together with a Morse-Smale metric. Following [17], the Morse cochains $C^*(f)$ form a deformation retract of the singular cochains on M. The cup product naturally endows the singular cochains $C^*_{sing}(M)$ with a dg algebra structure. Theorem 1.6.1 then ensures that it can be transferred to an A_∞-algebra structure on the Morse cochains $C^*(f)$. The following question then naturally arises. The differential on the Morse cochains is defined by a count of negative gradient trajectories connecting critical points of f. Is it possible to define higher multiplications m_n on $C^*(f)$ by couting the points of 0-dimensional moduli spaces, such that they fit into a structure of A_∞-algebra ?

We have seen in the previous part that the polytopes encoding the operad A_∞ are the associahedra and that they can be realized as the compactified moduli spaces of stable metric ribbon trees. A natural candidate would thus be an interpretation of metric ribbon trees in Morse theory. A naive approach would be to define trees whose internal edges correspond to finite Morse trajectories and whose external edges correspond to semi-infinite Morse trajectories, as in Figure 6.1. These moduli spaces are however not well defined, as two trajectories coming from two distinct critical points cannot intersect. A second problem is that moduli spaces of trajectories issued from the same critical point do not intersect transversely. Abouzaid bypasses this problem in [3] by perturbing the equation around each vertex, so that a transverse intersection can be achieved. This is illustrated in Figure 6.1.

Trees obtained in this way will be called *perturbed Morse gradient trees*. Let t be a stable ribbon tree type and $y, x_1, \ldots, x_n$ a collection of critical points of the Morse function f. We prove in this section that for a generic choice of perturbation data $\mathbb{X}_t$ on the moduli space $\mathcal{T}_n(t)$,

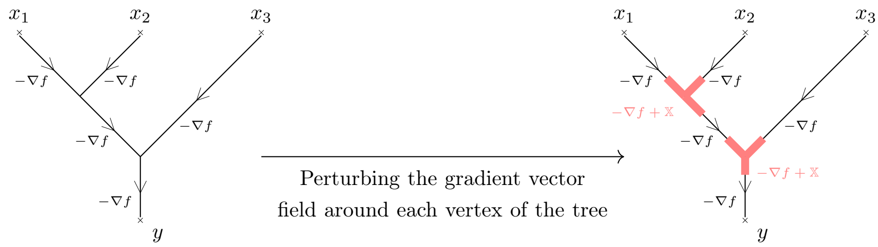

Figure 6.1

the moduli space of perturbed Morse gradient trees modeled on t and connecting $x_1, \dots, x_n$ to y, denoted $\mathcal{T}_t(y; x_1, \dots, x_n)$, is an orientable manifold (Proposition 6.3.3). Under some additional generic assumptions on the choices of perturbation data $\mathbb{X}_t$, these moduli spaces are compact in the 0-dimensional case, and can be compactified to compact manifolds with boundary in the 1-dimensional case (Theorems 6.4.5 and 6.4.6). We are finally able to define operations on the Morse cochains $C^*(f)$ through counts of perturbed Morse gradient trees: these operations define an ΩBAs-algebra structure on $C^*(f)$ (Theorem 6.5.1). Our constructions are carried out using the viewpoint of [3, Sections 2 and 7] on perturbed Morse gradient trees that we recall in Section 6.2, and borrowing some terminology and notations used in [35]. Technical details are moreover postponed to Sections 8 and 9.

6.1 Conventions We will study Morse theory of the Morse function $f : M \to \mathbb{R}$ using its negative gradient vector field $-\nabla f$. Denote d the dimension of the manifold M and ϕ^s the flow of $-\nabla f$. For a critical point x define its unstable and stable manifolds

$$W^U(x) := \{z \in M, \lim_{s \to -\infty} \phi^s(z) = x\}$$
$$W^S(x) := \{z \in M, \lim_{s \to +\infty} \phi^s(z) = x\} .$$

Their dimensions are such that $\dim(W^U(x)) + \dim(W^S(x)) = d$. We then define the *degree of a critical point* x to be $|x| := \dim(W^S(x))$. This degree is often referred to as the *coindex of* x in the litterature.

We will moreover work with Morse cochains. For two critical point $x \neq y$, define

$$\mathcal{T}(y; x) := W^S(y) \cap W^U(x)/\mathbb{R}$$

to be the moduli space of negative gradient trajectories connecting x to y. Denote moreover $\mathcal{T}(x; x) = \emptyset$. Under the Morse-Smale assumption on f and the Riemannian metric on M, for $x \neq y$ the moduli space $\mathcal{T}(y; x)$ has dimension $\dim(\mathcal{T}(y; x)) = |y| - |x| - 1$. The Morse differential $\partial_{Morse} : C^*(f) \to C^*(f)$ is then defined to count descending negative gradient trajectories

$$\partial_{Morse}(x) := \sum_{|y| = |x|+1} \#\mathcal{T}(y; x) \cdot y .$$

We refer to Section 9.2 for additional details on the moduli spaces introduced in this section.

6.2 Perturbed Morse gradient trees

Definition 6.2.1 ([3]). Let $T := (t, \{l_e\}_{e \in E(t)})$ be a metric tree, where $\{l_e\}_{e \in E(t)}$ are the lengths of its internal edges. A *choice of perturbation data* on T consists of the following data:

(i) a vector field

$$[0, l_e] \times M \underset{\mathbb{X}_e}{\longrightarrow} TM \ ,$$

that vanishes on $[1, l_e - 1]$, associated to each internal edge e of t ;

(ii) a vector field

$$[0, +\infty[\times M \underset{\mathbb{X}_{e_0}}{\longrightarrow} TM \ ,$$

that vanishes away from $[0, 1]$, associated to the outgoing edge e_0 of t ;

(iii) a vector field

$$] - \infty, 0] \times M \underset{\mathbb{X}_{e_i}}{\longrightarrow} TM \ ,$$

that vanishes away from $[-1, 0]$, associated to each incoming edge e_i ($1 \leqslant i \leqslant n$) of t.

Note that when $l_e \leqslant 2$, the vanishing condition on $[1, l_e - 1]$ is empty, that is we do not require any specific vanishing property for $\mathbb{X}_e$. For brevity's sake we will write D_e for all segments $[0, l_e]$ as well as for all semi-infinite segments $] - \infty, 0]$ and $[0, +\infty[$ in the rest of the paper.

Definition 6.2.2 ([3]). A *perturbed Morse gradient tree* T^{Morse} associated to $(T, \mathbb{X})$ is the data for each edge e of t of a smooth map $\gamma_e : D_e \to M$ such that γ_e is a trajectory of the perturbed negative gradient $-\nabla f + \mathbb{X}_e$, i.e.

$$\dot{\gamma}_e(s) = -\nabla f(\gamma_e(s)) + \mathbb{X}_e(s, \gamma_e(s)) \ ,$$

and such that the endpoints of these trajectories coincide as prescribed by the edges of the tree T.

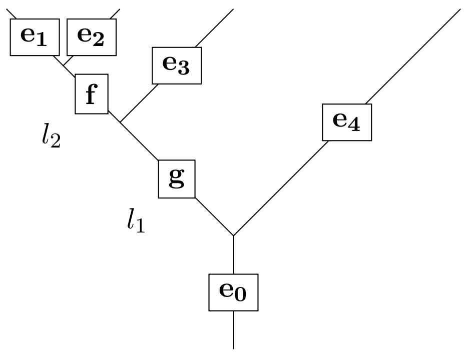

Figure 6.2: Choosing perturbation data $\mathbb{X}$ for this metric tree, we have that $\phi_{1,\mathbb{X}} = \phi^{l_1}_{g,\mathbb{X}} \circ \phi^{l_2}_{f,\mathbb{X}} \circ \phi^{1}_{e_1,\mathbb{X}}$, $\phi_{2,\mathbb{X}} = \phi^{l_1}_{g,\mathbb{X}} \circ \phi^{l_2}_{f,\mathbb{X}} \circ \phi^{1}_{e_2,\mathbb{X}}$, $\phi_{3,\mathbb{X}} = \phi^{l_1}_{g,\mathbb{X}} \circ \phi^{1}_{e_3,\mathbb{X}}$ and $\phi_{4,\mathbb{X}} = \phi^{1}_{e_4,\mathbb{X}}$

A perturbed Morse gradient tree T^{Morse} associated to $(T, \mathbb{X})$ is determined by the data of the time -1 points on its incoming edges plus the time 1 point on its outgoing edge. Indeed, for each edge e of t, we write $\phi_{e,\mathbb{X}}$ for the flow of $-\nabla f + \mathbb{X}_e$. We moreover define for every incoming edge e_i ($1 \leqslant i \leqslant n$) of T, the diffeomorphism $\phi_{i,\mathbb{X}}$ to be the composition of all flows obtained by following the time -1 point of the metric tree on e_i along the only non-self crossing path connecting it to the root. We also set $\phi_{0,\mathbb{X}}$ for the flow of $\phi_{e_0,\mathbb{X}}$ at time -1, where e_0 is the outgoing edge of t. This is depicted on Figure 6.2. Setting

$$\Phi_{T,\mathbb{X}} : M \times \cdots \times M \underset{\phi_{0,\mathbb{X}} \times \cdots \times \phi_{n,\mathbb{X}}}{\longrightarrow} M \times \cdots \times M \ ,$$

and Δ for the thin diagonal of $M \times \cdots \times M$, it is then clear that:

Proposition 6.2.3 ([3]). *There is a one-to-one correspondence*

$$\left\{ \begin{array}{c} \text{perturbed Morse gradient trees} \\ \text{associated to } (T,\mathbb{X}) \end{array} \right\} \longleftrightarrow (\Phi_{T,\mathbb{X}})^{-1}(\Delta) \quad .$$

The vector fields on the external edges are equal to $-\nabla f$ away from a length 1 segment, hence the trajectories associated to these edges all converge to critical points of the function f. For critical points y and $x_1, \dots, x_n$, the map $\Phi_{T,\mathbb{X}}$ can be restricted to

$$W^S(y) \times W^U(x_1) \times \cdots \times W^U(x_n) \ ,$$

such that the inverse image of the diagonal yields all perturbed Morse gradient trees associated to $(T, \mathbb{X})$ connecting $x_1, \dots, x_n$ to y.

6.3 Moduli spaces of perturbed Morse gradient trees Let t be a stable ribbon tree and Ω be an ordering on t (Definition 5.1.1). Recall that $E(t)$ stands for the set of internal edges of t, and $\overline{E}(t)$ for the set of all its edges. We previously saw that a choice of perturbation data on a metric ribbon tree $T := (t, (l_e)_{e \in E(t)})$ is the data of maps $\mathbb{X}_{T,f} : D_f \times M \longrightarrow TM$, for every edge $f \in \overline{E}(t)$ of t. Define the cone $C_f \subset \mathcal{T}_n(t,\Omega) \times \mathbb{R} \simeq]0,+\infty[^{e(t)} \times \mathbb{R}$ to be

(i) $\{((l_e)_{e \in E(t)}, s)$ such that $0 \leqslant s \leqslant l_f\}$ if f is an internal edge ;
(ii) $\{((l_e)_{e \in E(t)}, s)$ such that $s \leqslant 0\}$ if f is an incoming edge ;
(iii) $\{((l_e)_{e \in E(t)}, s)$ such that $s \geqslant 0\}$ if f is the outgoing edge.

Then a choice of perturbation data for every metric ribbon tree in $\mathcal{T}_n(t)$ yields a map

$$\mathbb{X}_{t,f} : C_f \times M \longrightarrow TM \ ,$$

for every edge f of t.

Definition 6.3.1. A choice of perturbation data $\mathbb{X}_t$ is said to be *smooth* if all the maps $\mathbb{X}_{t,f} : C_f \times M \to TM$ extend to smooth maps $]0,+\infty[^{e(t)} \times \mathbb{R} \times M \longrightarrow TM$.

Definition 6.3.2. Let $\mathbb{X}_t$ be a smooth choice of perturbation data on $\mathcal{T}_n(t)$. For critical points y and $x_1, \dots, x_n$, we define the moduli space

$$\mathcal{T}_t^{\mathbb{X}_t}(y; x_1, \dots, x_n) := \left\{ \begin{array}{c} \text{perturbed Morse gradient trees associated to } (T, \mathbb{X}_T) \\ \text{and connecting } x_1, \dots, x_n \text{ to } y, \text{ for } T \in \mathcal{T}_n(t) \end{array} \right\} .$$

Introduce now the map

$$\phi_{\mathbb{X}_t} : \mathcal{T}_n(t) \times W^S(y) \times W^U(x_1) \times \cdots \times W^U(x_n) \longrightarrow M^{\times n+1} \ ,$$

whose restriction to every $T \in \mathcal{T}_n(t)$ is as defined at the end of Section 6.2:

Proposition 6.3.3. *(i) The moduli space $\mathcal{T}_t^{\mathbb{X}_t}(y; x_1, \dots, x_n)$ can be rewritten as*

$$\mathcal{T}_t^{\mathbb{X}_t}(y; x_1, \dots, x_n) = \phi_{\mathbb{X}_t}^{-1}(\Delta) \ ,$$

where Δ is the thin diagonal of $M^{\times n+1}$.

(ii) Given a choice of perturbation data $\mathbb{X}_t$ making $\phi_{\mathbb{X}_t}$ transverse to the diagonal Δ, the moduli space $\mathcal{T}_t^{\mathbb{X}_t}(y; x_1, \dots, x_n)$ is an orientable manifold of dimension

$$\dim\left(\mathcal{T}_t(y; x_1, \dots, x_n)\right) = e(t) + |y| - \sum_{i=1}^{n} |x_i| \ .$$

(iii) Choices of perturbation data $\mathbb{X}_t$ such that $\phi_{\mathbb{X}_t}$ is transverse to Δ exist.

Proof. Item (i) is straightforward and Item (ii) stems from the fact that if $\phi_{\mathbb{X}_t}$ is transverse to Δ, the moduli spaces $\mathcal{T}_t^{\mathbb{X}_t}(y; x_1, \dots, x_n)$ are manifolds of codimension

$$\operatorname{codim}(\mathcal{T}_t(y; x_1, \dots, x_n)) = \operatorname{codim}_{M^{\times n+1}}(\Delta) = nd \ ,$$

where $d := \dim(M)$. Note that we have chosen to grade the Morse cochains using the coindex in order for this convenient dimension formula to hold. We refer to Section 8.2 for details on Item (iii). □

6.4 Compactifications

6.4.1 Compactification of the 1-dimensional manifolds $\mathcal{T}_t^{\mathbb{X}_t}(y; x_1, \dots, x_n)$

We now would like to compactify the 1-dimensional moduli spaces $\mathcal{T}_t^{\mathbb{X}_t}(y; x_1, \dots, x_n)$ to 1-dimensional manifolds with boundary. They are defined as the inverse image in $\mathcal{T}_n(t) \times W^S(y) \times W^U(x_1) \times \dots \times W^U(x_n)$ of the diagonal Δ under $\phi_{\mathbb{X}_t}$. The boundary components in the compactification should hence come from those of $\mathcal{T}_n(t)$, of the unstable manifolds $W^U(x_i)$, and of the stable manifold $W^S(y)$. In other words, they should respectively come from internal edges of the perturbed Morse gradient tree collapsing, or breaking at a critical point (boundary of $\mathcal{T}_n(t)$), its semi-infinite incoming edges breaking at a critical point (boundary of $W^U(x_i)$) and its semi-infinite outgoing edge breaking at a critical point (boundary of $W^S(y)$). We illustrate some of these phenomena in Figure 6.3.

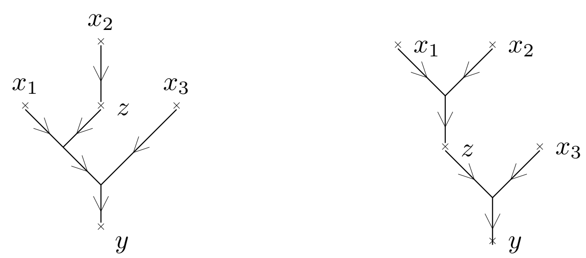

Figure 6.3: Two examples of perturbed Morse gradient trees breaking at a critical point

Definition 6.4.1. Given a smooth perturbation data $\mathbb{X}_t$ for all $t \in SRT_i$, $2 \leqslant i \leqslant n$, we denote $\mathbb{X}_n := (\mathbb{X}_t)_{t \in SRT_n}$ and call it a *choice of perturbation data on the moduli space $\mathcal{T}_n$*.

Following the previous discussion, we would like the boundary of the compactification of the moduli space $\mathcal{T}_t^{\mathbb{X}_t}(y; x_1, \dots, x_n)$ to be given by the following spaces:

(i) corresponding to an internal edge collapsing (int-collapse):

$$\mathcal{T}_{t'}^{\mathbb{X}_{t'}}(y; x_1, \dots, x_n)$$

where $t' \in SRT_n$ are all the trees obtained by collapsing exactly one internal edge of t ;

(ii) corresponding to an internal edge breaking (int-break):

$$\mathcal{T}_{t_1}^{\mathbb{X}_{t_1}}(y; x_1, \dots, x_{i_1}, z, x_{i_1+i_2+1}, \dots, x_n) \times \mathcal{T}_{t_2}^{\mathbb{X}_{t_2}}(z; x_{i_1+1}, \dots, x_{i_1+i_2}),$$

where t_2 is seen to lie above the $(i_1 + 1)$-th incoming edge of t_1 ;

(iii) corresponding to an external edge breaking (Morse):

$$\mathcal{T}(y;z) \times \mathcal{T}_t^{\mathbb{X}_t}(z;x_1,\dots,x_n) \text{ and } \mathcal{T}_t^{\mathbb{X}_t}(y;x_1,\dots,z,\dots,x_n) \times \mathcal{T}(z;x_i) \ .$$

While the (Morse) boundary simply comes from the fact that external edges are Morse trajectories away from a length 1 segment, the analysis for the (int-collapse) and (int-break) boundaries requires some additional conditions on the perturbation data.

6.4.2 Smooth choices of perturbation data

We begin by tackling the conditions coming with the (int-collapse) boundary. Let t be a stable ribbon tree type and consider a choice of perturbation data on $\mathcal{T}_n(t)$: it is a choice of perturbation data $\mathbb{X}_T$ for every $T \in \mathcal{T}_n(t) \simeq]0,+\infty[^{e(t)}$. Denote $coll(t) \subset SRT_n$ the set of all trees obtained by collapsing internal edges of t. A choice of perturbation data $(\mathbb{X}_{t'})_{t' \in coll(t)}$ then corresponds to a choice of perturbation data $\mathbb{X}_T$ for every $T \in [0,+\infty[^{e(t)}$. Following Section 6.3, such a choice of perturbation data is equivalent to a map

$$\tilde{\mathbb{X}}_{t,f} : \tilde{C}_f \times M \longrightarrow TM \ ,$$

for every edge f of t, where $\tilde{C}_f \subset [0,+\infty[^{e(t)} \times \mathbb{R} \subset \mathbb{R}^{e(t)} \times \mathbb{R}$ is defined in a similar fashion to C_f.

Definition 6.4.2. A choice of perturbation data $(\mathbb{X}_{t'})_{t' \in coll(t)}$ is said to be *smooth* if all maps $\tilde{\mathbb{X}}_{t,f}$ extend to smooth maps $\mathbb{R}^{e(t)} \times \mathbb{R} \times M \to TM$. A choice of perturbation data $\mathbb{X}_n$ is said to be *smooth* if for every $t \in SRT_n$, the choice of perturbation data $(\mathbb{X}_{t'})_{t' \in coll(t)}$ is smooth.

6.4.3 Gluing-compatible choices of perturbation data

We now tackle the conditions coming with the (int-break) boundary. We work again with a fixed stable ribbon tree type t. Consider a choice of perturbation data $\mathbb{X}_t = (\mathbb{X}_{t,e})_{e \in \overline{E}(t)}$ on $\mathcal{T}_n(t)$. We have to specify what happens on the $\mathbb{X}_{t,e}$ when the length of an internal edge f of t, denoted l_f, goes towards $+\infty$. Write t_1 and t_2 for the trees obtained by breaking t at the edge f.

(i) For $e \in \overline{E}(t)$ and $\neq f$, assuming for instance that $e \in t_1$, we require that

$$\lim_{l_f \to +\infty} \mathbb{X}_{t,e} = \mathbb{X}_{t_1,e} \ .$$

(ii) For $f = e$, $\mathbb{X}_{t,f}$ yields two parts when $l_f \to +\infty$: the part corresponding to the infinite edge in t_1 and the part corresponding to the infinite edge in t_2. We then require that they coincide respectively with $\mathbb{X}_{t_1,f}$ and $\mathbb{X}_{t_2,f}$.

We now illustrate each of these two cases with an example. Begin with an example of the first case, where $e \neq f$. This is represented on Figure 6.4. We only represent the perturbation $\mathbb{X}_{t,f_3}$ on this figure for clarity's sake. The perturbation datum $\mathbb{X}^{\infty}_{t,f_3}$ could a priori depend on l_{f_1}: the requirement $\mathbb{X}^{\infty}_{t,f_3} = \mathbb{X}_{t_1,f_3}$ says in particular that it is independent of l_{f_1}. Similarly, we illustrate the second case, where $e = f$, on Figure 6.5. A priori, $\mathbb{X}^{+}_{t,f_2}$ and $\mathbb{X}^{-}_{t,f_2}$ can depend on both l_{f_1} and l_{f_3}: the requirement $\mathbb{X}^{+}_{t,f_2} = \mathbb{X}_{t_2,f_2}$ says in particular that $\mathbb{X}^{+}_{t,f_2}$ is independent of l_{f_3}, and the same goes for $\mathbb{X}^{-}_{t,f_2} = \mathbb{X}_{t_1,f_2}$ with respect to l_{f_1}.

Definition 6.4.3. A choice of perturbation data $(\mathbb{X}_i)_{2 \leqslant i \leqslant n}$ is said to be *gluing-compatible* if it satisfies the conditions of Items (i) and (ii) for lengths of edges going toward $+\infty$.

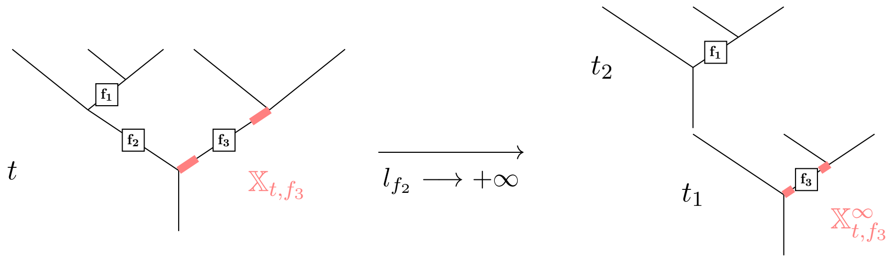

Figure 6.4

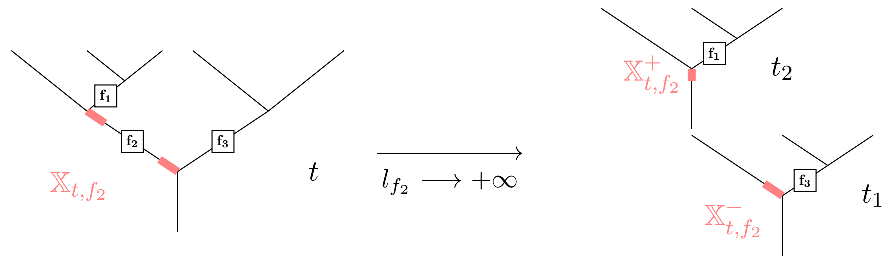

Figure 6.5

As explained in the two previous examples, a gluing-compatible choice of perturbation data has in particular the property that when lengths of edges go towards $+\infty$, the perturbation datum on each edge only depends on the lengths of the tree that the edge belongs to. If we only required that perturbation data on each edge have limits when lengths of edges go towards $+\infty$ without further assumptions, the (int-break) boundary component of Section 6.4.1 would in fact appear as a fiber product over the codimension 1 boundary of the compactified moduli space $\overline{\mathcal{T}}_n(t)$, since these limits might depend on the lengths of all edges of the broken tree obtained from t.

6.4.4 Admissible choices of perturbation data

Definition 6.4.4. A choice of perturbation data $(\mathbb{X}_n)_{n\geqslant 2}$ being smooth and gluing-compatible, and such that all maps $\phi_{\mathbb{X}_t}$ are transverse to Δ is said to be *admissible.*

Theorem 6.4.5. *Admissible choices of perturbation data on the moduli spaces $\mathcal{T}_n$ exist.*

Proof. See Section 8.2. □

Theorem 6.4.6. *Let $(\mathbb{X}_n)_{n\geqslant 2}$ be an admissible choice of perturbation data. The 0-dimensional moduli spaces $\mathcal{T}_t^{\mathbb{X}}(y; x_1, \dots, x_n)$ are compact. The 1-dimensional moduli spaces $\mathcal{T}_t^{\mathbb{X}}(y; x_1, \dots, x_n)$ can be compactified to 1-dimensional manifolds with boundary $\overline{\mathcal{T}}_t^{\mathbb{X}}(y; x_1, \dots, x_n)$, whose boundary is described in Section 6.4.1.*

Proof. This theorem results from the techniques of [35, Chapter 6]. □

Consider in fact an internal edge $f \in E(t)$ and write t_1 and t_2 for the trees obtained by breaking t at the edge f, where t_2 is seen to lie above t_1. Given critical points $y, z, x_1, \dots, x_n$ suppose moreover that the moduli spaces $\mathcal{T}_{t_1}(y; x_1, \dots, x_{i_1}, z, x_{i_1+i_2+1}, \dots, x_n)$ and $\mathcal{T}_{t_2}(z; x_{i_1+1}, \dots, x_{i_1+i_2})$ are 0-dimensional. Let T_1^{Morse} and T_2^{Morse} be two perturbed Morse gradient trees which belong respectively to the former and the latter moduli spaces. Theorem 6.4.6 implies in particular that there exists $R > 0$ and an embedding

$$\#_{T_1^{Morse},T_2^{Morse}} : [R, +\infty] \longrightarrow \overline{\mathcal{T}}_t(y; x_1, \ldots, x_n)$$

parametrizing a neighborhood of the boundary $\{T_1^{Morse}\} \times \{T_2^{Morse}\} \subset \partial \overline{\mathcal{T}}_t^{Morse}$, i.e. sending $+\infty$ to $(T_1^{Morse}, T_2^{Morse}) \in \partial \overline{\mathcal{T}}_t^{Morse}$. Such a map is called a *gluing map* for T_1^{Morse} and T_2^{Morse}. We will construct explicit gluing maps in Section 9.4.3.

6.5 ΩBAs -algebra structure on the Morse cochains We now have all the necessary material to define an ΩBAs-algebra structure on the Morse cochains $C^*(f)$.

Theorem 6.5.1. *Let $\mathbb{X} := (\mathbb{X}_n)_{n \geqslant 2}$ be an admissible choice of perturbation data. Defining for every n and $t \in SRT_n$ the operations m_t as*

$$\begin{aligned} m_t : C^*(f) \otimes \cdots \otimes C^*(f) &\longrightarrow C^*(f) \\ x_1 \otimes \cdots \otimes x_n &\longmapsto \sum_{|y| = \sum_{i=1}^n |x_i| - e(t)} \# \mathcal{T}_t^{\mathbb{X}}(y; x_1, \cdots, x_n) \cdot y \ , \end{aligned}$$

they endow the Morse cochains $C^*(f)$ with an ΩBAs-algebra structure.

Proof. The proof of this theorem is the subject of Section 9.4. Putting it shortly, counting the boundary points of the 1-dimensional orientable compactified moduli spaces $\overline{\mathcal{T}}_t^{\mathbb{X}}(y; x_1, \cdots, x_n)$ whose boundary is described in Section 6.4.1 yields the ΩBAs-equations

$$[\partial_{Morse}, m_t] = \sum_{t' \in coll(t)} \pm m_{t'} + \sum_{t_1 \#_i t_2 = t} \pm m_{t_1} \circ_i m_{t_2} \ . \qquad \square$$

In fact, the collection of operations $\{m_t\}$ does not exactly define an ΩBAs-algebra structure: one of the two differentials ∂_{Morse} appearing in the bracket $[\partial_{Morse}, \cdot]$ has to be twisted by a specific sign for the ΩBAs-equations to hold. We will speak about a *twisted ΩBAs-algebra structure* (Definition 9.3.1). In the case when M is odd-dimensional, this twisted ΩBAs-algebra is exactly an ΩBAs-algebra.

Remark 6.5.2. If we want to recover an A_∞-algebra structure on the Morse cochains, it suffices to apply the morphism of operads $A_\infty \to \Omega BAs$ of Proposition 3.1.15. In [3], Abouzaid constructs a geometric A_∞-morphism $C^*_{sing}(M) \to C^*(f)$, where the Morse cochains are endowed with the A_∞-algebra structure induced by the ΩBAs-algebra structure of Theorem 6.5.1. This A_∞-morphism is in fact a quasi-isomorphism. This implies in particular that the Morse cochains $C^*(f)$ endowed with the A_∞-algebra structure of Theorem 6.5.1 are quasi-isomorphic as an A_∞-algebra to the Morse cochains endowed with the A_∞-algebra structure induced by Theorem 1.6.1. Abouzaid's construction of the A_∞-morphism $C^*_{sing}(M) \to C^*(f)$ could be adapted to our present framework, and lifted to an ΩBAs-morphism. We will however not give more details on that matter.

Remark 6.5.3. We point out that Morse theory is the natural viewpoint that connects symplectic topology to differential topology, as pseudo-holomorphic curves tend to degenerate in the low-energy regime to Morse gradient flow trees: if symplectic topology is to be thought of as a quantization of differential topology, then pseudo-holomorphic curve theory is the quantization of Morse theory (see [14] and [11]). While the ΩBAs-algebra structure on the Morse cochains stems from Lemma 3.1.13, the A_∞-category structure on the Fukaya category of a symplectic manifold then stems from the fact that the compactified moduli spaces of stable disks with $n+1$ marked boundary points $\overline{\mathcal{D}}_{n,1}$ are naturally isomorphic to the associahedra K_n endowed with their A_∞-cell decomposition (see [37] for instance).

7. A_∞ and ΩBAs-morphisms between the Morse cochains

Let M be an oriented closed Riemannian manifold endowed with a Morse function f together with a Morse-Smale metric. We have proven in Section 6 that upon choosing admissible perturbation data on the moduli spaces of stable metric ribbon trees $\mathcal{T}_n(t)$, we can define moduli spaces of perturbed Morse gradient trees, whose count will define the operations m_t, $t \in SRT$, of an ΩBAs-algebra structure on the Morse cochains $C^*(f)$.

Consider now another Morse function g on M. Apply again Theorem 1.6.1 to the Morse cochains $C^*(f)$ and $C^*(g)$, which are deformation retracts of the singular cochains on M. Endowing them with their induced A_∞-algebra structures, this yields a diagram

$$(C^*(f), m_n^{ind}) \xrightarrow{\sim} (C^*_{sing}(M), \cup) \xrightarrow{\sim} (C^*(g), m_n^{ind}) ,$$

where each arrow is an A_∞-quasi-isomorphism, hence an A_∞-quasi-isomorphism $(C^*(f), m_n^{ind}) \to (C^*(g), m_n^{ind})$. Let moreover $\mathbb{X}^g$ be an admissible perturbation data for g. The previous quasi-isomorphism motivates the following question: endowing $C^*(f)$ and $C^*(g)$ with the ΩBAs-algebra structures of Theorem 6.5.1, can we construct an ΩBAs-morphism

$$(C^*(f), m_t^{\mathbb{X}^f}) \longrightarrow (C^*(g), m_t^{\mathbb{X}^g})$$

by counting perturbed Morse trees ?

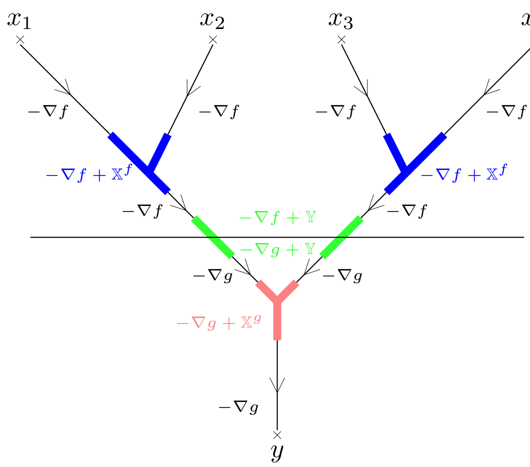

Figure 7.1: An example of a perturbed 2-colored Morse gradient tree, where the x_i are critical points of f and y is a critical point of g

While stable metric ribbon trees encode ΩBAs-algebra structures, we have seen that 2-colored stable metric ribbon trees encode ΩBAs-morphisms. The answer to the previous question is then positive, and the morphism will be constructed using moduli spaces of *2-colored perturbed Morse gradient trees*. As in Section 6, 2-colored Morse gradient trees will be defined by perturbing Morse gradient equations around each vertex of the tree, where the Morse gradient is $-\nabla f$

above the gauge and $-\nabla g$ below the gauge. This is illustrated in Figure 7.1. The figure is incorrect, because we will not choose the perturbation to be equal to $\mathbb{X}^f$ above the gauge and to $\mathbb{X}^g$ below, but conveys the correct intuition on the construction we unfold in this section.

The structure of this section follows the same lines as Section 6, and the only difficulty will consist in adapting properly our arguments to the combinatorics of 2-colored ribbon trees. Under a generic choice of perturbation data on the moduli spaces $\mathcal{CT}_n$, the moduli spaces of 2-colored perturbed Morse gradient trees connecting $x_1, \dots, x_n \in \mathrm{Crit}(g)$ to $y \in \mathrm{Crit}(g)$, that we denote $\mathcal{CT}_{t_c}(y; x_1, \dots, x_n)$, are orientable manifolds. They are moreover compact when 0-dimensional and can be compactified to compact manifolds with boundary when 1-dimensional (Theorems 7.3.3 and 7.3.4). Counting 2-colored Morse gradient trees then defines an ΩBAs-morphism from $C^*(f)$ to $C^*(g)$, called a *continuation morphism* (Theorem 7.4.1). We prove in Theorem 7.4.5 that continuation morphisms are in fact quasi-isomorphisms. We finally discuss in Section 7.5 the two problems that naturally arise from our construction of continuation morphisms and that will be the respective starting points to the part II and part III to this series of articles.

7.1 Perturbed 2-colored Morse gradient trees A 2-colored metric ribbon tree T_c will be written $(t_c, \{L_{f_c}\}_{f_c \in E(t_c)})$ from the viewpoint of Definition 3.2.1 and $(t_c, \lambda, \{l_e\}_{e \in E(t)})$ from the viewpoint of Definition 3.2.2, where t denotes the underlying stable ribbon tree of t_c.

Definition 7.1.1. A *choice of perturbation data* $\mathbb{Y}$ on a 2-colored metric ribbon tree T_c is defined to be a choice of perturbation data on the metric ribbon tree $(t_c, \{L_{f_c}\})$ in the sense of Definition 6.2.1.

Definition 7.1.2. A *2-colored perturbed Morse gradient tree* T_c^{Morse} associated to a pair 2-colored metric ribbon tree and perturbation data $(T_c, \mathbb{Y})$ is the data

(i) for each edge f_c of t_c which is above the gauge of a smooth map
$$D_{f_c} \xrightarrow[\gamma_{f_c}]{} M ,$$
such that γ_{f_c} is a trajectory of the perturbed negative gradient $-\nabla f + \mathbb{Y}_{f_c}$,

(ii) for each edge f_c of t_c which is below the gauge of a smooth map
$$D_{f_c} \xrightarrow[\gamma_{f_c}]{} M ,$$
such that γ_{f_c} is a trajectory of the perturbed negative gradient $-\nabla g + \mathbb{Y}_{f_c}$,

and such that the endpoints of these trajectories coincide as prescribed by the edges of the tree t_c.

Remark 7.1.3. We point out that the above definitions still work for $+$. A choice of perturbation data for $+$ is the data of vector fields
$$[0, +\infty[\times M \xrightarrow[\mathbb{Y}_+]{} TM \qquad]-\infty, 0] \times M \xrightarrow[\mathbb{Y}_-]{} TM ,$$
which vanish away from a length 1 segment, and a 2-colored perturbed Morse gradient tree associated to $(+, \mathbb{Y})$ is then simply the data of two smooth maps
$$]-\infty, 0] \xrightarrow[\gamma_-]{} M \qquad [0, +\infty[\xrightarrow[\gamma_+]{} M ,$$
such that γ_- is a trajectory of $-\nabla f + \mathbb{Y}_-$ and γ_+ is a trajectory of $-\nabla g + \mathbb{Y}_+$.

A 2-colored perturbed Morse gradient tree can be equivalently defined by following the flows of $-\nabla f + \mathbb{Y}$ and $-\nabla g + \mathbb{Y}$ along the metric ribbon tree (t_c, L_{f_c}), as it is determined by the data of the time -1 points on its incoming edges plus the time 1 point on its outgoing edge. Introduce again the map

$$\Phi_{T_c,\mathbb{Y}} : M \times \cdots \times M \underset{\phi_{0,\mathbb{Y}} \times \cdots \times \phi_{n,\mathbb{Y}}}{\longrightarrow} M \times \cdots \times M ,$$

defined as in Section 6.2, and set Δ for the diagonal of $M^{\times n+1}$

Proposition 7.1.4. *There is a one-to-one correspondence*

$$\left\{ \begin{array}{c} \textit{2-colored perturbed Morse gradient trees} \\ \textit{associated to } (T_c, \mathbb{Y}) \end{array} \right\} \longleftrightarrow (\Phi_{T_c,\mathbb{Y}})^{-1}(\Delta) \quad .$$

The vector fields on the incoming edges are equal to $-\nabla f$ away from a length 1 segment, hence the trajectories associated to these edges all converge to critical points of the function f, while the vector field on the outgoing edge is equal to $-\nabla g$ away from a length 1 segment, hence the trajectory associated to these edge converges to a critical point of the function g. For critical points y of the function g and $x_1, \dots, x_n$ of the function f, the map $\Phi_{T_c,\mathbb{Y}}$ can be restricted to

$$W^S_g(y) \times W^U_f(x_1) \times \cdots \times W^U_f(x_n) ,$$

such that the inverse image of the diagonal yields all 2-colored perturbed Morse gradient trees associated to $(T_c, \mathbb{Y})$ connecting $x_1, \dots, x_n$ to y.

7.2 Moduli spaces of 2-colored perturbed Morse gradient trees Let t_c be a 2-colored stable ribbon tree of arity n together with an ordering Ω on t_c. We write $(*)_{t_c}$ for the set of inequalities and equalities on $(l_e)_{e \in E(t)}$ and λ, which define the polyhedral cone $\mathcal{CT}_n(t_c, \Omega) \subset \mathbb{R}^{e(t)+1}$ in Definition 5.2.5. Define for all $f_c \in \overline{E}(t_c)$, the cone $C_{f_c} \subset \mathcal{CT}_n(t_c, \Omega) \times \mathbb{R} \subset \mathbb{R}^{e(t)+1} \times \mathbb{R}$ to be

(i) $\{(\lambda, (l_e)_{e \in E(T)}, s)$ such that $(*)_{t_c}$, $0 \leqslant s \leqslant L_{f_c}(\lambda, \{l_e\}_{e \in E(T)})\}$ if f_c is an internal edge ;
(ii) $\{(\lambda, (l_e)_{e \in E(T)}, s)$ such that $(*)_{t_c}$, $s \leqslant 0\}$ if f_c is an incoming edge ;
(iii) $\{(\lambda, (l_e)_{e \in E(T)}, s)$ such that $(*)_{t_c}$, $s \geqslant 0\}$ if f_c is the outgoing edge.

Example 7.2.1. We consider the following 2-colored tree t_c with ordering $e_1 < e_2$ on the underlying ribbon tree t

$t_c :=$ 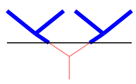 $t :=$ 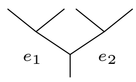

.

We then denote f_1, f_2 and f_3 the following three edges of the 2-colored tree t_c

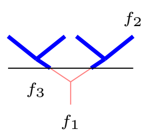

.

The cones $C_{f_i} \subset \mathbb{R}^4$ are then equal to

$$C_{f_1} = \{(\lambda, l_1, l_2, s),\ 0 < -\lambda < l_1, l_2 \text{ and } s \geqslant 0\} ,$$
$$C_{f_2} = \{(\lambda, l_1, l_2, s),\ 0 < -\lambda < l_1, l_2 \text{ and } s \leqslant 0\} ,$$
$$C_{f_3} = \{(\lambda, l_1, l_2, s),\ 0 < -\lambda < l_1, l_2 \text{ and } 0 \leqslant s \leqslant -\lambda\} .$$

Then a choice of perturbation data for every 2-colored metric ribbon tree in $\mathcal{CT}_n(t_c)$, yields maps $\mathbb{Y}_{t_c,f_c} : C_{f_c} \times M \longrightarrow TM$ for every edge f_c of t_c.

Definition 7.2.2. A choice of perturbation data $\mathbb{Y}_{t_c}$ is said to be *smooth* if all the maps $\mathbb{Y}_{t_c,f_c}$ extend to smooth maps $\mathbb{R}^{e(t)+1} \times \mathbb{R} \times M \to TM$.

Definition 7.2.3. Let $\mathbb{Y}_{t_c}$ be a smooth choice of perturbation data on the moduli space $\mathcal{CT}_n(t_c)$. Given $y \in \mathrm{Crit}(g)$ and $x_1, \dots, x_n \in \mathrm{Crit}(f)$, we define the moduli spaces

$$\mathcal{CT}_{t_c}^{\mathbb{Y}_{t_c}}(y; x_1, \dots, x_n) := \left\{ \begin{array}{c} \text{2-colored perturbed Morse gradient trees associated to } (T_c, \mathbb{Y}_{T_c}) \\ \text{and connecting } x_1, \dots, x_n \text{ to } y \text{ for } T_c \in \mathcal{CT}_n(t_c) \end{array} \right\} .$$

Using the smooth map

$$\phi_{\mathbb{Y}_{t_c}} : \mathcal{CT}_n(t_c) \times W^S(y) \times W^U(x_1) \times \cdots \times W^U(x_n) \longrightarrow M^{\times n+1} ,$$

this moduli space can be rewritten as

$$\mathcal{CT}_{t_c}^{\mathbb{Y}_{t_c}}(y; x_1, \dots, x_n) = \phi_{\mathbb{Y}_{t_c}}^{-1}(\Delta) .$$

Proposition 7.2.4. *(i) Given a choice of perturbation data $\mathbb{Y}_{t_c}$ making $\phi_{\mathbb{Y}_{t_c}}$ transverse to the diagonal $\Delta \subset M^{\times n+1}$, the moduli spaces $\mathcal{CT}_{t_c}^{\mathbb{Y}_{t_c}}(y; x_1, \dots, x_n)$ are orientable manifolds of dimension*

$$\dim\left(\mathcal{CT}_{t_c}(y; x_1, \dots, x_n)\right) = +|y| - \sum_{i=1}^n |x_i| - |t_c| .$$

(ii) Choices of perturbation data $\mathbb{Y}_{t_c}$ such that $\phi_{\mathbb{Y}_{t_c}}$ is transverse to the diagonal Δ exist.

Proof. The proof of this proposition is identical to the proof of Proposition 6.3.3. □

7.3 Compactifications

7.3.1 Compactification of the 1-dimensional manifolds $\mathcal{CT}_{t_c}^{\mathbb{Y}_{t_c}}(y; x_1, \dots, x_n)$

We would like to compactify the 1-dimensional moduli spaces $\mathcal{CT}_{t_c}^{\mathbb{Y}_{t_c}}(y; x_1, \dots, x_n)$ to 1-dimensional manifolds with boundary. Their boundary components are going to be given by those coming from the compactification of the moduli space $\mathcal{CT}_n(t_c)$, and the compactifications of the unstable manifolds $W^U(x_i)$ and of the stable manifold $W^S(y)$.

Choose admissible perturbation data $\mathbb{X}^f$ and $\mathbb{X}^g$ for the functions f and g. Choose moreover smooth perturbation data $\mathbb{Y}_{t_c}$ for all $t_c \in SCRT_i$, $1 \leqslant i \leqslant n$. We will again denote $\mathbb{Y}_n := (\mathbb{Y}_{t_c})_{t_c \in SCRT_n}$, and call it a choice of perturbation data on $\mathcal{CT}_n$. Fixing a 2-colored stable ribbon tree $t_c \in SCRT_n$ we would like to compactify the 1-dimensional moduli space $\mathcal{CT}_{t_c}^{\mathbb{Y}_{t_c}}(y; x_1, \dots, x_n)$ using the perturbation data $\mathbb{X}^f$, $\mathbb{X}^g$ and $(\mathbb{Y}_i)_{1 \leqslant i \leqslant n}$, such that its boundary would be given by the following spaces:

(i) an external edge breaks at a critical point (Morse):

$$\mathcal{T}(y; z) \times \mathcal{CT}_{t_c}^{\mathbb{Y}_{t_c}}(z; x_1, \dots, x_n) \text{ and } \mathcal{CT}_{t_c}^{\mathbb{Y}_{t_c}}(y; x_1, \dots, z, \dots, x_n) \times \mathcal{T}(z; x_i) ;$$

(ii) an internal edge of the tree t collapses (int-collapse):

$$\mathcal{CT}_{t'_c}^{\mathbb{Y}_{t'_c}}(y; x_1, \dots, x_n)$$

where $t'_c \in SCRT_n$ are all the 2-colored trees obtained by collapsing exactly one internal edge, which does not cross the gauge ;

(iii) the gauge moves to cross exactly one additional vertex of the underlying stable ribbon tree (gauge-vertex):

$$\mathcal{CT}_{t'_c}^{\mathbb{Y}_{t'_c}}(y; x_1, \dots, x_n)$$

where $t'_c \in SCRT_n$ are all the 2-colored trees obtained by moving the gauge to cross exactly one additional vertex of t ;

(iv) an internal edge located above the gauge or intersecting it breaks or, when the gauge is below the root, the outgoing edge breaks between the gauge and the root (above-break):

$$\mathcal{CT}_{t_c^1}^{\mathbb{Y}_{t_c^1}}(y; x_1, \dots, x_{i_1}, z, x_{i_1+i_2+1}, \dots, x_n) \times \mathcal{T}_{t^2}^{\mathbb{X}^f_{t^2}}(z; x_{i_1+1}, \dots, x_{i_1+i_2}) \ ;$$

(v) edges (internal or incoming) that are possibly intersecting the gauge, break below it, such that there is exactly one edge breaking in each non-self crossing path from an incoming edge to the root (below-break):

$$\mathcal{T}_{t^1}^{\mathbb{X}^g_{t^0}}(y; y_1, \dots, y_s) \times \mathcal{CT}_{t_c^1}^{\mathbb{Y}_{t_c^1}}(y_1; x_1, \dots) \times \dots \times \mathcal{CT}_{t_c^s}^{\mathbb{Y}_{t_c^s}}(y_s; \dots, x_n) \ .$$

7.3.2 Smooth and gluing-compatible choices of perturbation data

The (Morse) boundaries are again a simple consequence of the fact that external edges are Morse trajectories away from a length 1 segment. Perturbation data that behave well with respect to the (int-collapse) and (gauge-vertex) boundaries are defined using simple adjustments of the discussion in Section 6.4.2, i.e. by asking that all maps $\tilde{\mathbb{Y}}_{t_c,f_c}$ extend to smooth maps $\mathbb{R}^{e(t)+1} \times \mathbb{R} \times M \to TM$. Hence, it only remains to specify the required behaviours under the breaking of edges.

We begin with the (above-break) boundary. Writing t_c for the 2-colored ribbon tree associated to t_c, it corresponds to the breaking of an internal edge f_c of t_c situated above the set of colored vertices. Denote t_c^1 and t^2 the trees obtained by breaking t_c at the edge f_c, where t^2 is seen to lie above t_c^1. We have to specify, for each edge $e_c \in \overline{E}(t_c)$, what happens to the perturbation $\mathbb{Y}_{t_c,e}$ at the limit.

(i) For $e_c \in \overline{E}(t^2)$ and $\neq f_c$, we require that

$$\lim \mathbb{Y}_{t_c,e_c} = \mathbb{X}^f_{t^2,e_c} \ .$$

(ii) For $e_c \in \overline{E}(t_c^1)$ and $\neq f_c$, we require that

$$\lim \mathbb{Y}_{t_c,e_c} = \mathbb{Y}_{t_c^1,e_c} \ .$$

(iii) For $f_c = e_c$, $\mathbb{Y}_{t_c,f_c}$ yields two parts at the limit: the part corresponding to the outgoing edge of t^1 and the part corresponding to the incoming edge of t_c^1. We then require that they coincide respectively with the perturbation $\mathbb{X}^f_{t^2,e_c}$ and $\mathbb{Y}_{t_c^1,e_c}$.

Leaving the notations aside, an example of each case is illustrated in Figure 7.2.

We conclude with the (below-break) boundary. Denote $t_c^1, \dots, t_c^s$ and t^0 the trees obtained by the chosen breaking of t_c below the gauge, where $t_c^1, \dots, t_c^s$ are seen to lie above t^0.

(i) For $e_c \in \overline{E}(t_c^i)$ and not among the breaking edges, we require that

$$\lim \mathbb{Y}_{t_c,e_c} = \mathbb{Y}_{t_c^i,e_c} \ .$$

(ii) For $e_c \in \overline{E}(t^1)$ and not among the breaking edges, we require that

$$\lim \mathbb{Y}_{t_c,e_c} = \mathbb{X}^g_{t^0,e_c} \ .$$

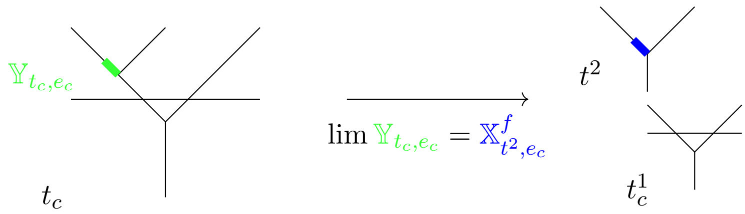

(above-break) case (i)

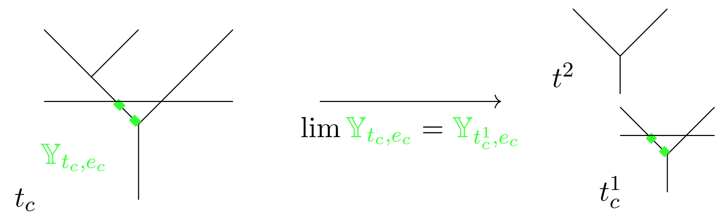

(above-break) case (ii)

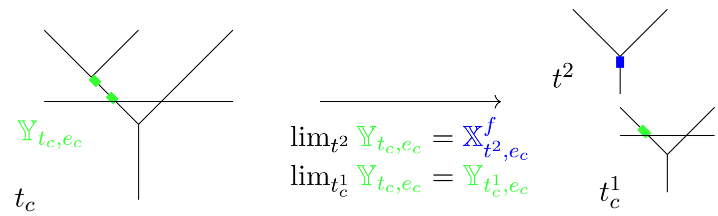

(above-break) case (iii)

Figure 7.2

(iii) For f_c among the breaking edges, $\mathbb{Y}_{t_c,f_c}$ yields two parts at the limit: the part corresponding to the outgoing edge of a t_c^j and the part corresponding to the incoming edge of t^0. We then require that they coincide respectively with the perturbation $\mathbb{Y}_{t_c^j}$ and $\mathbb{X}^g_{t^0}$.

This is again illustrated on Figure 7.3.

Definition 7.3.1. (i) A choice of perturbation data $\mathbb{Y}$ on the moduli spaces $\mathcal{CT}_n$ is said to be *smooth* if it is compatible with the (int-collapse) and (gauge-vertex) boundaries.

(ii) A smooth choice of perturbation data is said to be *gluing-compatible w.r.t.* $\mathbb{X}^f$ *and* $\mathbb{X}^g$ if it satisfies the (above-break) and (below-break) conditions described in this section.

As we explained in Section 6.4.3, a gluing-compatible choice of perturbation data has in particular the property that when lengths of edges go towards $+\infty$, the perturbation datum on each edge only depends on the lengths of the tree/the 2-colored tree that the edge belongs to. This ensures that the (above-break) and (below-break) boundary components of Section 7.3.1 actually appear as standard products and not as fiber products over the codimension 1 boundary of the compactified moduli spaces $\overline{\mathcal{CT}}_n(t_c)$.

7.3.3 Admissible choices of perturbation data

Definition 7.3.2. Smooth and consistent choices of perturbation data $(\mathbb{Y}_n)_{n\geqslant 1}$ such that all maps $\phi_{\mathbb{Y}_{t_c}}$ are transverse to the diagonal Δ are called *admissible w.r.t.* $\mathbb{X}^f$ *and* $\mathbb{X}^g$ or simply *admissible*.

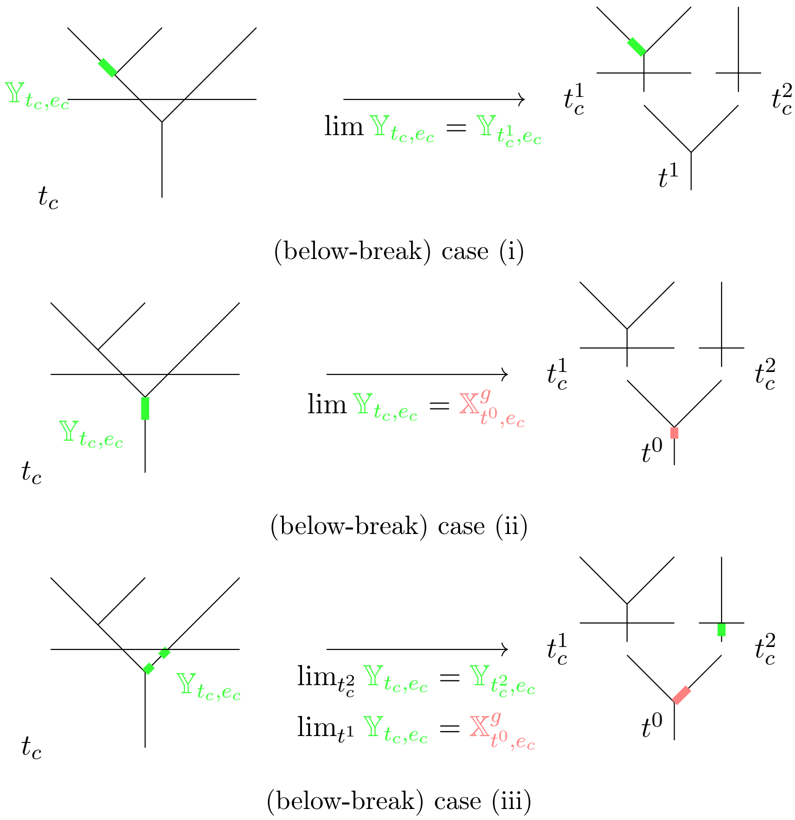

Figure 7.3

Theorem 7.3.3. *Given admissible choices of perturbation data $\mathbb{X}^f$ and $\mathbb{X}^g$ on the moduli spaces $\mathcal{T}_n$, choices of perturbation data on the moduli spaces $\mathcal{CT}_n$ that are admissible w.r.t. $\mathbb{X}^f$ and $\mathbb{X}^g$ exist.*

Proof. The proof is identical to the proof of Theorem 6.4.5. □

Theorem 7.3.4. *Let $(\mathbb{Y}_n)_{n\geqslant 1}$ be an admissible choice of perturbation data on the moduli spaces $\mathcal{CT}_n$. The 0-dimensional moduli spaces $\mathcal{CT}^{\mathbb{Y}}_{t_c}(y; x_1, \dots, x_n)$ are compact. The 1-dimensional moduli spaces $\mathcal{CT}^{\mathbb{Y}}_{t_c}(y; x_1, \dots, x_n)$ can be compactified to 1-dimensional manifolds with boundary, whose boundary is described in Section 7.3.1.*

Proof. This theorem is again a consequence of the techniques of [35, Chapter 6]. □

We point out that Theorem 7.3.4 implies in particular the existence of gluing maps

$$\#^{above-break}_{T_c^{1,Morse},T^{2,Morse}} : [R, +\infty] \longrightarrow \overline{\mathcal{CT}}_{t_c}(y; x_1, \dots, x_n)$$
$$\#^{below-break}_{T^{0,Morse},T_c^{1,Morse},\dots,T_c^{s,Morse}} : [R, +\infty] \longrightarrow \overline{\mathcal{CT}}_{t_c}(y; x_1, \dots, x_n)$$

where our choice of notation is as in Section 6.4.4. We will construct explicit gluing maps in Section 9.5.4.

7.4 Continuation morphisms Let $\mathbb{X}^f$ and $\mathbb{X}^g$ be admissible choices of perturbation data for the Morse functions f and g. Denote $(C^*(f), m_t^{\mathbb{X}^f})$ and $(C^*(g), m_t^{\mathbb{X}^g})$ the ΩBAs-algebras constructed in Theorem 6.5.1.

Theorem 7.4.1. *Let $(\mathbb{Y}_n)_{n \geqslant 1}$ be a choice of perturbation on the moduli spaces $\mathcal{CT}_n$ that is admissible w.r.t. $\mathbb{X}^f$ and $\mathbb{X}^g$. Defining for every n and $t_c \in SCRT_n$ the operations μ_{t_c} as*

$$\begin{aligned} \mu^{\mathbb{Y}}_{t_c} : C^*(f) \otimes \cdots \otimes C^*(f) &\longrightarrow C^*(g) \\ x_1 \otimes \cdots \otimes x_n &\longmapsto \sum_{|y| = \sum_{i=1}^{n} |x_i| + |t_c|} \# \mathcal{CT}^{\mathbb{Y}}_{t_c}(y; x_1, \cdots, x_n) \cdot y \ . \end{aligned}$$

they fit into an ΩBAs-morphism $\mu^{\mathbb{Y}} : (C^*(f), m_t^{\mathbb{X}^f}) \to (C^*(g), m_t^{\mathbb{X}^g})$.

Proof. The proof is similar to the proof of Theorem 6.5.1, and postponed to Section 9.5. In fact, we will prove that the collection of operations $\{\mu_{t_c}\}$ does not exactly define an ΩBAs-morphism but rather a *twisted ΩBAs-morphism*. In the case when M is odd-dimensional, this twisted ΩBAs-morphism is exactly an ΩBAs-morphism between two ΩBAs-algebras. □

Remark 7.4.2. If we want to go back to the algebraic framework of A_∞-algebras, an A_∞-morphism between the induced A_∞-algebra structures on the Morse cochains is simply obtained under the morphism of operadic bimodules $M_\infty \to M_{\Omega BAs}$ of Proposition 3.2.25.

Remark 7.4.3. In symplectic topology, A_∞-functors between Fukaya categories are constructed by couting pseudo-holomorphic quilted disks with marked boundary points and Lagrangian boundary and seam conditions. This is the subject of the work of [31] and [30].

Definition 7.4.4. ΩBAs-morphisms $\mu^{\mathbb{Y}}$ associated to admissible choices of perturbation data $\mathbb{Y}$ will be called *continuation morphisms.*

Theorem 7.4.5. *Continuations morphisms are quasi-isomorphisms.*

Proof. We want to prove that the arity 1 component $\mu^{\mathbb{Y}}_{+} : C^*(f) \to C^*(g)$ is a map which induces an isomorphism in cohomology. In this regard, consider three perturbation data on $\mathcal{CT}_1 := \{+\}$, $\mathbb{Y}^{fg}_{+}$, $\mathbb{Y}^{gf}_{+}$ and $\mathbb{Y}^{ff}_{+}$, defining chain maps

$$\mu^{\mathbb{Y}^{ij}_{+}} : C^*(i) \longrightarrow C^*(j) \ .$$

We will introduce in Section 9.6 moduli spaces of perturbed trees $\mathcal{H}(y; x)$ and prove that their count defines a homotopy $h : C^*(f) \to C^*(f)$ between the chain maps $\mu^{\mathbb{Y}^{gf}}_{+} \circ \mu^{\mathbb{Y}^{fg}}_{+}$ and $\mu^{\mathbb{Y}^{ff}}_{+}$ in Lemma 9.6.2. Specializing to the case where $\mathbb{Y}^{ff}_{+}$ is null, the equality $\mu^{\mathbb{Y}^{ff}_{+}} = \mathrm{id}$ then concludes the proof. □

Remark 7.4.6. In Remark 6.5.2, we explained that given any Morse function f together with an admissible choice of perturbation data $\mathbb{X}^f$, the Morse cochains $C^*(f)$ and the singular cochains $C^*_{sing}(M)$ are quasi-isomorphic as ΩBAs-algebras. In particular, given another Morse function g together with an admissible choice of perturbation data $\mathbb{X}^g$, the Morse cochains $C^*(f)$ and $C^*(g)$ are quasi-isomorphic as ΩBAs-algebras. Continuation morphisms realize such quasi-isomorphisms explicitly.

7.5 Towards higher algebra Two questions naturally arise from our construction of continuation morphisms. They will respectively be the starting point to the part II and part III to this series of articles.

Problem 1. Given two Morse functions f, g, choices of perturbation data $\mathbb{X}^f$ and $\mathbb{X}^g$, and choices of perturbation data $\mathbb{Y}$ and $\mathbb{Y}'$, is $\mu^{\mathbb{Y}}$ always A_∞-homotopic (resp. ΩBAs-homotopic) to $\mu^{\mathbb{Y}'}$? I.e., when can the following diagram be filled in the A_∞ (resp. ΩBAs) world

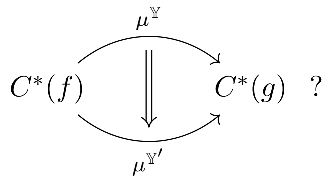

In which sense, with which notion of homotopy can it be filled ? And in general, which notion of higher operadic algebra naturally encodes this type of problem ?

This problem is solved in [32] by introducing the notions of n-A_∞-morphisms and n-ΩBAs-morphisms. In this article, we will show that the simplicial set consisting of higher morphisms defined by a count of perturbed Morse gradient trees is a Kan complex which is contractible, giving a higher categorical meaning to the fact that continuation morphisms in Morse theory are well-defined up to homotopy at chain level.

Problem 2. Given three Morse functions f_0, f_1, f_2, choices of perturbation data $\mathbb{X}^i$, and choices of perturbation data $\mathbb{Y}^{ij}$ defining continuation morphisms

$$\begin{aligned}
\mu^{\mathbb{Y}^{01}} &: (C^*(f_0), m_t^{\mathbb{X}^0}) \longrightarrow (C^*(f_1), m_t^{\mathbb{X}^1}) \ , \\
\mu^{\mathbb{Y}^{12}} &: (C^*(f_1), m_t^{\mathbb{X}^1}) \longrightarrow (C^*(f_2), m_t^{\mathbb{X}^2}) \ , \\
\mu^{\mathbb{Y}^{02}} &: (C^*(f_0), m_t^{\mathbb{X}^0}) \longrightarrow (C^*(f_2), m_t^{\mathbb{X}^2}) \ ,
\end{aligned}$$

can we construct an A_∞-homotopy (or an ΩBAs-homotopy) such that $\mu^{\mathbb{Y}^{12}} \circ \mu^{\mathbb{Y}^{01}} \simeq \mu^{\mathbb{Y}^{02}}$ through this homotopy ? That is can the following diagram be filled in the A_∞ (resp. ΩBAs) world

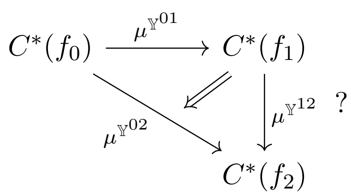

Which higher operadic algebra naturally arises from this basic question ?

We point out that the proof of Theorem 7.4.5 solves the arity 1 step of this problem. It will be adressed in an upcoming paper, in which it will appear that the combinatorics of n-A_∞-morphisms and of multicolored trees provide a natural framework to solve this question. This question is moreover closely related to the work of Mau, Wehrheim and Woodward on pseudo-holomorphic quilted disks ([30]) and of Bottman on witch curves and the 2-associahedra ([7, 8]).

8. Transversality

The goal of this section is to prove Theorem 6.4.5. In this regard, we recall at first the parametric transversality lemma and then build an admissible choice of perturbation data $(\mathbb{X}_n)_{n\geqslant 2}$ on the moduli spaces $\mathcal{T}_n$, proceeding by induction on the number of internal edges $e(t)$ of a stable ribbon tree t. It moreover appears in our construction that all arguments adapt nicely to the framework of 2-colored trees and admissible choices of perturbation data $(\mathbb{Y}_n)_{n\geqslant 1}$ on the moduli spaces $\mathcal{CT}_n$.

8.1 Parametric transversality lemma

We begin by recalling Smale's generalization of the classical Sard theorem. See [38] or [34] for a complete proof:

Theorem 8.1.1 (Sard-Smale theorem). *Let X and Y be separable Banach manifolds. Suppose that $f : X \to Y$ is a Fredholm map of class C^l with $l \geqslant \max(1, \mathrm{ind}(f) + 1)$. Then the set $Y_{reg}(f)$ of regular values of f is residual in Y in the sense of Baire.*

Theorem 8.1.1 implies in particular the following corollary in transversality theory, that will constitute the cornerstone of our proof of Theorem 6.4.5:

Corollary 8.1.2 (Parametric transversality lemma). *Let $\mathfrak{X}$ be a Banach space, M and N two finite-dimensional manifolds and $S \subset N$ a submanifold of N. Suppose that $f : \mathfrak{X} \times M \to N$ is a map of class C^l with $l \geqslant \max(1, \dim(M) + \dim(S) - \dim(N) + 1)$ and that it is transverse to S. Then the set*

$$\mathfrak{X}_{\pitchfork S} := \{\mathbb{X} \in \mathfrak{X} \text{ such that } f_{\mathbb{X}} \pitchfork S\}$$

is residual in $\mathfrak{X}$ in the sense of Baire.

Proof. The map f being transverse to S, the inverse image $f^{-1}(S)$ is a Banach submanifold of $\mathfrak{X} \times M$. Consider the standard projection $p_{\mathfrak{X}} : \mathfrak{X} \times M \to \mathfrak{X}$ and denote $\pi := p_{\mathfrak{X}}|_{f^{-1}(S)}$. Following [4, Lemma 19.2], this map is Fredholm and has index $\dim(M) + \dim(S) - \dim(N)$. Moreover, drawing from an argument in [34, Section 3.2], there is an equality $\mathfrak{X}_{reg}(\pi) = \mathfrak{X}_{\pitchfork S}$. One can then conclude by applying Theorem 8.1.1 to the map π. □

8.2 Proof of Theorem 6.4.5

8.2.1 The case $e(t) = 0$

If $e(t) = 0$, the tree t is a corolla. Fix an integer l such that

$$l \geqslant \max\left(1, |y| - \sum_{i=1}^{n} |x_i| + 1\right) .$$

We define C^l-choices of perturbation data in a similar fashion to smooth choices of perturbation data. A C^l-choice of perturbation data $\mathbb{X}_t$ on $\mathcal{T}_n(t)$ then simply corresponds to a C^l-choice of perturbation datum on each external edge of t. Define the parametrization space

$$\mathfrak{X}_t^l := \{C^l\text{-perturbation data } \mathbb{X}_t \text{ on the moduli space } \mathcal{T}_n(t)\} .$$

This parametrization space is a Banach space. The linear combination of choices of perturbation data is simply defined as the linear combination of each perturbation datum $\mathbb{X}_{t,e}$ with e an external edge of t. The vector space $\mathfrak{X}_t^l$ is moreover Banach as each perturbation datum $\mathbb{X}_{t,e}$ vanishes away from a length 1 segment in D_e.

Given critical points y and $x_1, \ldots, x_n$, introduce the C^l-map

$$\phi_t : \mathfrak{X}_t^l \times \mathcal{T}_n(t) \times W^S(y) \times W^U(x_1) \times \cdots \times W^U(x_n) \longrightarrow M^{\times n+1} ,$$

such that for every $\mathbb{X}_t \in \mathfrak{X}_t^l$, $\phi_t(\mathbb{X}_t, \cdot) = \phi_{\mathbb{X}_t}$. Note that we should in fact write $\phi_t^{y,x_1,\ldots,x_n}$ as the domain of ϕ_t depends on $y, x_1, \ldots, x_n$. The map ϕ_t is then a submersion. This is proven in [3, Lemma 7.3] and Abouzaid explains it informally in the following terms: "[this lemma] is the infinitesimal version of the fact that perturbing the gradient flow equation on a bounded subset of an edge integrates to an essentially arbitrary diffeomorphism".

In particular the map ϕ_t is transverse to the diagonal $\Delta \subset M^{\times n+1}$. Applying Corollary 8.1.2, there exists a residual set $\mathfrak{Y}_t^{l;y,x_1,\dots x_n} \subset \mathfrak{X}_t^l$ such that for every choice of perturbation data $\mathbb{X}_t \in \mathfrak{Y}_t^{l;y,x_1,\dots x_n}$ the map $\phi_{\mathbb{X}_t}$ is transverse to the diagonal $\Delta \subset M^{\times n+1}$. Considering the intersection

$$\mathfrak{Y}_t^l := \bigcap_{y,x_1,\dots,x_n} \mathfrak{Y}_t^{y,x_1,\dots x_n} \subset \mathfrak{X}_t$$

which is again residual, any $\mathbb{X}_t \in \mathfrak{Y}_t^l$ yields a C^l-choice of perturbation data on $\mathcal{T}_n(t)$ such that all the maps $\phi_{\mathbb{X}_t}$ are transverse to the diagonal $\Delta \subset M^{\times n+1}$. It remains to prove this statement in the smooth case.

8.2.2 Achieving smoothness à la Taubes

Using an argument drawn from [34, Section 3.2] and attributed to Taubes, we now prove that the set

$$\mathfrak{Y}_t := \left\{ \begin{array}{l} \text{smooth choices of perturbation data } \mathbb{X}_t \text{ on } \mathcal{T}_n(t) \text{ such that} \\ \text{all the maps } \phi_{\mathbb{X}_t} \text{ are transverse to the diagonal } \Delta \subset M^{\times n+1} \end{array} \right\}$$

is residual in the Fréchet space

$$\mathfrak{X}_t := \{\text{smooth choices of perturbation data } \mathbb{X}_t \text{ on } \mathcal{T}_n(t)\} \ .$$

Choose an exhaustion by compact sets $L_0 \subset L_1 \subset L_2 \subset \cdots$ of the space $\mathcal{T}_n(t) \times W^S(y) \times W^U(x_1) \times \cdots \times W^U(x_n)$. Define

$$\mathfrak{Y}_{t,L_m} := \left\{ \begin{array}{l} \text{smooth choices of perturbation data } \mathbb{X}_t \text{ on } \mathcal{T}_n(t) \text{ such that} \\ \text{all maps } \phi_{\mathbb{X}_t} \text{ are transverse on } L_m \text{ to the diagonal of } M^{\times n+1} \end{array} \right\}$$

and note that

$$\mathfrak{Y}_t = \bigcap_{m=0}^{+\infty} \mathfrak{Y}_{t,L_m} \ .$$

We will prove that each $\mathfrak{Y}_{t,L_m} \subset \mathfrak{Y}_t$ is open and dense in $\mathfrak{X}_t$ to conclude that $\mathfrak{Y}_t$ is indeed residual.

Fix $m \geqslant 0$. To prove that the set $\mathfrak{Y}_{t,L_m}$ is open in $\mathfrak{X}_t$ it suffices to prove that for every l, the set $\mathfrak{Y}_{t,L_m}^l$ is open in $\mathfrak{X}_t^l$, where $\mathfrak{Y}_{t,L_m}^l$ is defined by replacing "smooth" by "C^l" in the definition of $\mathfrak{Y}_{t,L_m}$. This last result is a simple consequence of the fact that "being transverse on a compact subset" is an open property: if the map $\phi_{\mathbb{X}_t^0}$ is transverse on L_m to the diagonal $\Delta \subset M^{\times n+1}$ then for $\mathbb{X}_t \in \mathfrak{X}_t^l$ sufficiently close to $\mathbb{X}_t^0$ the map $\phi_{\mathbb{X}_t}$ is again transverse on L_m to the diagonal on L_m.

Let now $\mathbb{X}_t \in \mathfrak{X}_t$. As $\mathbb{X}_t \in \mathfrak{X}_t^l$ and the set $\mathfrak{Y}_t^l$ is dense in $\mathfrak{X}_t^l$, there exists a sequence $\mathbb{X}_t^l \in \mathfrak{Y}_t^l$ such that for all l

$$||\mathbb{X}_t - \mathbb{X}_t^l||_{\mathcal{C}^l} \leqslant 2^{-l} \ .$$

Note that $\mathbb{X}_t^l \in \mathfrak{Y}_{t,L_m}^l$. Now since the set $\mathfrak{Y}_{t,L_m}^l$ is open in $\mathfrak{X}_t^l$ for the $\mathcal{C}^l$-topology, there exists $\varepsilon_l > 0$ such that for all $\mathbb{X}_t'^l \in \mathfrak{X}_t^l$ if

$$||\mathbb{X}_t^l - \mathbb{X}_t'^l||_{\mathcal{C}^l} \leqslant \min(2^{-l}, \varepsilon_l) \ ,$$

then $\mathbb{X}_t'^l \in \mathfrak{Y}_{t,L_m}^l$. Choosing $\mathbb{X}_t'^l$ to be smooth, this yields a sequence of smooth choices of perturbation data lying in $\mathfrak{Y}_{t,L_m}$ and converging to $\mathbb{X}_t$, which concludes the proof.

8.2.3 Induction step and conclusion

Let $k \geqslant 0$ and suppose that we have constructed an admissible choice of perturbation data $(\mathbb{X}_t^0)_{e(t) \leqslant k}$. This notation should not be confused with the notation $(\mathbb{X}_i)_{i \leqslant k}$: the former corresponds to a choice of perturbation data on the strata $\mathcal{T}(t)$ of dimension $\leqslant k$ while the latter corresponds to a choice of perturbation data on the moduli spaces $\mathcal{T}_i$ with $i \leqslant k$. Let t be a stable ribbon tree with $e(t) = k+1$ and choose

$$l \geqslant \max\left(1, e(t) + |y| - \sum_{i=1}^{n} |x_i| + 1\right) .$$

We want to construct a choice of perturbation data $\mathbb{X}_t$ on $\mathcal{T}_n(t)$ which is smooth, gluing-compatible and such that each map $\phi_{\mathbb{X}_t}$ is transverse to the diagonal $\Delta \subset M^{\times n+1}$.

Under a choice of identification $\overline{\mathcal{T}}_n(t) \simeq [0, +\infty]^{e(t)}$, define $\underline{\mathcal{T}_n}(t) \subset \overline{\mathcal{T}}_n(t)$ as the inverse image of $[0, +\infty[^{e(t)}$. Introduce the parametrization space

$$\mathfrak{X}_t^l := \left\{ \begin{array}{l} C^l\text{-perturbation data } \mathbb{X}_t \text{ on } \underline{\mathcal{T}_n}(t) \text{ such that} \\ \mathbb{X}_t|_{\mathcal{T}(t')} = \mathbb{X}_{t'}^0 \text{ for all } t' \in coll(t) \text{ and such that} \\ \lim\limits_{l_e \to +\infty} \mathbb{X}_t = \mathbb{X}_{t_1}^0 \#_e \mathbb{X}_{t_2}^0 \text{ for all } e \in E(t) \end{array} \right\} ,$$

where $t_1 \#_e t_2 = t$, and $\lim_{l_e \to +\infty} \mathbb{X}_t = \mathbb{X}_{t_1}^0 \#_e \mathbb{X}_{t_2}^0$ denotes the gluing-compatibility condition described in Section 6.4.3. Following [35] this parametrization space is an affine space which is Banach. One can indeed show that the $l_e \to +\infty$ conditions imply that each $\mathbb{X}_t \in \mathfrak{X}_t^l$ is bounded in the C^l-norm, and that the C^l-norm is thus well defined on $\mathfrak{X}_t^l$ although $\underline{\mathcal{T}_n}(t)$ is not compact.

Consider the C^l-map

$$\phi_t : \mathfrak{X}_t^l \times \mathcal{T}_n(t) \times W^S(y) \times W^U(x_1) \times \cdots \times W^U(x_n) \longrightarrow M^{\times n+1} .$$

Using the same argument as in Section 8.2.1, the map ϕ_t is again transverse to the diagonal $\Delta \subset M^{\times n+1}$. Applying Corollary 8.1.2 and proceeding as in the case $e(t) = 0$, there exists a residual set $\mathfrak{Y}_t^l \subset \mathfrak{X}_t^l$ such that for every choice of perturbation data $\mathbb{X}_t \in \mathfrak{Y}_t^l$ the map $\phi_{\mathbb{X}_t}$ is transverse to the diagonal $\Delta \subset M^{\times n+1}$. Using the previous argument à la Taubes, we can moreover prove the same statement in the smooth context. By definition of the parametrization spaces $\mathfrak{X}_t$ this construction yields indeed an admissible choice of perturbation data $(\mathbb{X}_t)_{e(t) \leqslant k+1}$, which concludes the proof of Theorem 6.4.5 by induction.

9. Signs, orientations and gluing

We now complete and conclude the proofs of Theorems 6.5.1, 7.4.1 and 7.4.5, by making explicit all orientation conventions on the moduli spaces of Morse gradient trees and computing the signs involved therein. We use to this extent the ad hoc formalism of signed short exact sequences of vector bundles. A particular attention will be paid to the behaviour of orientations under gluing in our proofs.

9.1 Orientations and short exact sequences

9.1.1 Signed short exact sequences of vector spaces

Consider a short exact sequence of vector spaces

$$0 \longrightarrow V_2 \longrightarrow W \longrightarrow V_1 \longrightarrow 0 \ .$$

It induces a direct sum decomposition $W = V_1 \oplus V_2$. Suppose that the vector spaces W, V_1 and V_2 are oriented. We denote $(-1)^\varepsilon$ the sign obtained by comparing the orientation on W to the one induced by the direct sum $V_1 \oplus V_2$. We will then say that the short exact sequence has sign $(-1)^\varepsilon$. In particular, when $(-1)^\varepsilon = 1$, we will say that the short exact sequence is *positive*.

Now, consider two short exact sequences

$$0 \longrightarrow V_2 \longrightarrow W \longrightarrow V_1 \longrightarrow 0 \ \text{ and } \ 0 \longrightarrow V_2' \longrightarrow W' \longrightarrow V_1' \longrightarrow 0 \ ,$$

of respective signs $(-1)^\varepsilon$ and $(-1)^{\varepsilon'}$. Then the short exact sequence obtained by summing them

$$0 \longrightarrow V_2 \oplus V_2' \longrightarrow W \oplus W' \longrightarrow V_1 \oplus V_1' \longrightarrow 0 \ ,$$

has sign $(-1)^{\varepsilon+\varepsilon'+\dim(V_1')\dim(V_2)}$. Indeed, the direct sum decomposition writes as

$$W \oplus W' = (-1)^\varepsilon (V_1 \oplus V_2) \oplus (-1)^{\varepsilon'}(V_1' \oplus V_2') \simeq (-1)^{\varepsilon+\varepsilon'+\dim(V_1')\dim(V_2)} V_1 \oplus V_1' \oplus V_2 \oplus V_2' \ .$$

9.1.2 Orientation and transversality

Given two manifolds M, N, a codimension k submanifold $S \subset N$ and a smooth map

$$\phi : M \longrightarrow N$$

which is tranverse to S, the inverse image $\phi^{-1}(S)$ is a codimension k submanifold of M. Moreover, choosing a complementary ν_S to TS, the transversality assumption yields the following short exact sequence of vector bundles

$$0 \longrightarrow T\phi^{-1}(S) \longrightarrow TM|_{\phi^{-1}(S)} \underset{d\phi}{\longrightarrow} \nu_S \longrightarrow 0 \ .$$

Suppose now that M is oriented and that S is cooriented (Definition 4.1.2). The submanifold $\phi^{-1}(S)$ is then oriented by requiring that the previous short exact sequence be positive.

Definition 9.1.1. This choice of orientation on $\phi^{-1}(S)$ will be called the *natural orientation on* $\phi^{-1}(S)$.

In the particular case of two submanifolds S and R of M which intersect transversely, we will use the inclusion map $S \hookrightarrow M$, which is transverse to $R \subset M$, to define the intersection $S \cap R$. The orientation will then be defined using the positive short exact sequence

$$0 \longrightarrow T(S \cap R) \longrightarrow TS|_{S \cap R} \longrightarrow \nu_R \longrightarrow 0 \ ,$$

or equivalently with the direct sum decomposition

$$TS = \nu_R \oplus T(S \cap R) \ .$$

The intersection $R \cap S$ (in contrast to $S \cap R$) is oriented by interchanging S and R in the above discussion. The two orientations on the intersection differ then by a $(-1)^{\operatorname{codim}(S)\operatorname{codim}(R)}$ sign.

9.2 Standard moduli spaces in Morse theory and their orientations

9.2.1 Orienting the unstable and stable manifolds

Recall that for a critical point x of a Morse function f, its unstable and stable manifolds are respectively defined as

$$W^U(x) := \{z \in M, \lim_{s \to -\infty} \phi^s(z) = x\}$$
$$W^S(x) := \{z \in M, \lim_{s \to +\infty} \phi^s(z) = x\} ,$$

where we denote ϕ^s the flow of $-\nabla f$, and its degree is defined as $|x| := \dim(W^S(x))$.

The unstable and stable manifolds are respectively diffeomorphic to a $(d - |x|)$-dimensional ball and a $|x|$-dimensional ball. They are hence orientable. They intersect moreover transversely in a unique point, which is x. Assume now that the manifold M is orientable and oriented. We choose for the rest of this section an arbitrary orientation on $W^U(x)$, and endow $W^S(x)$ with the unique orientation such that the concatenation of orientations $or_{W^U(x)} \wedge or_{W^S(x)}$ at x coincides with the orientation or_M.

9.2.2 Orienting the moduli spaces $\mathcal{T}(y;x)$

For two critical points $x \neq y$, the moduli spaces of negative gradient trajectories $\mathcal{T}(y;x)$ can be defined in two ways. The first point of view hinges on the fact that $\mathbb{R}$ acts on $W^S(y) \cap W^U(x)$, by defining $s \cdot p = \phi^s(p)$ for $s \in \mathbb{R}$ and $p \in W^S(y) \cap W^U(x)$. The moduli space $\mathcal{T}(y;x)$ is then defined as the quotient associated to this action, i.e. by defining $\mathcal{T}(y;x) := W^S(y) \cap W^U(x)/\mathbb{R}$. The second point of view is to consider the transverse intersection with the level set of a regular value a such that $f(x) > f(a) > f(y)$,

$$\mathcal{T}(y;x) := W^S(y) \cap W^U(x) \cap f^{-1}(a) .$$

Using this description, and coorienting the level set $f^{-1}(a)$ with $-\nabla f$, the spaces $\mathcal{T}(y;x)$ can easily be oriented with the formalism of Section 9.1.2 on transverse intersections:

$$TW^S(y) \simeq TW^S(x) \oplus T\left(W^S(y) \cap W^U(x)\right) \simeq TW^S(x) \oplus -\nabla f \oplus T\mathcal{T}(y;x) .$$

Note that the space $W^S(y) \cap W^U(x)$ consists in a union of negative gradient trajectories $\gamma : \mathbb{R} \to M$. We will therefore use the notation $\dot{\gamma}$ for $-\nabla f$, which will become handy in Section 9.2.3.

We point out that the moduli spaces $\mathcal{T}(y;x)$ are constructed in a different way than the moduli spaces $\mathcal{T}_t(y;x_1,\ldots,x_n)$: they cannot naturally be viewed as an arity 1 case of the moduli spaces of gradient trees. This observation will be of importance in our upcoming discussion on signs for the ΩBAs-algebra structure on the Morse cochains.

Finally, the moduli spaces $\mathcal{T}(y;x)$ are manifolds of dimension

$$\dim(\mathcal{T}(y;x)) = |y| - |x| - 1 ,$$

which can be compactified to manifolds with corners $\overline{\mathcal{T}}(y;x)$, by allowing convergence towards broken negative gradient trajectories. See for instance [42]. In the case when they are 1-dimensional, their boundary is given by the signed union

$$\partial\overline{\mathcal{T}}(y;x) = \bigcup_{z \in \mathrm{Crit}(f)} -\mathcal{T}(y;z) \times \mathcal{T}(z;x) .$$

We moreover recall from Section 6.1 that we work under the convention $\mathcal{T}(x;x) = \emptyset$.

9.2.3 Compactifications of the unstable and stable manifolds

Using the moduli spaces $\mathcal{T}(y;x)$, we can now compactify the manifolds $W^S(y)$ and $W^U(x)$ to compact manifolds with corners $\overline{W^S}(y)$ and $\overline{W^U}(x)$, as in[17]. With the choices of orientations made in Section 9.2.2, the top dimensional strata in their boundary are given by

$$\partial\overline{W^S}(y) = \bigcup_{z\in\mathrm{Crit}(f)} (-1)^{|z|+1} W^S(z)\times\mathcal{T}(y;z) \ ,$$
$$\partial\overline{W^U}(x) = \bigcup_{z\in\mathrm{Crit}(f)} (-1)^{(d-|z|)(|x|+1)} W^U(z)\times\mathcal{T}(z;x) \ ,$$

where d is the dimension of the ambient manifold M.

The pictures in the neighborhood of the critical point z are represented in Figure 9.1. For instance, in the case of $\partial\overline{W^S}(y)$, an element of $W^S(y)$ is seen as lying on a negative semi-infinite trajectory converging to y, and an outward-pointing vector to the boundary is given by $-\dot\gamma$. We hence have that

$$-\dot\gamma\oplus TW^S(z)\oplus T\mathcal{T}(y;z) = (-1)^{|z|}TW^S(z)\oplus -\dot\gamma\oplus T\mathcal{T}(y;z) = (-1)^{|z|+1}TW^S(y) \ .$$

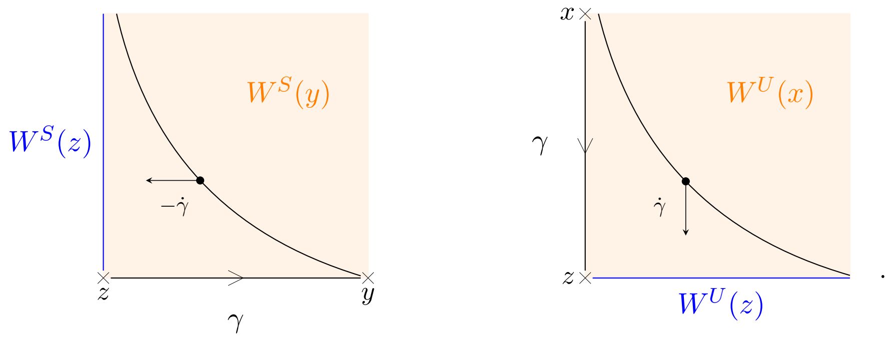

Figure 9.1

9.2.4 Euclidean neighborhood of a critical point

Following [42], we will assume in the rest of this part that the pair consisting of the Morse function and the metric on the manifold M is Euclidean. Denote $B^k_\delta := \{x\in\mathbb{R}^k,\ |x|<\delta\}$. Such a pair is said to *Euclidean* if it is Morse-Smale and is such that for each critical point $z\in\mathrm{Crit}(f)$ there exists a local chart $\phi : B^{d-|z|}_\delta\times B^{|z|}_\delta \xrightarrow{\sim} U_z\subset M$, such that $\phi(0)=z$ and such that the function f and the metric g read as

$$f(x_1,\dots,x_{n-|z|},y_1,\dots,y_{|z|}) = f(p)-\frac{1}{2}(x_1^2+\cdots+x_{n-|z|}^2)+\frac{1}{2}(y_1^2+\cdots+y_{|z|}^2)$$
$$g=\sum_{i=1}^{n-|z|}dx_i\otimes dx_i+\sum_{i=1}^{|z|}dy_i\otimes dy_i$$

in the chart ϕ. In this chart, we then have that

$$W^U(z) := \{y_1=\cdots=y_{|z|}=0\}$$
$$W^S(z) := \{x_1=\cdots=x_{n-|z|}=0\} \ ,$$

and $M = W^U(z) \times W^S(z)$. Hence any point of U_z can be uniquely written as a sum $x+y$ where $x \in W^U(z)$ and $y \in W^S(z)$. Choosing now $s \in \mathbb{R}$ such that the the image of $x+y$ under the Morse flow map ϕ^s still lies in U_z, we have that

$$\phi^s(x+y) = e^s x + e^{-s} y \ .$$

These observations will prove crucial in the proof of Proposition 9.4.2 in Section 9.4.3.

9.3 Preliminaries for the proofs of Theorems 6.5.1, 7.4.1 and 7.4.5

9.3.1 Counting the points on the boundary of an oriented 1-dimensional manifold

Consider an oriented 1-dimensional manifold with boundary. Then its boundary ∂M is oriented. Assume it can be written set-theoretically as a disjoint union

$$\partial M = \bigsqcup_i N_i \ .$$

Suppose now that each N_i comes with its own orientation, and write $(-1)^{\dagger_i}$ for the sign obtained by comparing this orientation to the boundary orientation. As oriented manifolds, the union writes as

$$\partial M = \bigsqcup_i (-1)^{\dagger_i} N_i \ .$$

The N_i being 0-dimensional, they can be seen as collections of points each coming with a + or − sign. Noticing that an orientable 1-dimensional manifold with boundary is either a segment or a circle, and writing $\# N_i$ for the signed count of points of N_i, the previous equality finally implies that

$$\sum (-1)^{\dagger_i} \# N_i = 0 \ .$$

This basic observation is key to constructing most algebraic structures arising Morse theory and in symplectic topology.

For instance, for a critical point x, counting the boundary points of the 1-dimensional manifolds $\overline{\mathcal{T}}(y;x)$ implies that

$$\partial^{Morse} \circ \partial^{Morse}(x) = \sum_{\substack{y \in \mathrm{Crit}(f) \\ |y|=|x|+2}} \sum_{\substack{z \in \mathrm{Crit}(f) \\ |z|=|x|+1}} \# \mathcal{T}(y;z) \# \mathcal{T}(z;x) \cdot y = 0 \ .$$

The equations for ΩBAs-algebras and ΩBAs-morphisms will be proven using this method.

9.3.2 Reformulating the ΩBAs-equations

We fix for each $t \in SRT_n$ an orientation ω_t. Given a $t \in SRT_n$ the orientation ω_t defines an orientation of the moduli space $\mathcal{T}_n(t)$, and we write moreover m_t for the operations (t, ω). The ΩBAs-equations for an ΩBAs-algebra then read as

$$[\partial, m_t] = \sum_{t' \in coll(t)} (-1)^{\dagger_{\Omega BAs}} m_{t'} + \sum_{t_1 \#_i t_2 = t} (-1)^{\dagger_{\Omega BAs}} m_{t_1} \circ_i m_{t_2} \ ,$$

where the notations for trees are as defined previously. The signs $(-1)^{\dagger_{\Omega BAs}}$ are obtained as in Section 5.1.3, by computing the signs of $\mathcal{T}_n(t')$ and $\mathcal{T}_{i_1+1+i_3}(t_1) \times_i \mathcal{T}_{i_2}(t_2)$ in the boundary of $\mathcal{T}_n(t)$. We will not need to compute their explicit value, and will hence keep this useful notation $(-1)^{\Omega BAs}$ to refer to them.

9.3.3 Twisted A_∞-algebras and twisted ΩBAs-algebras

It is clear using the method of Section 9.3.1 that the operations m_t of Theorem 6.5.1 will endow the Morse cochains $C^*(f)$ with a structure of ΩBAs-algebra over $\mathbb{Z}/2$. Working over integers will prove more difficult and we introduce first to this extent the notion of twisted A_∞-algebras and twisted ΩBAs-algebras.

Definition 9.3.1. (i) A *twisted A_∞-algebra* is a dg module A endowed with two different differentials ∂_1 and ∂_2, and a sequence of degree $2-n$ operations $m_n : A^{\otimes n} \to A$ such that

$$[\partial, m_n] = -\sum_{\substack{i_1+i_2+i_3=n \\ 2\leqslant i_2\leqslant n-1}} (-1)^{i_1+i_2 i_3} m_{i_1+1+i_3}(\mathrm{id}^{\otimes i_1} \otimes m_{i_2} \otimes \mathrm{id}^{\otimes i_3}) ,$$

where $[\partial, \cdot]$ denotes the bracket for the maps $(A^{\otimes n}, \partial_1) \to (A, \partial_2)$.

(ii) A *twisted ΩBAs-algebra* is defined similarly.

We refer to them as *twisted*, as these algebras will occur in the upcoming lines by setting $\partial_2 := (-1)^\sigma \partial_1$, that is by simply twisting the differential ∂_1 by a specific sign.

We now make explicit the formulae obtained by evaluating the ΩBAs-equations on $A^{\otimes n}$, as we will need them in our proof of Theorem 6.5.1:

$$\begin{aligned}
&-\partial_2 m_t(a_1,\dots,a_n) + (-1)^{|t|+\sum_{j=1}^{i-1}|a_j|} m_t(a_1,\dots,a_{i-1},\partial_1 a_i, a_{i+1},\dots,a_n) \\
&+ \sum_{t_1 \# t_2 = t} (-1)^{\dagger_{\Omega BAs}+|t_2|\sum_{j=1}^{i_1}|a_j|} m_{t_1}(a_1,\dots,a_{i_1}, m_{t_2}(a_{i_1+1},\dots,a_{i_1+i_2}), a_{i_1+i_2+1},\dots,a_n) \\
&+ \sum_{t'\in coll(t)} (-1)^{\dagger_{\Omega BAs}} m_{t'}(a_1,\dots,a_n) \\
&= 0 .
\end{aligned}$$

REMARK 9.3.2. We point out that these two definitions cannot be phrased in terms of operads, as $\mathrm{Hom}((A,\partial_1),(A,\partial_2))$ is an $(\mathrm{End}_{(A,\partial_1)}, \mathrm{End}_{(A,\partial_2)})$-operadic bimodule but is NOT an operad: the composition maps on $\mathrm{Hom}((A,\partial_1),(A,\partial_2))$ are associative, but they fail to be compatible with the differential $[\partial,\cdot]$. As a result, a twisted A_∞-algebra cannot be described as a morphism of operads from A_∞ to $\mathrm{Hom}((A,\partial_1),(A,\partial_2))$. However, a twisted ΩBAs-algebra structure always transfers to a twisted A_∞-algebra structure. Indeed, while the functorial proof of Proposition 3.1.15 does not work anymore, we point out that it still contains the proof that a sequence of operations m_t defining a twisted ΩBAs-algebra structure on A can always be arranged in a sequence of operations m_n defining a twisted A_∞-algebra structure on A.

9.3.4 The maps $\psi_{e_i,\mathbb{X}_t}$

Consider again a stable ribbon tree t and order its external edges clockwise, starting with e_0 at the outgoing edge. Given a choice of perturbation data $\mathbb{X}_t$, we illustrate in Figure 9.2 a mean to visualize the map

$$\phi_{\mathbb{X}_t} : \mathcal{T}_n(t) \times W^S(y) \times W^U(x_1) \times \cdots \times W^U(x_n) \longrightarrow M^{\times n+1}$$

defined in Section 6.3. We introduce a family of maps defined in a similar fashion. Consider e_i an incoming edge of t. Define the map

$$\psi_{e_i,\mathbb{X}_t} : \mathcal{T}_n(t) \times W^S(y) \times W^U(x_1) \times \cdots \times \widehat{W^U(x_i)} \times \cdots \times \cdots \times W^U(x_n) \longrightarrow M^{\times n}$$

to be the map which, for a fixed metric tree T, takes a point of a $W^U(x_j)$ for $j \neq i$ to the point in M obtained by following the only non-self crossing path from the time -1 point on e_j to the time -1 point on e_i in T through the perturbed gradient flow maps associated to $\mathbb{X}_T$, and which takes a point of $W^s(y)$ to the point in M obtained by following the only non-self crossing path from the time 1 point on e_0 to the time -1 point on e_i in T through the perturbed gradient flow maps associated to $\mathbb{X}_T$. The map $\psi_{e_0,\mathbb{X}_t}$ is defined similarly for the outgoing edge e_0. These two definitions are illustrated on two examples in Figure 9.2.

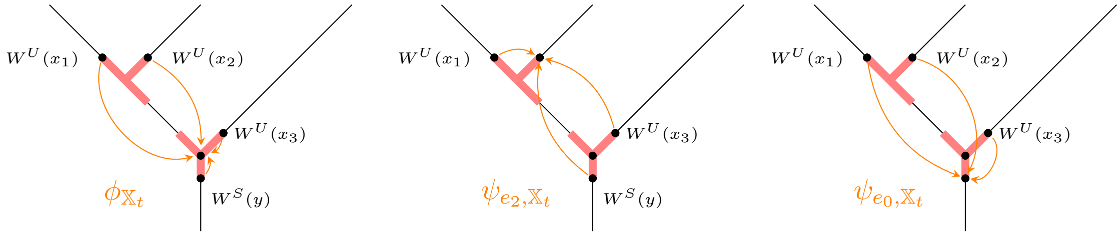

Figure 9.2: Representations of a map $\phi_{\mathbb{X}_t}$, a map $\psi_{e_2,\mathbb{X}_t}$ and a map $\psi_{e_0,\mathbb{X}_t}$

9.4 The twisted ΩBAs-algebra structure on the Morse cochains

9.4.1 Proof of Theorem 6.5.1

Definition 9.4.1. (i) The space $\widetilde{\mathcal{T}}_t^{\mathbb{X}}(y; x_1, \dots, x_n)$ is defined to be the oriented manifold $\mathcal{T}_t^{\mathbb{X}}(y; x_1, \dots, x_n)$ whose natural orientation (see Definition 9.1.1) has been twisted by a sign of parity

$$\sigma(t; y; x_1, \dots, x_n) := dn(1 + |y| + |t|) + |t||y| + d\sum_{i=1}^{n} |x_i|(n-i) .$$

(ii) Similarly, we define $\widetilde{\mathcal{T}}(y; x)$ to be the oriented manifold $\mathcal{T}(y; x)$ whose natural orientation has been twisted by a sign of parity

$$\sigma(y; x) := 1 .$$

The operations m_t and the differential on $C^*(f)$ are then defined as

$$m_t(x_1, \dots, x_n) = \sum_{|y| = \sum_{i=1}^{n} |x_i| + |t|} \# \widetilde{\mathcal{T}}_t^{\mathbb{X}}(y; x_1, \dots, x_n) \cdot y ,$$
$$\partial_{Morse}(x) = \sum_{|y| = |x| + 1} \# \widetilde{\mathcal{T}}(y; x) \cdot y .$$

Proposition 9.4.2. *If $\widetilde{\mathcal{T}}_t(y; x_1, \dots, x_n)$ is 1-dimensional, the boundary of its compactification decomposes as the disjoint union of the following components*

(i) $(-1)^{|y| + \dagger_{\Omega BAs} + |t_2| \sum_{i=1}^{i_1} |x_i|} \widetilde{\mathcal{T}}_{t_1}(y; x_1, \dots, x_{i_1}, z, x_{i_1+i_2+1}, \dots, x_n) \times \widetilde{\mathcal{T}}_{t_2}(z; x_{i_1+1}, \dots, x_{i_1+i_2})$ *;*

(ii) $(-1)^{|y| + \dagger_{\Omega BAs}} \widetilde{\mathcal{T}}_{t'}(y; x_1, \dots, x_n)$ *for* $t' \in coll(t)$ *;*

(iii) $(-1)^{|y| + \dagger_{Koszul} + (d+1)|x_i|} \widetilde{\mathcal{T}}_t(y; x_1, \dots, z, \dots, x_n) \times \widetilde{\mathcal{T}}(z; x_i)$ *where* $\dagger_{Koszul} = |t| + \sum_{j=1}^{i-1} |x_j|$ *;*

(iv) $(-1)^{|y|+1} \widetilde{\mathcal{T}}(y; z) \times \widetilde{\mathcal{T}}_t(z; x_1, \dots, x_n)$.

Proof. See Sections 9.4.2 to 9.4.4. □

Theorem 6.5.1 is then a simple corollary to Proposition 9.4.2, that is proven by applying the method of Section 9.3.1:

Theorem 6.5.1. *The operations m_t endow $(C^*(f), \partial^{Tw}_{Morse}, \partial_{Morse})$ with a twisted ΩBAs-algebra structure, where*

$$(\partial^{Tw}_{Morse})^k := (-1)^{(d+1)k} \partial^k_{Morse} \ .$$

It appears in particular from the definition of ∂^{Tw}_{Morse} that when M is odd-dimensional, this ΩBAs-algebra structure is untwisted, i.e. $\partial^{Tw}_{Morse} = \partial_{Morse}$.

Remark 9.4.3. We point out that the twisted structure arise from the two uncompatible orientation conventions on an intersection $R \cap S$ and $S \cap R$ as explained in Section 9.1.2. Indeed, we decided to orient $\mathcal{T}(y;x)$ inside the intersection $W^S(y) \cap W^U(x)$. The signs then compute nicely for the boundary component $\widetilde{\mathcal{T}}(y;z) \times \widetilde{\mathcal{T}}_t(z;x_1,\dots,x_n)$, and the twist in ∂^{Tw}_{Morse} arises in the boundary component $\widetilde{\mathcal{T}}_t(y;x_1,\dots,z,\dots,x_n) \times \widetilde{\mathcal{T}}(z;x_i)$. Orienting $\mathcal{T}(y;x)$ inside the intersection $W^U(x) \cap W^S(y)$ would make these two boundary components switch roles. In that case, redefining the twist on the orientation of the moduli space $\mathcal{T}(y;x)$ as given by the parity of $\sigma(y;x) := 1 + |x|$, we check that the operations m_t would define a twisted ΩBAs-algebra structure on $(C^*(f), \partial_{Morse}, \partial^{Tw}_{Morse})$.

9.4.2 Proof of Proposition 9.4.2: Item (i)

We resort to the formalism of short exact sequences of vector bundles (Section 9.1) to handle orientations in this section. For the sake of readability, we will write N rather than TN for the tangent bundle of a manifold N in the upcoming computations.

The moduli space $\mathcal{T}_t(y;x_1,\dots,x_n)$ is defined as the inverse image of the diagonal $\Delta \subset M^{\times n+1}$ under the map

$$\phi_{\mathbb{X}_t} : \mathcal{T}_n(t) \times W^S(y) \times W^U(x_1) \times \cdots \times W^U(x_n) \longrightarrow M^{\times n+1} \ ,$$

where the factors of $M^{\times n+1}$ are labeled in the order $M_y \times M_{x_1} \times \cdots \times M_{x_n}$. Orienting the domain and codomain of $\phi_{\mathbb{X}_t}$ by taking the product orientations, and orienting Δ as M, defines the natural orientation on $\mathcal{T}_t(y;x_1,\dots,x_n)$ as in Section 9.1.2. Choose $M^{\times n}$ labeled by $x_1,\dots,x_n$ as complementary to Δ. Then the orientation induced on $M^{\times n}$ by the orientations on $M^{\times n+1}$ and on Δ, differs by a $(-1)^{d^2 n}$ sign from the product orientation of $M^{\times n}$. In the language of short exact sequences, $\mathcal{T}_t(y;x_1,\dots,x_n)$ is oriented by the short exact sequence

$$0 \longrightarrow \mathcal{T}_t(y;x_1,\dots,x_n) \longrightarrow \mathcal{T}_n(t) \times W^S(y) \times \prod_{i=1}^{n} W^U(x_i) \longrightarrow M^{\times n} \longrightarrow 0 \ ,$$

which has a sign of parity

$$dn \ . \tag{A}$$

In the case of $\mathcal{T}^{Morse}_{t_1} := \mathcal{T}_{t_1}(y;x_1,\dots,x_{i_1},z,x_{i_1+i_2+1},\dots,x_n)$, we choose $M^{\times i_1+1+i_3}$ labeled by $y,x_1,\dots,x_{i_1},x_{i_1+i_2+1},\dots,x_n$ as complementary to Δ. The orientation induced on $M^{\times i_1+1+i_3}$, by the orientations on $M^{\times i_1+2+i_3}$ and on Δ, differs by a $(-1)^{d^2 i_3}$ sign from the product orientation of $M^{\times i_1+1+i_3}$. Hence the short exact sequence

$$0 \longrightarrow \mathcal{T}^{Morse}_{t_1} \longrightarrow \mathcal{T}_{i_1+1+i_3}(t_1) \times W^S(y) \times \prod_{i=1}^{i_1} W^U(x_i) \times W^U(z) \times \prod_{i=i_1+i_2+1}^{n} W^U(x_i) \longrightarrow M^{\times i_1+1+i_3} \to 0 \ ,$$

has a sign of parity

$$di_3 \ . \tag{B}$$

In the case of $\mathcal{T}_{t_2}^{Morse} := \mathcal{T}_{t_2}(z; x_{i_1+1}, \dots, x_{i_1+i_2})$, we choose $M^{\times i_2}$ labeled by $x_{i_1+1}, \dots, x_{i_1+i_2}$ as complementary to Δ. The orientation induced on $M^{\times i_2}$ differs this time by a $(-1)^{d^2 i_2}$ sign from the product orientation. The short exact sequence

$$0 \longrightarrow \mathcal{T}_{t_2}^{Morse} \longrightarrow \mathcal{T}_{i_2}(t_2) \times W^S(z) \times \prod_{i=i_1+1}^{i_1+i_2} W^U(x_i) \longrightarrow M^{\times i_2} \to 0 \ ,$$

has now a sign given by the parity of

$$di_2 \ . \tag{C}$$

Following the convention on the sum of signed short exact sequences in Section 9.1.1, taking the product

$$0 \longrightarrow \mathcal{T}_{t_1}^{Morse} \times \mathcal{T}_{t_2}^{Morse} \longrightarrow \mathcal{T}_{i_1+1+i_3}(t_1) \times W^S(y) \times \prod_{i=1}^{i_1} W^U(x_i) \times W^U(z) \times \prod_{i=i_1+i_2+1}^{n} W^U(x_i) \times \mathcal{T}_{i_2}(t_2) \times W^S(z) \times \prod_{i=i_1+1}^{i_1+i_2} W^U(x_i)$$
$$\longrightarrow M^{\times i_1+1+i_3} \times M^{\times i_2} \to 0$$

doesn't introduce a sign, as $\mathcal{T}_{t_1}^{Morse}$ and $\mathcal{T}_{t_2}^{Morse}$ are 0-dimensional.

In the previous short exact sequence, $M^{\times i_1+1+i_3} \times M^{\times i_2}$ is labeled by

$$y, x_1, \dots, x_{i_1}, x_{i_1+i_2+1}, \dots, x_n, x_{i_1+1}, \dots, x_{i_1+i_2} \ .$$

We rearrange this labeling into

$$y, x_1, \dots, x_n \ ,$$

which induces a sign given by the parity of

$$di_2 i_3 \ . \tag{D}$$

We also rearrange the expression

$$\mathcal{T}_{i_1+1+i_3}(t_1) \times W^S(y) \times \prod_{i=1}^{i_1} W^U(x_i) \times W^U(z) \times \prod_{i=i_1+i_2+1}^{n} W^U(x_i) \times \mathcal{T}_{i_2}(t_2) \times W^S(z) \times \prod_{i=i_1+1}^{i_1+i_2} W^U(x_i) \ ,$$

into

$$W^U(z) \times W^S(z) \times \mathcal{T}_{i_1+1+i_3}(t_1) \times \mathcal{T}_{i_2}(t_2) \times W^S(y) \times \prod_{i=1}^{n} W^U(x_i) \ .$$

The parity of the produced sign is that of

$$|z| \left(|t_2| + \sum_{i=i_1+i_2+1}^{n} (d - |x_i|) \right) + m \left(|t_1| + |y| + \sum_{i=1}^{i_1} (d - |x_i|) \right) \tag{E}$$
$$+ |t_2| \left(|y| + \sum_{i=1}^{i_1} (d - |x_i|) + \sum_{i=i_1+i_2+1}^{n} (d - |x_i|) \right) + \left(\sum_{i=i_1+1}^{i_1+i_2} (d - |x_i|) \right) \left(\sum_{i=i_1+i_2+1}^{n} (d - |x_i|) \right) \ .$$

Introduce now the factor $[L, +\infty[$, corresponding to the length l_e increasing towards $+\infty$, where e is the edge of t whose breaking produces t_1 and t_2 and where L is chosen to be large enough as in Section 9.4.3. Following the convention of Section 9.1.2, the short exact sequence

$$0 \longrightarrow [L,+\infty[\times \mathcal{T}_{t_1}^{Morse} \times \mathcal{T}_{t_2}^{Morse} \longrightarrow [L,+\infty[\times W^U(z) \times W^S(z) \times \mathcal{T}(t_1) \times \mathcal{T}(t_2) \times \times W^S(y) \times \prod_{i=1}^n W^U(x_i) \longrightarrow M^{\times n+1} \longrightarrow 0 ,$$

induces a sign change whose parity is given by

$$d(n+1) \ . \tag{F}$$

Define the map

$$\psi : M \times \mathcal{T}_n(t) \times W^S(y) \times \prod_{i=1}^n W^U(x_i) \longrightarrow M \times M^{\times n+1} ,$$

which is defined on the factors $\mathcal{T}_n(t) \times W^S(y) \times \prod_{i=1}^n W^U(x_i)$ as ϕ and is defined on $M \times \mathcal{T}_n(t)$ by seeing M as the point lying in the middle of the edge e in t. This map is depicted on Figure 9.3. The inverse image of the diagonal of $M \times M^{\times n+1}$ is exactly $\mathcal{T}_t(y; x_1, \dots, x_n)$. Fix now a sufficiently great $L > 0$. We prove in Section 9.4.3 that after orienting $[L, +\infty[\times \mathcal{T}_{t_1}^{Morse} \times \mathcal{T}_{t_2}^{Morse}$ with the previous short exact sequence, the orientation obtained on $\mathcal{T}_t^{Morse}$ by gluing is exactly the one given by the short exact sequence

$$0 \longrightarrow \mathcal{T}_t^{Morse} \longrightarrow [L,+\infty[\times M \times \mathcal{T}(t_1) \times \mathcal{T}(t_2) \times W^S(y) \times \textstyle\prod_{i=1}^n W^U(x_i) \xrightarrow[d\psi]{} M^{\times n+1} \longrightarrow 0$$

where our convention on orientations for the unstable and stable manifolds of z implies that $W^U(z) \times W^S(z)$ yields indeed the orientation of M, and $M^{\times n+1}$ is labeled by $y, x_1, \dots, x_n$.

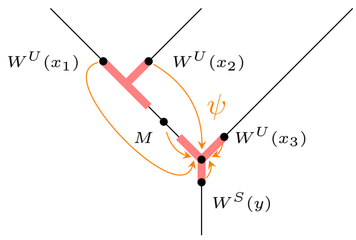

Figure 9.3: Representation of the map ψ

Transform the coorientation labeled by $y, x_1, \dots, x_n$ into the coorientation labeled by $M, x_1, \dots, x_n$ and rearrange the factors $[L, +\infty[\times M \times \mathcal{T}(t_1) \times \mathcal{T}(t_2) \times \cdots$ into $M \times [L, +\infty[\times \mathcal{T}(t_1) \times \mathcal{T}(t_2) \times \cdots$ This produces a sign change of parity

$$d + d \equiv 0 \ . \tag{G}$$

We can moreover now delete the two M factors associated to the label M in $M^{\times n+1}$ and in $M \times [L, +\infty[\times \mathcal{T}(t_1) \times \mathcal{T}(t_2) \times \cdots$ in order to obtain the short exact sequence

$$0 \longrightarrow \mathcal{T}_t(y; x_1, \dots, x_n) \longrightarrow [L,+\infty[\times \mathcal{T}(t_1) \times \mathcal{T}(t_2) \times W^S(y) \times \prod_{i=1}^n W^U(x_i) \longrightarrow M^{\times n} \longrightarrow 0 ,$$

where $M^{\times n} = M_{x_1} \times \cdots \times M_{x_n}$.

Transforming finally $[L,+\infty[\times\mathcal{T}(t_1)\times\mathcal{T}(t_2)$ into $\mathcal{T}_n(t)$ gives a sign of parity

$$\dagger_{\Omega BAs} \ . \tag{H}$$

In closing, the short exact sequence

$$0 \longrightarrow \mathcal{T}_t(y;x_1,\dots,x_n) \longrightarrow \mathcal{T}_n(t)\times W^S(y)\times\prod_{i=1}^n W^U(x_i) \longrightarrow M^{\times n} \longrightarrow 0 \ ,$$

has sign given by the parity of A when $\mathcal{T}_t^{Morse}$ is endowed with its natural orientation. It has sign given by the parity of $B+C+D+E+F+G+H$ when $\mathcal{T}_t^{Morse}$ is endowed with the orientation induced by $[L,+\infty[\times\mathcal{T}_{t_1}^{Morse}\times\mathcal{T}_{t_2}^{Morse}$, where the first factor is the length l_e obtained after gluing (see Section 9.4.3) and determines the outward-pointing direction ν_e to the boundary component $\mathcal{T}_{t_1}^{Morse}\times\mathcal{T}_{t_2}^{Morse}$.

We thus obtain that with our choice of orientation on the moduli spaces $\mathcal{T}_t^{Morse}$, the sign of $\mathcal{T}_{t_1}(y;x_1,\dots,x_{i_1},z,x_{i_1+i_2+1},\dots,x_n)\times\mathcal{T}_{t_2}(z;x_{i_1+1},\dots,x_{i_1+i_2})$ in the boundary of the moduli space of dimension 1 $\mathcal{T}_t(y;x_1,\dots,x_n)$ is given by the parity of

$$(*)\quad A+B+C+D+E+F+G+H$$
$$= |z||t_2|+d|y|+d|t_1|+(n+1)d+\sum_{i=1}^{i_1}d|x_i|+|t_2||y|+di_1|t_2|+di_2\sum_{i=i_1+i_2+1}^{n}|x_i|+\dagger_{\Omega BAs}+|t_2|\sum_{i=1}^{i_1}|x_i| \ .$$

Hence the sign of $\widetilde{\mathcal{T}}_{t_1}(y;x_1,\dots,x_{i_1},z,x_{i_1+i_2+1},\dots,x_n)\times\widetilde{\mathcal{T}}_{t_2}(z;x_{i_1+1},\dots,x_{i_1+i_2})$ in the boundary of the 1-dimensional moduli space $\widetilde{\mathcal{T}}_t(y;x_1,\dots,x_n)$ is given by the parity of

$$\sigma(t;y;x_1,\dots,x_n)+\sigma(t_1;y;x_1,\dots,x_{i_1},z,x_{i_1+i_2+1},\dots,x_n)+\sigma(t_2;z;x_{i_1+1},\dots,x_{i_1+i_2})+(*)$$
$$= |y|+\dagger_{\Omega BAs}+|t_2|\sum_{i=1}^{i_1}|x_i| \ .$$

This concludes the proof of Item (i) in Proposition 9.4.2.

9.4.3 Proof of Proposition 9.4.2: gluing and orientations

We prove in this subsection that after orienting $[L,+\infty[\times\mathcal{T}_{t_1}^{Morse}\times\mathcal{T}_{t_2}^{Morse}$ with the short exact sequence

$$0 \longrightarrow [L,+\infty[\times\mathcal{T}_{t_1}^{Morse}\times\mathcal{T}_{t_2}^{Morse} \longrightarrow [L,+\infty[\times W^U(z)\times W^S(z)\times\mathcal{T}(t_1)\times\mathcal{T}(t_2)\times W^S(y)\times\textstyle\prod_{i=1}^n W^U(x_i) \longrightarrow M^{\times n+1} \longrightarrow 0 \ ,$$

the orientation induced on $\mathcal{T}_t^{Morse}$ by gluing is the one given by the short exact sequence

$$0 \longrightarrow \mathcal{T}_t^{Morse} \longrightarrow [L,+\infty[\times M\times\mathcal{T}(t_1)\times\mathcal{T}(t_2)\times W^S(y)\times\textstyle\prod_{i=1}^n W^U(x_i) \xrightarrow[d\psi]{} M^{\times n+1} \longrightarrow 0 \ .$$

The proof boils down to the following lemma.

Lemma 9.4.4. *Let M and N be manifolds and $S\subset N$ a submanifold of N. Suppose that M, N and S are orientable and oriented. Let $f:[0,1]\times M\to N$ be a smooth map such that $f_1:=f(1,\cdot):M\to N$ is transverse to S. Let $x\in f_1^{-1}(S)$. Then there exist an open subset V of M containing x and $0\leqslant t_1<1$ such that*

(i) The map $f|_{[t_1,1]\times V}:[t_1,1]\times V\to N$ is transverse to S. In particular the inverse image $f|_{[t_1,1]\times V}^{-1}(S)$ is then a submanifold of $[t_1,1]\times V$.

(ii) There exists an orientation-preserving embedding

$$f|^{-1}_{[t_1,1]\times V}(S) \longrightarrow [t_1,1] \times f_1^{-1}(S)$$

equal to the identity on $f_1|_V^{-1}(S)$ and preserving the t coordinate, where we orient $[t_1,1] \times f_1^{-1}(S)$ with the short exact sequence

$$0 \longrightarrow [t_1,1] \times f_1^{-1}(S) \longrightarrow [0,1] \times M \longrightarrow \nu_S \longrightarrow 0$$

and we orient $f|^{-1}_{[t_1,1]\times V}(S)$ with the short exact sequence

$$0 \longrightarrow f|^{-1}_{[t_1,1]\times V}(S) \longrightarrow [0,1] \times M \longrightarrow \nu_S \longrightarrow 0 \ .$$

Proof. Choose an adapted chart for S around $f_1(x)$, i.e. a chart $\phi : U' \subset N \to \mathbb{R}^n$ such that

$$\phi(U' \cap S) = \{(y_1, \ldots, y_{n-s}, x_1, \ldots, x_s) \in \mathbb{R}^n, \ y_1 = \cdots = y_{n-s} = 0\} \ ,$$

where n and s respectively denote the dimensions of N and S. Using the local normal form theorem for submersions, there exists a local chart $\psi : U \subset M \to \mathbb{R}^m$ around x such that the map f_1 reads as

$$(y_1, \ldots, y_{n-s}, x_1, \ldots, x_{m+s-n}) \longmapsto (y_1, \ldots, y_{n-s}, F_1(\vec{y}, \vec{x}), \ldots, F_s(\vec{y}, \vec{x}))$$

in the local charts ψ and ϕ, where the F_i are smooth maps and $\vec{y} := y_1, \ldots, y_{n-s}$, $\vec{x} := x_1, \ldots, x_{m+s-n}$ and $m := \dim(M)$. In these local charts,

$$U \cap f_1^{-1}(U' \cap S) = \{(y_1, \ldots, y_{n-s}, x_1, \ldots, x_{m+s-n}) \in \mathbb{R}^m, \ y_1 = \cdots = y_{n-s} = 0\} \ .$$

The property "being transverse to S" being open, there exists a neighborhood W of x in M and $t_0 \in [0,1[$ such that the map $f|_{[t_0,1]\times W} : [t_0,1] \times W \to N$ is transverse to S. Suppose $W \subset U$ and consider now the projection $\pi : \mathbb{R}^m \to \mathbb{R}^{m+s-n}$ given by

$$(y_1, \ldots, y_{n-s}, x_1, \ldots, x_{m+s-n}) \longmapsto (x_1, \ldots, x_{m+s-n})$$

and define the smooth map

$$\iota := \mathrm{id}_t \times \pi : f|^{-1}_{[t_0,1]\times W}(S) \longrightarrow [0,1] \times f_1^{-1}(S)$$

in the local charts ϕ and ψ. The differential of this map is invertible at $(1,x)$. The inverse function theorem then ensures that there exits $t_1 \in [t_0, 1[$ and a neighborhood $V \subset W$ of x such that the map

$$\iota : f|^{-1}_{[t_1,1]\times V}(S) \longrightarrow [0,1] \times f_1^{-1}(S)$$

is a diffeomorphism on its image.

Orient now $[0,1] \times f_1^{-1}(S)$ and $f|^{-1}_{[t_1,1]\times V}(S)$ with the previous short exact sequences. It remains to show that the map ι is orientation-preserving. The proof of this result can be reduced to a proof in linear algebra, i.e. by considering a smooth family of linear maps $f : [0,1]\times\mathbb{R}^m \to \mathbb{R}^n$ such that f_1 reads as

$$(y_1, \ldots, y_{n-s}, x_1, \ldots, x_{m+s-n}) \longmapsto (y_1, \ldots, y_{n-s}, F_1(\vec{y}, \vec{x}), \ldots, F_s(\vec{y}, \vec{x})) \ ,$$

and the linear subspace $S = \{0\} \times \mathbb{R}^s \subset \mathbb{R}^n$. Then there exists $t_0 \in [0,1]$ such that $f|_{[t_0,1]\times\mathbb{R}^m}$ is transverse to S, and we can consider the smooth map

$$\iota := \mathrm{id}_t \times \pi : f|^{-1}_{[t_0,1]\times\mathbb{R}^m}(S) \longrightarrow [0,1] \times f_1^{-1}(S)$$

which is a diffeomorphism on its image. Basic computations finally show that the map ι is indeed orientation-preserving. □

We now go back to our initial problem. Let $T_1^{Morse} \in \mathcal{T}_1^{Morse}$ and $T_2^{Morse} \in \mathcal{T}_2^{Morse}$, where we refer to Section 9.4.2 for notations. Consider a local Euclidean chart $\phi_z : U_z \to \mathbb{R}^d$ for the critical point z as in Section 9.2.4. Introduce the map $ev : [0, +\infty] \times U_z \to U_z \times U_z$ reading as

$$(\delta, x + y) \longmapsto (e^{-2\delta}x + y, x + e^{-2\delta}y)$$

in the chart ϕ_z. The pair $ev(\delta, x+y)$ corresponds to the two endpoints of the unique finite Morse trajectory parametrized by $[-\delta, \delta]$ and meeting $e^{-\delta}x + e^{-\delta}y$ at time 0.

Consider the trajectory $\gamma_{e,1} :]-\infty, 0] \to M$ and the trajectory $\gamma_{e,2} : [0, +\infty[\to M$, respectively associated to the incoming edge of T_1^{Morse} and to the outgoing edge of T_2^{Morse} which result from the breaking of the edge e in t. Choose L large enough such that $\gamma_{e,1}(-L)$ and $\gamma_{e,2}(L)$ belong to U_z. Introduce the map $f := ev \times (\phi^{-(L-1)})^{\times i_1+1+i_3} \circ \psi_{e,\mathbb{X}_{t_1}} \times (\phi^{L-1})^{\times i_2} \circ \psi_{e,\mathbb{X}_{t_2}}$ acting as

$$[0, +\infty] \times U_z \times \mathcal{T}_{i_1+1+i_3}(t_1) \times W^S(y) \times \prod_{i=1}^{i_1} W^U(x_i) \times \prod_{i=i_1+i_2+1}^{n} W^U(x_i) \times \mathcal{T}_{i_2}(t_2) \times \prod_{i=i_1+1}^{i_1+i_2} W^U(x_i)$$
$$\longrightarrow M^{\times 2} \times M^{\times i_1+1+i_3} \times M^{\times i_2} ,$$

where ϕ^{L-1} stands for the time $L-1$ Morse flow and the maps $\psi_{e,\mathbb{X}_{t_2}}$ and $\psi_{e,\mathbb{X}_{t_1}}$ have been introduced in Section 9.2.4. This map is depicted in Figure 9.4.

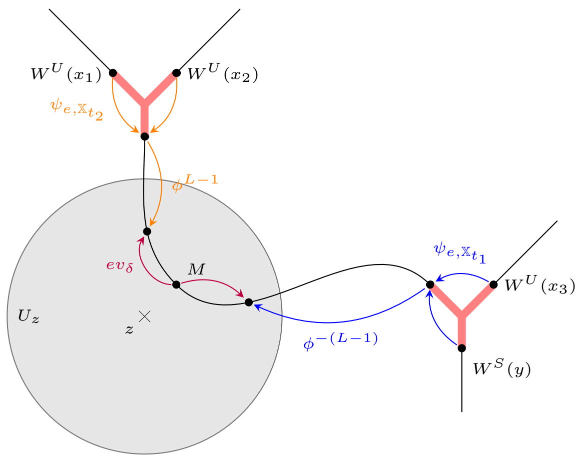

Figure 9.4: Representation of the map f. Beware that the label M corresponds to the point $e^{-\delta}x + e^{-\delta}y$ and not to the point $x + y$.

Define the $2d$-dimensional submanifold $\Lambda \subset M^{\times 2} \times M^{\times i_1+1+i_3} \times M^{\times i_2}$ to be

$$\Lambda := \left\{ \begin{array}{l} (m_z^1, m_z^2, m_y, m_1, \dots, m_{i_1}, m_{i_1+1+i_2}, \dots, m_n, m_{i_1+1}, \dots, m_{i_1+i_2}) \\ \text{such that } m_z^1 = m_{i_1+1} = \cdots = m_{i_1+i_2} \quad \text{and} \\ m_z^2 = m_y = m_1 = \cdots = m_{i_1} = m_{i_1+1+i_2} = \cdots = m_n \end{array} \right\} .$$

The pair $(T_1^{Morse}, T_2^{Morse})$ then belongs to the inverse image $f_{+\infty}^{-1}(\Lambda)$. By assumption on the choice of perturbation data $(\mathbb{X}_n)_{n \geqslant 2}$, the map $f_{+\infty}$ is moreover transverse to Λ. Applying Lemma 9.4.4 to the map f at the point $(T_1^{Morse}, T_2^{Morse})$, there exists $R > 0$ and an embedding

$$\#_{T_1^{Morse}, T_2^{Morse}} : [R, +\infty] \longrightarrow \overline{\mathcal{T}}_t(y; x_1, \dots, x_n) .$$

Note that the parameter δ corresponds to an edge of length $2L + 2\delta$ in the resulting glued tree. Upon reordering the factors of the domain of f, it is finally easy to check that this lemma also implies the result on orientations stated at the beginning of this subsection.

9.4.4 Proof of Proposition 9.4.2: Items (ii) to (iv)

Repeating the beginning of Section 9.4.2, for the moduli spaces $\mathcal{T}_{t'}(y; x_1, \dots, x_n)$, where $t' \in coll(t)$, and $\mathcal{T}_t(y; x_1, \dots, x_n)$, we choose $M^{\times n}$ labeled by $x_1, \dots, x_n$ as complementary to the diagonal $\Delta \subset M^{\times n+1}$. The parity of the total sign change coming from these coorientation choices is

$$dn + dn = 0 \ . \tag{A}$$

Introduce the factor $]0, L]$, corresponding to the length l_e going towards 0, where e is the edge of t whose collapsing produces t'. Applying again Lemma 9.4.4 and following convention of Section 9.1.1, the short exact sequence

$$0 \longrightarrow \mathcal{T}_t(y; x_1, \dots, x_n) =]0, L] \times \mathcal{T}_{t'}(y; x_1, \dots, x_n) \longrightarrow]0, L] \times \mathcal{T}_n(t') \times W^S(y) \times \prod_{i=1}^{n} W^U(x_i) \longrightarrow M^{\times n} \longrightarrow 0 \ ,$$

introduces a sign change whose parity is given by

$$dn \ . \tag{B}$$

Transforming finally $]0, L] \times \mathcal{T}_n(t')$ into $\mathcal{T}_n(t)$ gives a sign of parity

$$\dagger_{\Omega BAs} \ . \tag{C}$$

Adding these contributions, we obtain that the sign of $\mathcal{T}_{t'}(y; x_1, \dots, x_n)$ in the boundary of the 1-dimensional moduli space $\mathcal{T}_t(y; x_1, \dots, x_n)$ is given by the parity of

$$A + B + C = dn + \dagger_{\Omega BAs} \ . \tag{*}$$

The sign of $\widetilde{\mathcal{T}}_{t'}(y; x_1, \dots, x_n)$ in the boundary of the 1-dimensional moduli space $\widetilde{\mathcal{T}}_t(y; x_1, \dots, x_n)$ is hence given by the parity of

$$\sigma(t; y; x_1, \dots, x_n) + \sigma(t'; y; x_1, \dots, x_n) + (*) = |y| + \dagger_{\Omega BAs} \ .$$

Finally, the signs for the (Morse) boundary can be computed following the exact same lines of the two previous proofs. This concludes the proof of Items (ii) to (iv) in Proposition 9.4.2.

9.5 The twisted ΩBAs-morphism between the Morse cochains

9.5.1 Reformulating the ΩBAs-equations

For the rest of this section, we endow each $t_c \in SCRT_n$ with the orientation chosen for the underlying ribbon tree t of t_c in Section 9.3.2. These choices of orientations endow each moduli space $\mathcal{CT}_n(t_c)$ with an orientation. We write moreover μ_{t_c} for the operations (t_c, ω) of $M_{\Omega BAs}$. The ΩBAs-equations for an ΩBAs-morphism then read as

$$\begin{aligned} [\partial, \mu_{t_c}] = & \sum_{t'_c \in coll(t_c)} (-1)^{\dagger_{\Omega BAs}} \mu_{t'_c} + \sum_{t'_c \in g-vert(t_c)} (-1)^{\dagger_{\Omega BAs}} \mu_{t'_c} + \sum_{t_c^1 \#_i t^2 = t_c} (-1)^{\dagger_{\Omega BAs}} \mu_{t_c^1} \circ_i m_{t^2} \\ & + \sum_{t^0 \#(t_c^1, \dots, t_c^s) = t_c} (-1)^{\dagger_{\Omega BAs}} m_{t^0} \circ (\mu_{t_c^1} \otimes \cdots \otimes \mu_{t_c^s}) \ , \end{aligned}$$

where the notations for trees are transparent. The signs $(-1)^{\dagger_{\Omega BAs}}$ are obtained as in Section 9.3.2.

9.5.2 Twisted A_∞-morphisms and twisted ΩBAs-morphisms

It is again clear using the method of Section 9.3.1 that the operations μ_{t_c} of Theorem 7.4.1 define an ΩBAs-morphism over $\mathbb{Z}/2$. Working over integers will require the following notions:

Definition 9.5.1. (i) Let $(A, \partial_1, \partial_2, m_n)$ and $(B, \partial_1, \partial_2, m_n)$ be two twisted A_∞-algebras. A *twisted A_∞-morphism* from A to B is defined to be a sequence of degree $1-n$ operations $f_n : A^{\otimes n} \to B$ such that

$$[\partial, f_n] = \sum_{\substack{i_1+i_2+i_3=n \\ i_2 \geqslant 2}} (-1)^{i_1+i_2 i_3} f_{i_1+1+i_3}(\mathrm{id}^{\otimes i_1} \otimes m_{i_2} \otimes \mathrm{id}^{\otimes i_3}) - \sum_{\substack{i_1+\cdots+i_s=n \\ s \geqslant 2}} (-1)^{\epsilon_B} m_s(f_{i_1} \otimes \cdots \otimes f_{i_s})$$

where $[\partial, \cdot]$ denotes the bracket for the maps $(A^{\otimes n}, \partial_1) \to (B, \partial_2)$.

(ii) A *twisted ΩBAs-morphism* between twisted ΩBAs-algebras is defined similarly.

The formulae obtained by evaluating the ΩBAs-equations on $A^{\otimes n}$ then read as

$$\begin{aligned}
&- \partial_2 \mu_{t_c}(a_1, \dots, a_n) + (-1)^{|t_c| + \sum_{j=1}^{i-1} |a_j|} \mu_{t_c}(a_1, \dots, a_{i-1}, \partial_1 a_i, a_{i+1}, \dots, a_n) \\
&+ \sum_{t_c^1 \# t^2 = t} (-1)^{\dagger_{\Omega BAs} + |t^2| \sum_{j=1}^{i_1} |a_j|} \mu_{t_c^1}(a_1, \dots, a_{i_1}, m_{t^2}(a_{i_1+1}, \dots, a_{i_1+i_2}), a_{i_1+i_2+1}, \dots, a_n) \\
&+ \sum_{t^1 \# (t_c^1, \dots, t_c^s) = t_c} (-1)^{\dagger_{\Omega BAs} + \dagger_{Koszul}} m_{t^0}(\mu_{t_c^1}(a_1, \dots, a_{i_1}), \dots, \mu_{t_c^s}(a_{i_1+\cdots+i_{s-1}+1}, \dots, a_n)) \\
&+ \sum_{t_c' \in coll(t_c)} (-1)^{\dagger_{\Omega BAs}} \mu_{t_c'}(a_1, \dots, a_n) + \sum_{t_c' \in g-vert(t_c)} (-1)^{\dagger_{\Omega BAs}} \mu_{t_c'}(a_1, \dots, a_n) \\
&= 0 \ ,
\end{aligned}$$

where

$$\dagger_{Koszul} = \sum_{r=1}^{s} |t_c^r| \left(\sum_{t=1}^{r-1} \sum_{j=1}^{i_t} |a_{i_1+\cdots+a_{i_{t-1}}+j}| \right) \ .$$

Remark 9.5.2. Again Definition 9.5.1 cannot be phrased using an operadic viewpoint. However, a twisted ΩBAs-morphism between twisted ΩBAs-algebras always descends to a twisted A_∞-morphism between twisted A_∞-algebras, for the same reason as in Remark 9.3.2.

9.5.3 Proof of Theorem 7.4.1

Definition 9.5.3. We define $\widetilde{\mathcal{CT}}_{t_c}^{\mathbb{Y}}(y; x_1, \dots, x_n)$ to be the oriented manifold $\mathcal{CT}_{t_c}^{\mathbb{Y}}(y; x_1, \dots, x_n)$ whose natural orientation has been twisted by a sign of parity

$$\sigma(t_c; y; x_1, \dots, x_n) := dn(1 + |y| + |t_c|) + |t_c||y| + d \sum_{i=1}^{n} |x_i|(n-i) \ .$$

The moduli spaces $\widetilde{\mathcal{T}}(y; x)$ and $\widetilde{\mathcal{T}}_t(y; x_1, \dots, x_n)$ are moreover defined as in Definition 9.4.1. The operations $\mu_{t_c} : C^*(f)^{\otimes n} \to C^*(g)$ are then defined as

$$\mu_{t_c}(x_1, \dots, x_n) = \sum_{|y| = \sum_{i=1}^{n} |x_i| + |t_c|} \# \widetilde{\mathcal{CT}}_{t_c}^{\mathbb{Y}}(y; x_1, \dots, x_n) \cdot y \ .$$

Proposition 9.5.4. *If $\widetilde{\mathcal{CT}}_{t_c}(y; x_1, \dots, x_n)$ is 1-dimensional, its boundary decomposes as the disjoint union of the following components* *(i)* $(-1)^{|y|+\dagger_{\Omega BAs}+|t^2|\sum_{i=1}^{i_1}|x_i|}\widetilde{\mathcal{CT}}_{t_c^1}(y;x_1,\dots,x_{i_1},z,x_{i_1+i_2+1},\dots,x_n)\times\widetilde{\mathcal{T}}_{t^2}(z;x_{i_1+1},\dots,x_{i_1+i_2})$;

(ii) $(-1)^{|y|+\dagger_{\Omega BAs}+\dagger_{Koszul}}\widetilde{\mathcal{T}}_{t^1}(y;y_1,\dots,y_s)\times\widetilde{\mathcal{CT}}_{t_c^1}(y_1;x_1,\dots)\times\cdots\times\widetilde{\mathcal{CT}}_{t_c^s}(y_s;\dots,x_n)$;

(iii) $(-1)^{|y|+\dagger_{\Omega BAs}}\widetilde{\mathcal{CT}}_{t_c'}(y;x_1,\dots,x_n)$ *for* $t'\in coll(t)$;

(iv) $(-1)^{|y|+\dagger_{\Omega BAs}}\widetilde{\mathcal{CT}}_{t_c'}(y;x_1,\dots,x_n)$ *for* $t'\in g-vert(t)$;

(v) $(-1)^{|y|+\dagger_{Koszul}+(m+1)|x_i|}\widetilde{\mathcal{CT}}_{t_c}(y;x_1,\dots,z,\dots,x_n)\times\widetilde{\mathcal{T}}(z;x_i)$ *where* $\dagger_{Koszul}=|t_c|+\sum_{j=1}^{i-1}|x_j|$;

(vi) $(-1)^{|y|+1}\widetilde{\mathcal{T}}(y;z)\times\widetilde{\mathcal{CT}}_{t_c}(z;x_1,\dots,x_n)$.

Proof. The proof relies on the same computations of signed short exact sequences as in the proof of Proposition 9.4.2. For the sake of concision, we choose not to include them. □

Theorem 7.4.1 is then again a simple corollary to Proposition 9.5.4, which is proven by applying the method of Section 9.3.1:

Theorem 7.4.1. *The operations μ_{t_c} define a twisted ΩBAs-morphism between the Morse cochains $(C^*(f),\partial^{Tw}_{Morse},\partial_{Morse})$ and $(C^*(g),\partial^{Tw}_{Morse},\partial_{Morse})$.*

When M is odd-dimensional, this twisted ΩBAs-morphism is a standard ΩBAs-morphism between ΩBAs-algebras, as $\partial^{Tw}_{Morse}=\partial_{Morse}$.

9.5.4 Gluing

We finally construct explicit gluing maps for the (above-break) and (below-break) boundary components using Lemma 9.4.4. Gluing maps for the (above-break) boundary components

$$\#^{above-break}_{T_c^{1,Morse},T^{2,Morse}}:[R,+\infty]\longrightarrow\overline{\mathcal{CT}}_{t_c}(y;x_1,\dots,x_n)$$

are built exactly as in Section 9.4.3.

In the (below-break) case, consider critical points $y,y_1,\dots,y_s\in\mathrm{Crit}(g)$ and $x_1,\dots,x_n\in\mathrm{Crit}(f)$ such that the moduli spaces $\mathcal{T}_{t^0}(y;y_1,\dots,y_s)$ and $\mathcal{CT}_{t_c^r}(y_r;x_{i_1+\dots+i_{r-1}+1},\dots,x_{i_1+\dots+i_r})$ both have dimension 0. Let $T^{0,Morse}\in\mathcal{T}^{Morse}_{t^0}$ and $T_c^{r,Morse}\in\mathcal{CT}^{Morse}_{t_c^r}$. Fix moreover an Euclidean neighborhood U_{z_r} of each critical point z_r and choose L large enough such that for $r=1,\dots,s$, $\gamma_{e_r,T^{0,Morse}}(-L)$ and $\gamma_{e_0,T_c^{r,Morse}}(L)$ belong to U_{z_r}. Define finally the map $\sigma_{e_0,\mathbb{X}_{t^0}}:M\to M^{\times s}$ in a similar fashion to the maps $\psi_{e_i,\mathbb{X}_t}$, as depicted for instance in Figure 9.5.

The gluing map for the perturbed Morse trees $T^{0,Morse}$ and $T_c^{r,Morse}$

$$\#^{below-break}_{T^{0,Morse},T_c^{1,Morse},\dots,T_c^{s,Morse}}:[R,+\infty]\longrightarrow\overline{\mathcal{CT}}_{t_c}(y;x_1,\dots,x_n)$$

can then be defined by applying Lemma 9.4.4 to the map

$$[0,+\infty]\times\prod_{r=1}^{s}U_{z_r}\times\mathcal{T}_s(t^0)\times W^S(y)\times\prod_{r=1}^{s}\left(\mathcal{CT}_{i_r}(t_c^r)\times\prod_{i=i_1+\dots+i_{r-1}+1}^{i_1+\dots+i_r}W^U(x_i)\right)\longrightarrow M^{\times 2s}\times M^{\times s}\times\prod_{r=1}^{s}M^{\times i_r}.$$

defined as follows:

(i) the factor $\mathcal{T}_s(t^0)\times W^S(y)$ is sent to $M^{\times s}$ under the map $(\phi^{-(L-1)})^{\times s}\circ\sigma_{e_0,t^0}$;

(ii) the factor $\mathcal{CT}_{i_r}(t_c^r)\times\prod W^U(x_i)$ is sent to $M^{\times i_r}$ under the map $(\phi^{(L-1)})^{\times i_r}\circ\sigma_{e_0,t_c^r}$;

(iii) the factor $[0,+\infty]\times\prod_{r=1}^{s}U_{z_r}$ is sent to $M^{\times 2s}$ under the map $ev^{U_{z_1}}_{l_\delta^1}\times\cdots\times ev^{U_{z_s}}_{l_\delta^s}$ where δ denotes the parameter in $[0,+\infty]$ and the lengths l_δ^r are defined as in the proof of Proposition 5.2.18 in order for them to define a 2-colored metric ribbon tree.

In particular, we have explicit formulae depending on δ for the resulting edges in the glued tree.

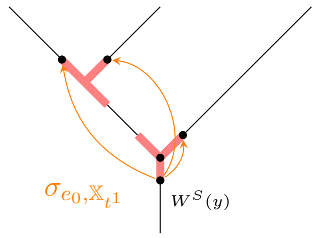

Figure 9.5: Representation of the map $\sigma_{e_0,\mathbb{X}_{t1}}$.

9.6 Proof of Theorem 7.4.5

9.6.1 The moduli spaces $\mathcal{H}(y;x)$

Consider three perturbation data on $\mathcal{CT}_1 := \{+\}$, $\mathbb{Y}^{fg}_{+}$, $\mathbb{Y}^{gf}_{+}$ and $\mathbb{Y}^{ff}_{+}$ For the sake of readability, we will write $\mathbb{Y}^{ij} := \mathbb{Y}^{ij}_{+}$ in the rest of this section. They define chain maps

$$\mu^{\mathbb{Y}^{ij}} : (C^*(i), \partial^{Tw}_{Morse}) \longrightarrow (C^*(j), \partial_{Morse}) \ .$$

Note also that the choices of perturbation data $\mathbb{X}^f$ and $\mathbb{X}^g$ are not necessary for this construction.

Begin by considering the moduli space of metric trees $\mathcal{H}$, represented in two equivalent ways in Figure 9.6. Adapting the discussions of Section 6.2, we infer without difficulty the notion of *smooth choice of perturbation data on $\mathcal{H}$*. Given such a choice of perturbation data $\mathbb{W}$, we then say that it is consistent with the $\mathbb{Y}^{ij}$ if it is such that, when $l \to 0$, $\lim(\mathbb{W}) = \mathbb{Y}^{ff}$, and when $l \to +\infty$, the limit $\lim(\mathbb{W})$ on the above part of the broken tree is $\mathbb{Y}^{fg}$ and the limit $\lim(\mathbb{W})$ on the bottom part of the broken tree is $\mathbb{Y}^{gf}$.

Figure 9.6: The moduli space $\mathcal{H}$

Definition 9.6.1. For x and y two critical points of the Morse function f, define $\mathcal{H}^{\mathbb{W}}(y;x)$ to be the moduli space of perturbed Morse gradient trees modeled on $\dagger$, and such that the two external edges correspond to perturbed Morse trajectories for f, and the internal edge corresponds to a perturbed Morse trajectory for g.

We then check that a generic choice of perturbation data $\mathbb{W}$ makes them into orientable manifolds of dimension

$$\dim(\mathcal{H}^{\mathbb{W}}(y;x)) = |y| - |x| + 1 \ .$$

The 1-dimensional moduli spaces $\mathcal{H}(y;x)$ can be compactified into compact manifolds with boundary $\overline{\mathcal{H}}(y;x)$, whose boundary is given by the three following phenomena:

(i) an external edge breaks at a critical point of f ;

(ii) the length of the internal edge tends towards 0: this yields the moduli spaces

$$\mathcal{CT}^{\mathbb{Y}^{ff}}(y;x) \ ;$$

(iii) the internal edge breaks at a critical point of g: this yields the moduli spaces

$$\bigcup_{z \in \mathrm{Crit}(g)} \mathcal{CT}^{\mathbb{Y}^{gf}}(y;z) \times \mathcal{CT}^{\mathbb{Y}^{fg}}(z;x) \ .$$

9.6.2 Proof of Theorem 7.4.5

Introduce now the degree -1 map $h : C^*(f) \to C^*(f)$ defined as

$$h(x) := \sum_{|y|=|x|-1} \# \mathcal{H}^{\mathbb{W}}(y;x) \cdot y \ .$$

Lemma 9.6.2. *The map h defines an homotopy between $(-1)^d \mu^{\mathbb{Y}^{gf}} \circ \mu^{\mathbb{Y}^{fg}}$ and $\mu^{\mathbb{Y}^{ff}}$ i.e. is such that*

$$(-1)^d \mu^{\mathbb{Y}^{gf}} \circ \mu^{\mathbb{Y}^{fg}} - \mu^{\mathbb{Y}^{ff}} = \partial_{Morse} h + h \partial_{Morse}^{Tw} \ .$$

Proof. We define the moduli space $\mathcal{H}(y;x)$ as before, by introducing the map

$$\phi_{\mathbb{W}} : \mathcal{H} \times W^S(y) \times W^U(x) \longrightarrow M \times M \ ,$$

and setting $\mathcal{H}(y;x) := \phi^{-1}(\Delta)$ where Δ is the diagonal of $M \times M$. We recall moreover that $\sigma(+;y;x) = d(1+|y|)$, $\sigma(y;x) = 1$ and that

$$\mu^{\mathbb{Y}^{ij}}(x) = \sum_{|y|=|x|} \# \widetilde{\mathcal{CT}}_{+}^{\mathbb{Y}^{ij}}(y;x) \cdot y \qquad\qquad \partial_{Morse}(x) = \sum_{|y|=|x|+1} \# \widetilde{\mathcal{T}}(y;x) \cdot y \ .$$

We then set

$$\sigma(\,\mid\,;y;x) = (d+1)|y| \ ,$$

and write $\widetilde{\mathcal{H}}(y;x)$ for the moduli space $\mathcal{H}(y;x)$ endowed with the orientation obtained by twisting its natural orientation by a sign of parity $\sigma(\,\mid\,;y;x)$. We can now define the map $h : C^*(f) \to C^*(f)$ by

$$h(x) := \sum_{|y|=|x|-1} \# \widetilde{\mathcal{H}}(y;x) \cdot y \ .$$

If $\widetilde{\mathcal{H}}(y;x)$ is 1-dimensional, its boundary decomposes as the disjoint union of the following four types of components

$$(-1)^{|y|+d} \widetilde{\mathcal{CT}}^{\mathbb{Y}^{gf}}(y;z) \times \widetilde{\mathcal{CT}}^{\mathbb{Y}^{fg}}(z;x) \qquad\qquad (-1)^{|y|+1} \widetilde{\mathcal{CT}}^{\mathbb{Y}^{ff}}(y;x)$$
$$(-1)^{|y|+1} \widetilde{\mathcal{T}}(y;z) \times \widetilde{\mathcal{H}}(z;x) \qquad\qquad (-1)^{|y|+1+(d+1)|x|} \widetilde{\mathcal{H}}(y;z) \times \widetilde{\mathcal{T}}(z;x) \ .$$

Counting the boundary points of these 1-dimensional moduli spaces implies that

$$(-1)^d \mu^{\mathbb{Y}^{gf}} \circ \mu^{\mathbb{Y}^{fg}} - \mu^{\mathbb{Y}^{ff}} = \partial_{Morse} h + h \partial_{Morse}^{Tw} \ . \qquad \square$$

Theorem 7.4.5 is then a simple corollary to the relation of Lemma 9.6.2, as it descends in cohomology to the relation

$$(-1)^d [\mu^{\mathbb{Y}^{gf}}] \circ [\mu^{\mathbb{Y}^{fg}}] = [\mu^{\mathbb{Y}^{ff}}] \ .$$

Acknowledgements

My first thanks go to my advisor Alexandru Oancea, for his continuous help and support through the settling of this series of papers. I also express my gratitude to Bruno Vallette for his constant reachability and his suggestions and ideas on the algebra underlying this work. I specially thank Jean-Michel Fischer and Guillaume Laplante-Anfossi who repeatedly took the time to offer explanations on higher algebra and ∞-categories. I finally adress my thanks to Florian Bertuol, Thomas Massoni, Amiel Peiffer-Smadja and Victor Roca Lucio for useful discussions.

References

[1] Hossein Abbaspour and Francois Laudenbach. Morse complexes and multiplicative structures. *Mathematische Zeitschrift*, pages 1–42, 2021.

[2] Mohammed Abouzaid. Morse homology, tropical geometry, and homological mirror symmetry for toric varieties. *Sel. Math., New Ser.*, 15(2):189–270, 2009.

[3] Mohammed Abouzaid. A topological model for the Fukaya categories of plumbings. *J. Differential Geom.*, 87(1):1–80, 2011.

[4] Ralph Abraham and Joel Robbin. *Transversal mappings and flows.* An appendix by Al Kelley. W. A. Benjamin, Inc., New York-Amsterdam, 1967.

[5] Dean Andrew Barber. *A comparison of models for the Fulton-MacPherson operads.* PhD thesis, University of Sheffield, 2017.

[6] J. M. Boardman and R. M. Vogt. *Homotopy invariant algebraic structures on topological spaces.* Lecture Notes in Mathematics, Vol. 347. Springer-Verlag, Berlin-New York, 1973.

[7] Nathaniel Bottman. 2-associahedra. *Algebr. Geom. Topol.*, 19(2):743–806, 2019.

[8] Nathaniel Bottman. Moduli spaces of witch curves topologically realize the 2-associahedra. *J. Symplectic Geom.*, 17(6):1649–1682, 2019.

[9] Ricardo Campos, Julien Ducoulombier, and Najib Idrissi. Boardman-Vogt resolutions and bar/cobar constructions of (co)operadic (co)bimodules. *High. Struct.*, 5(1):310–383, 2021.

[10] Pierre-Louis Curien and Guillaume Laplante-Anfossi. Topological proofs of categorical coherence. *Cahiers de topologie et géométrie différentielle catégoriques*, LXV(4), 2024.

[11] Tobias Ekholm. Morse flow trees and Legendrian contact homology in 1-jet spaces. *Geom. Topol.*, 11:1083–1224, 2007.

[12] Stefan Forcey. Convex hull realizations of the multiplihedra. *Topology Appl.*, 156(2):326–347, 2008.

[13] Kenji Fukaya. Morse homotopy and its quantization. In *Geometric topology (Athens, GA, 1993)*, volume 2 of *AMS/IP Stud. Adv. Math.*, pages 409–440. Amer. Math. Soc., Providence, RI, 1997.

[14] Kenji Fukaya and Yong-Geun Oh. Zero-loop open strings in the cotangent bundle and Morse homotopy. *Asian J. Math.*, 1(1):96–180, 1997.

[15] Ezra Getzler and John DS Jones. Operads, homotopy algebra and iterated integrals for double loop spaces. *hep-th/9403055*, 1994.

[16] M. Haiman. Constructing the associahedron, 1984. available for download at http://math.berkeley.edu/mhaiman/ftp/assoc/manuscript.pdf.

[17] Michael Hutchings. Floer homology of families. I. *Algebr. Geom. Topol.*, 8(1):435–492, 2008.

[18] Norio Iwase and Mamoru Mimura. Higher homotopy associativity. In *Algebraic topology (Arcata, CA, 1986)*, volume 1370 of *Lecture Notes in Math.*, pages 193–220. Springer, Berlin, 1989.

[19] T. V. Kadeišvili. On the theory of homology of fiber spaces. *Uspekhi Mat. Nauk*, 35(3(213)):183–188, 1980. International Topology Conference (Moscow State Univ., Moscow, 1979).

[20] Guillaume Laplante-Anfossi and Thibaut Mazuir. The diagonal of the multiplihedra and the tensor product of A_∞-morphisms. *Journal de l'École polytechnique—Mathématiques*, 10:405–446, 2023.

[21] Carl W. Lee. The associahedron and triangulations of the n-gon. *European J. Combin.*, 10(6):551–560, 1989.

[22] Kenji Lefevre-Hasegawa. *Sur les A_∞-catégories*. PhD thesis, Ph. D. thesis, Université Paris 7, UFR de Mathématiques, 2003, math. CT/0310337, 2002.

[23] Jean-Louis Loday. Realization of the Stasheff polytope. *Arch. Math. (Basel)*, 83(3):267–278, 2004.

[24] Jean-Louis Loday and Bruno Vallette. *Algebraic operads*, volume 346 of *Grundlehren der Mathematischen Wissenschaften [Fundamental Principles of Mathematical Sciences]*. Springer, Heidelberg, 2012.

[25] Martin Markl. Models for operads. *Commun. Algebra*, 24(4):1471–1500, 1996.

[26] Martin Markl. Homotopy diagrams of algebras. In *Proceedings of the 21st Winter School "Geometry and Physics" (Srní, 2001)*, number 69, pages 161–180, 2002.

[27] Martin Markl. Transferring A_∞ (strongly homotopy associative) structures. *Rend. Circ. Mat. Palermo (2) Suppl.*, (79):139–151, 2006.

[28] Martin Markl and Steve Shnider. Associahedra, cellular W-construction and products of A_∞-algebras. *Trans. Amer. Math. Soc.*, 358(6):2353–2372, 2006.

[29] Naruki Masuda, Hugh Thomas, Andy Tonks, and Bruno Vallette. The diagonal of the associahedra. *Journal de l'École polytechnique — Mathématiques*, 8:121–146, 2021.

[30] S. Ma'u, K. Wehrheim, and C. Woodward. A_∞ functors for Lagrangian correspondences. *Selecta Math. (N.S.)*, 24(3):1913–2002, 2018.

[31] S. Ma'u and C. Woodward. Geometric realizations of the multiplihedra. *Compos. Math.*, 146(4):1002–1028, 2010.

[32] Thibaut Mazuir. Higher algebra of A_∞ and ΩBAs-algebras in Morse theory II. ArXiv:2102.08996, 2021.

[33] Thibaut Mazuir. *Théorie de Morse et algèbre supérieure des A_∞-algèbres*. PhD thesis, Sorbonne Université, IMJ-PRG, 2022.

[34] Dusa McDuff and Dietmar Salamon. *J-holomorphic curves and symplectic topology*, volume 52 of *American Mathematical Society Colloquium Publications*. American Mathematical Society, Providence, RI, second edition, 2012.

[35] Stephan Mescher. *Perturbed gradient flow trees and A_∞-algebra structures in Morse cohomology*, volume 6 of *Atlantis Studies in Dynamical Systems*. Atlantis Press, [Paris]; Springer, Cham, 2018.

[36] John W. Milnor. *Morse theory. Based on lecture notes by M. Spivak and R. Wells*, volume 66 of *Texts Read. Math.* New Delhi: Hindustan Book Agency, reprint of the 1963 original published by Princeton University Press edition, 2013.

[37] Paul Seidel. *Fukaya categories and Picard-Lefschetz theory*. Zurich Lectures in Advanced Mathematics. European Mathematical Society (EMS), Zürich, 2008.

[38] S. Smale. An infinite dimensional version of Sard's theorem. *Amer. J. Math.*, 87:861–866, 1965.

[39] James Dillon Stasheff. Homotopy associativity of H-spaces. I, II. *Trans. Amer. Math. Soc. 108 (1963), 275-292; ibid.*, 108:293–312, 1963.

[40] Dov Tamari. Monoïdes préordonnés et chaînes de Malcev. *Bulletin de la Société mathématique de France*, 82:53–96, 1954.

[41] Bruno Vallette. Algebra + homotopy = operad. In *Symplectic, Poisson, and noncommutative geometry*, volume 62 of *Math. Sci. Res. Inst. Publ.*, pages 229–290. Cambridge Univ. Press, New York, 2014.

[42] Katrin Wehrheim. Smooth structures on Morse trajectory spaces, featuring finite ends and associative gluing. In *Proceedings of the Freedman Fest*, volume 18 of *Geom. Topol. Monogr.*, pages 369–450. Geom. Topol. Publ., Coventry, 2012.

[43] Donald Yau. *Colored operads*, volume 170 of *Graduate Studies in Mathematics*. American Mathematical Society, Providence, RI, 2016.